High-Redshift Quasars at the Epoch of Cosmic Reionization

Linhua Jiang (江林华)
(KIAA-PKU)

KIAA/DoA, PKU, Dec 12, 2019

Outline

- Introduction
  - Cosmic reionization and quasars at z ≥ 6
- Surveys of z ≥ 6 quasars
  - How to find high-z quasars
  - Modern quasar surveys
  - Quasar luminosity functions
- Quasar properties
  - Metalliticity in broad-line regions
  - Quasar host galaxies
  - ......
- Supermassive black holes (SMBHs)
  - Measurement of SMBH masses
  - Formation of SMBHs
- Probing cosmic reionization
  - Different methods to study the IGM state

Cosmic Reionization

- Neutral IGM ionized by the first astrophysical objects at $6 < z < 12$
- Evidence: CMB polarization + high-z quasars + high-z galaxies …

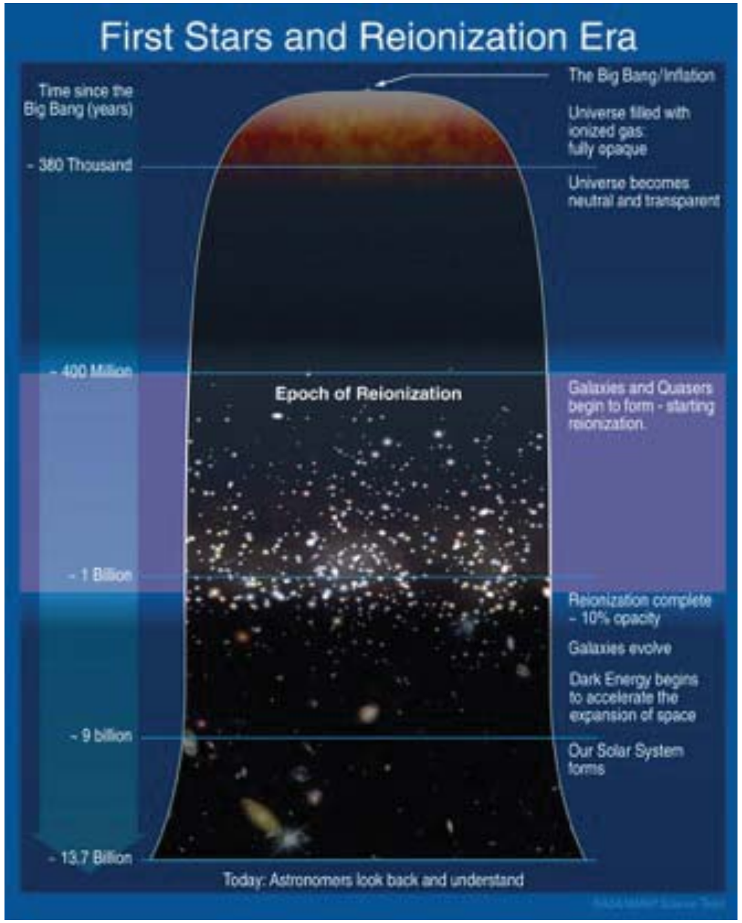

(By M. Alvarez & T. Abel)

Probing reionization

- Quasars at z ≥ 6
- Galaxies at z ≥ 6
- SNe and GRBs at z ≥ 6
- 21cm radiation
- CMB
- …

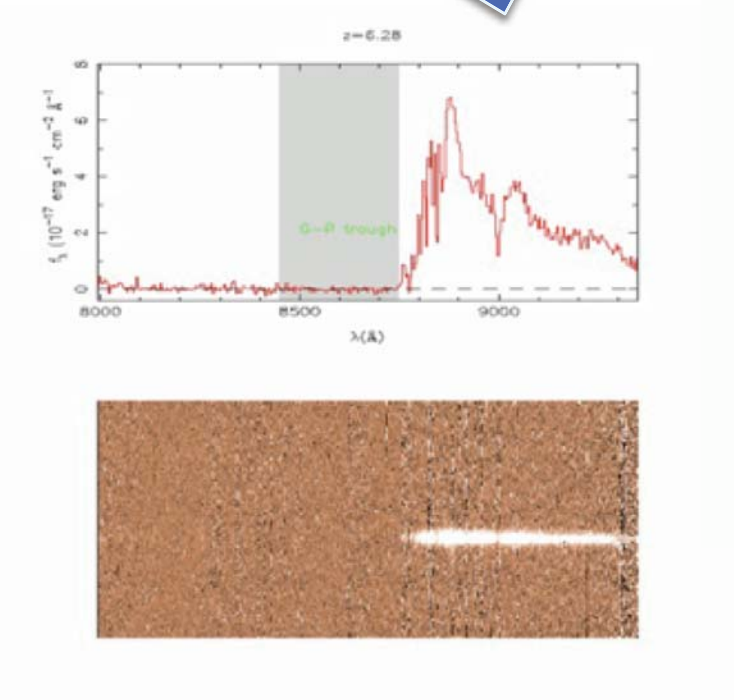

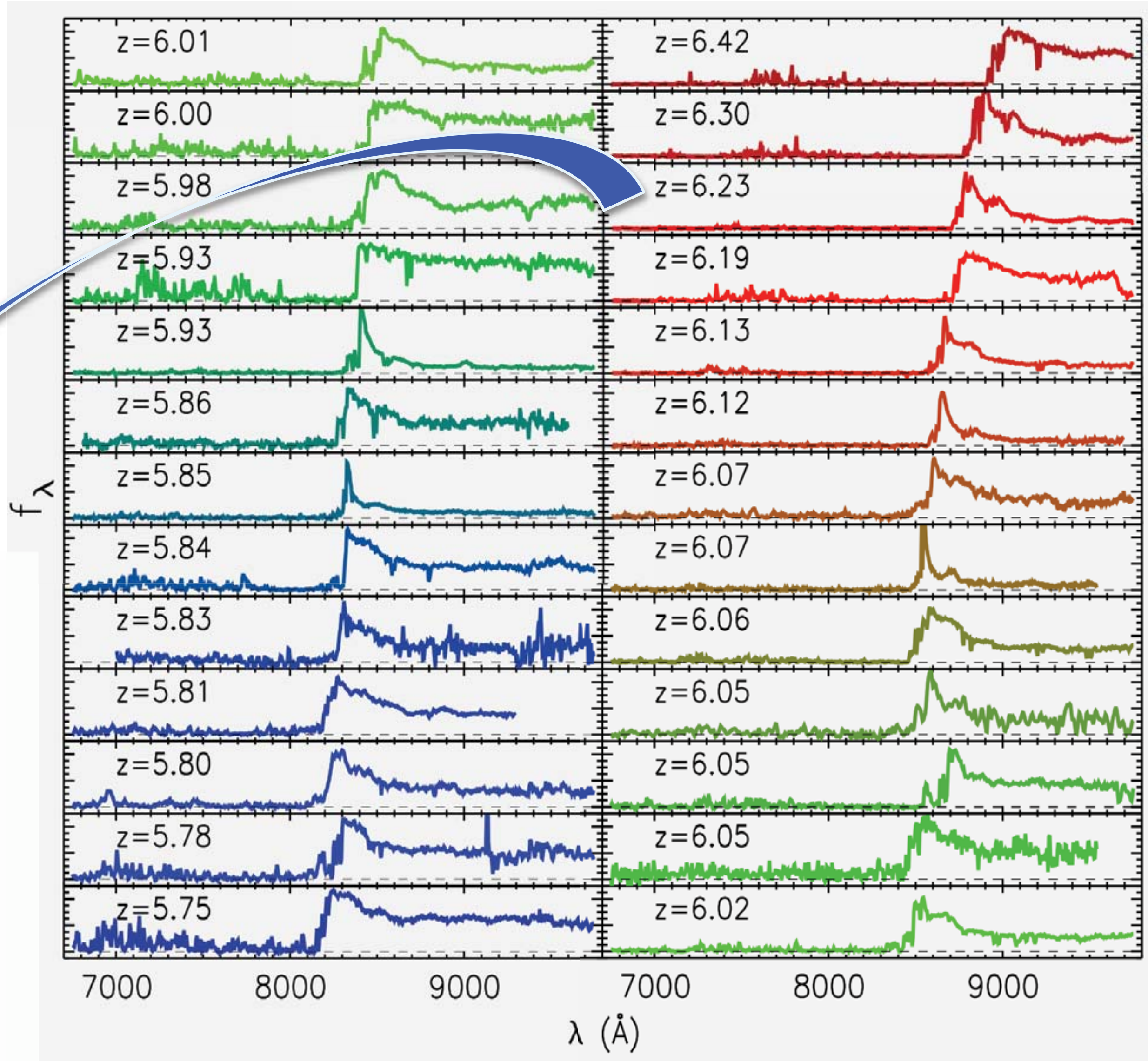

26 SDSS quasars at z > 5.7 before 2010

(Fan et al. 2000–2006; Jiang et al. 2008, 2009)

High-redshift (z≥6) quasars

- Direct evidence: cosmic reionization ends at z~6
- Reionization history, quasar contribution to reionization, etc.
- Birth and growth of early supermassive black holes
- Quasar host galaxies: extreme places to form stars
- Many others

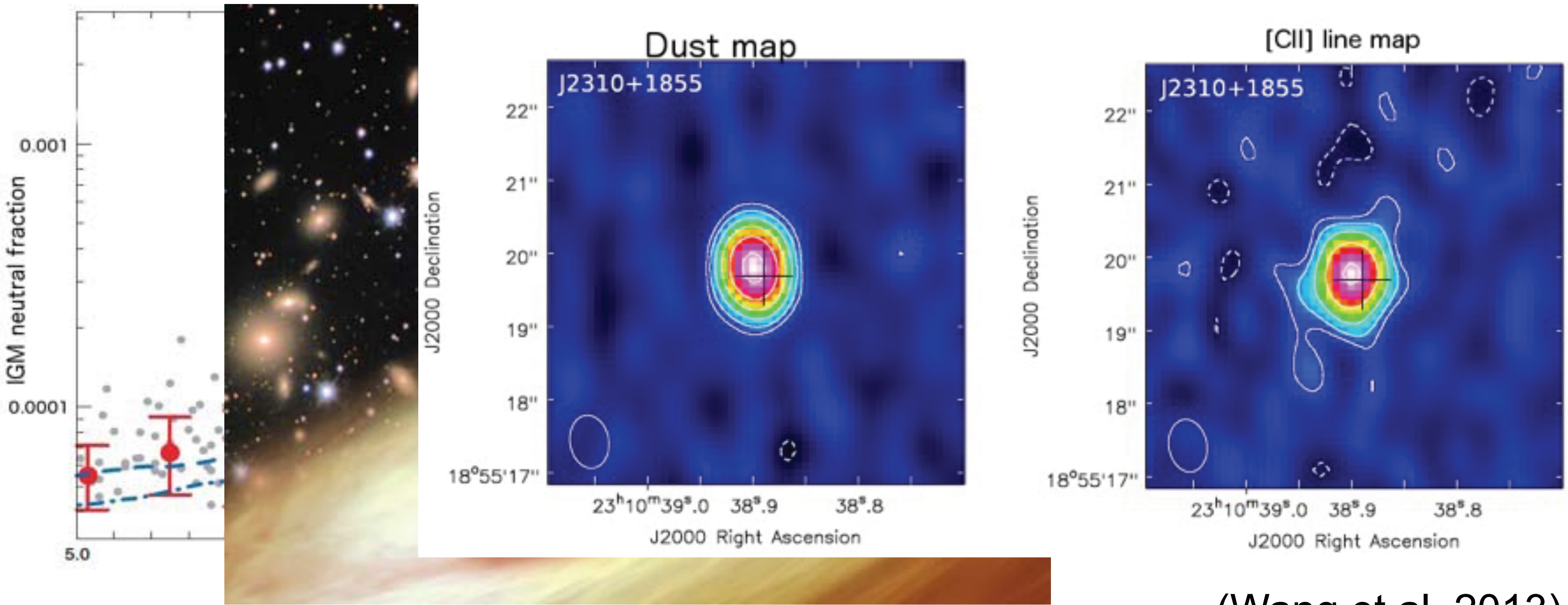

(Wang et al. 2013)

Quasar selection

- Star-like morphology
- Non-stellar colors
- Color-color diagrams
- Photo-z, KDE, …
- Variability
- …

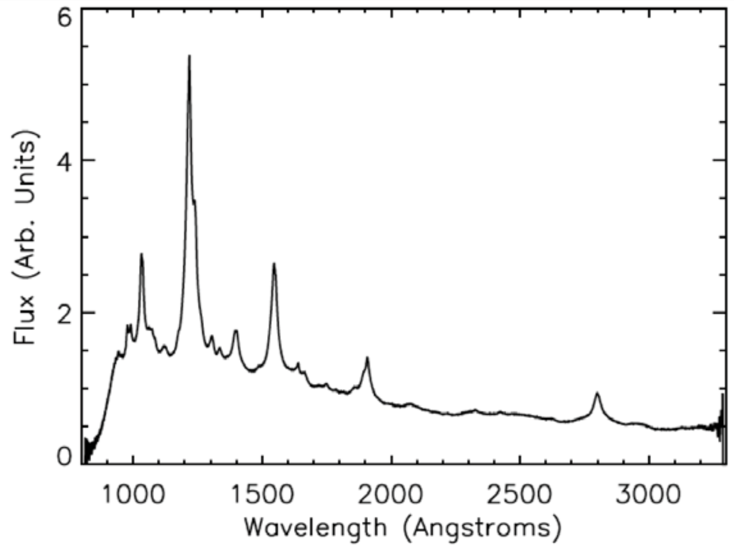

Low-z quasar composite spectrum

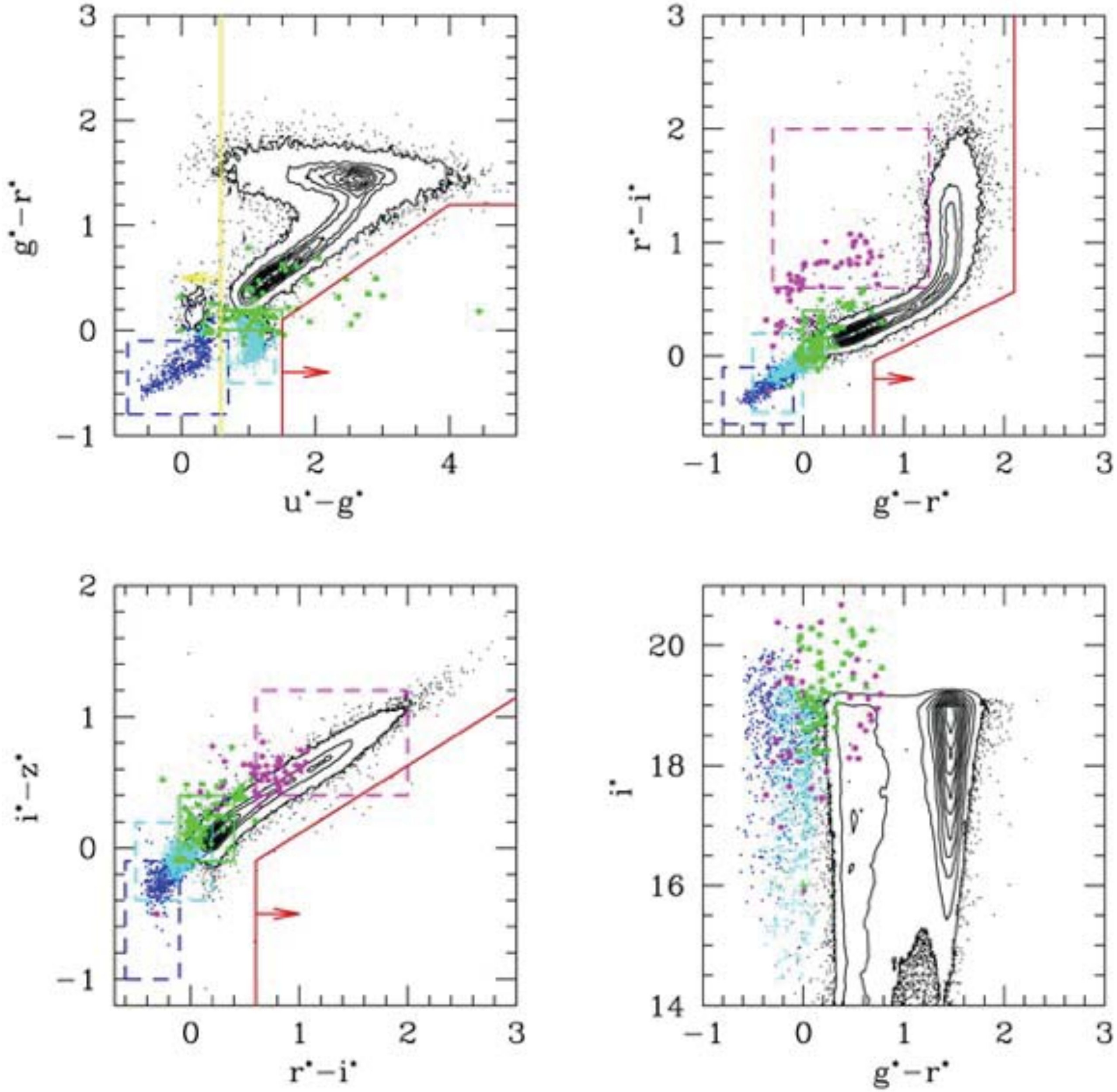

(Richards et al. 2002)

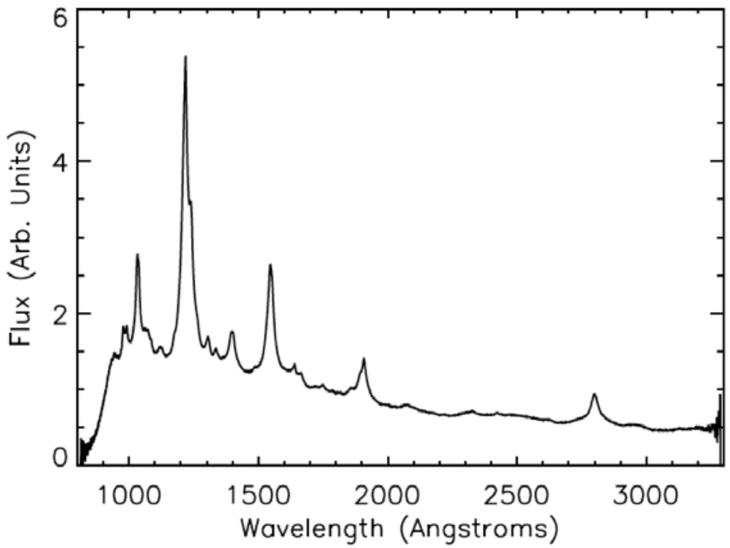
Flux (Arb. Units)
Wavelength (Angstroms)

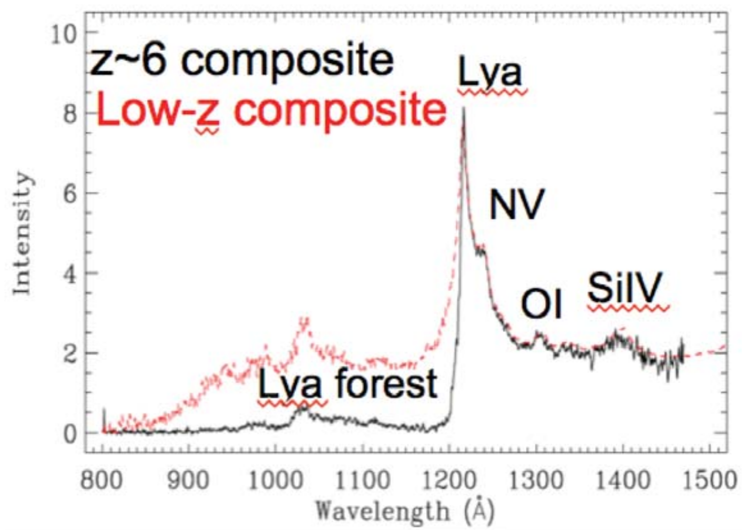
z~6 composite
Low-z composite
Lya
NV
OI
SiIV
Lya forest
Intensity
Wavelength (Å)

(By A. Pontzen)

➢ Selection procedure of quasars at z ~ 6

- Selection of i-band dropout objects
- J-band photometry to remove late type dwarf stars
- Optical spectroscopy to identify quasar candidates

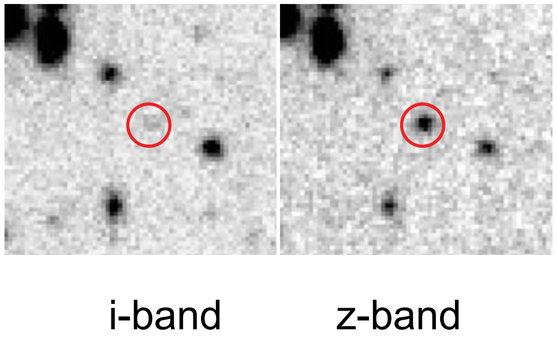

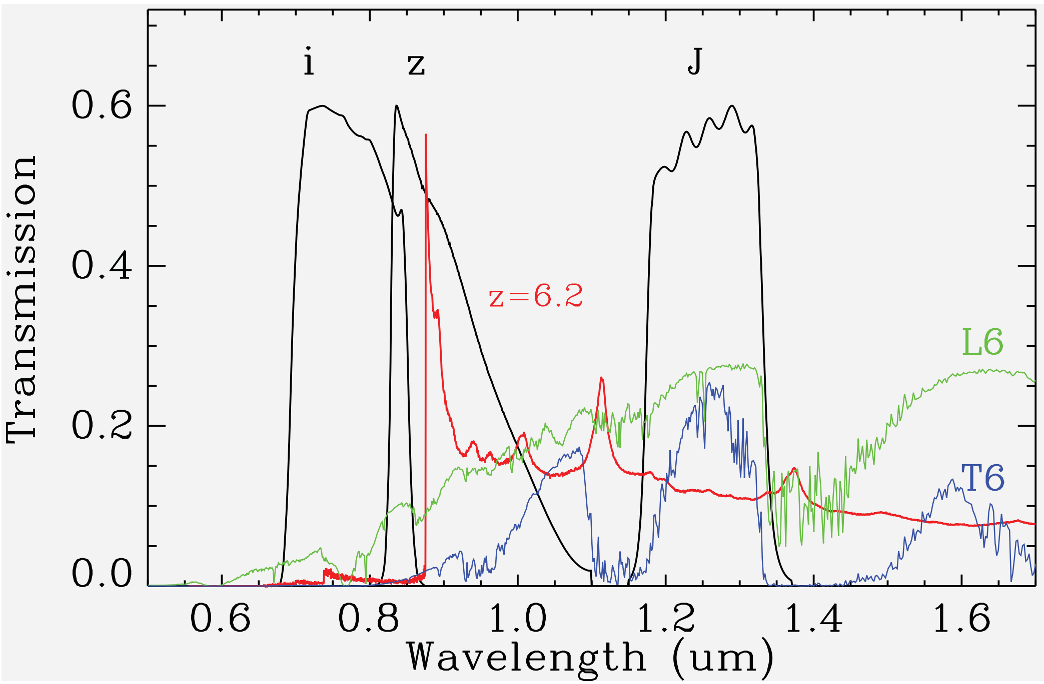

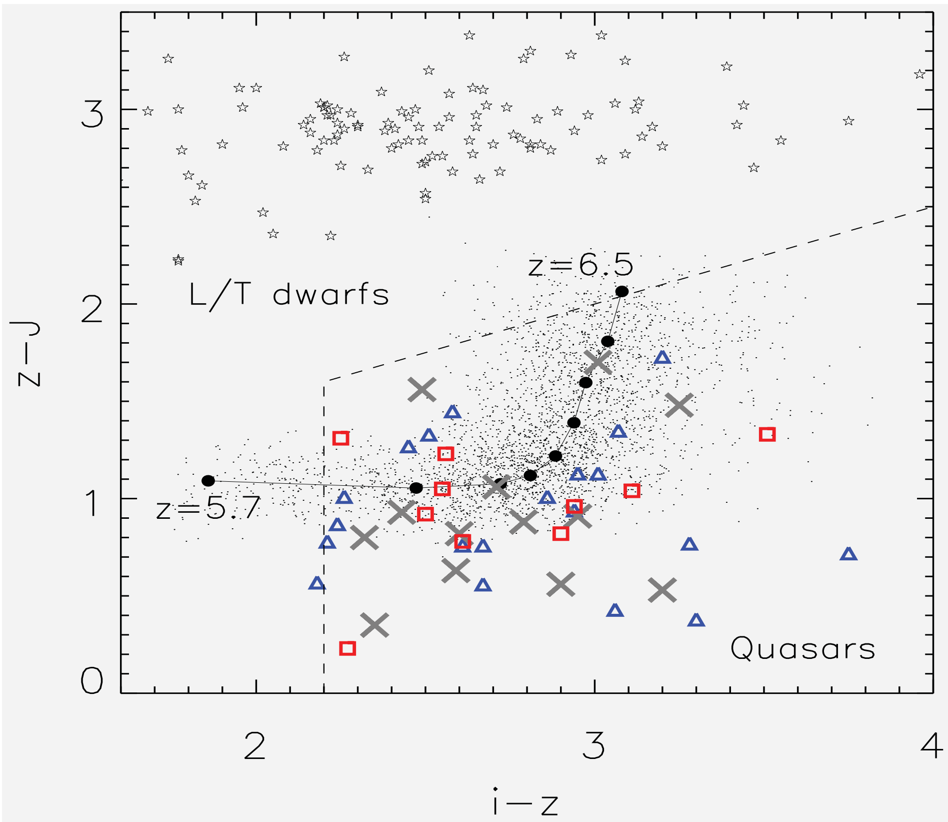

Current status of quasar searches

- The first z~6 quasars found in the SDSS (Fan et al. 2000−2006)
- Followed by
  - A complete survey of SDSS quasars (Jiang et al. 2008−2016)
  - CFHTQS (Willott et al. 2005−2010)
  - UKIDSS (Venemans et al. 2007, Mortlock et al. 2009, 2011)

An extra-luminous quasar
at z = 6.3 (Wu et al. 2015)

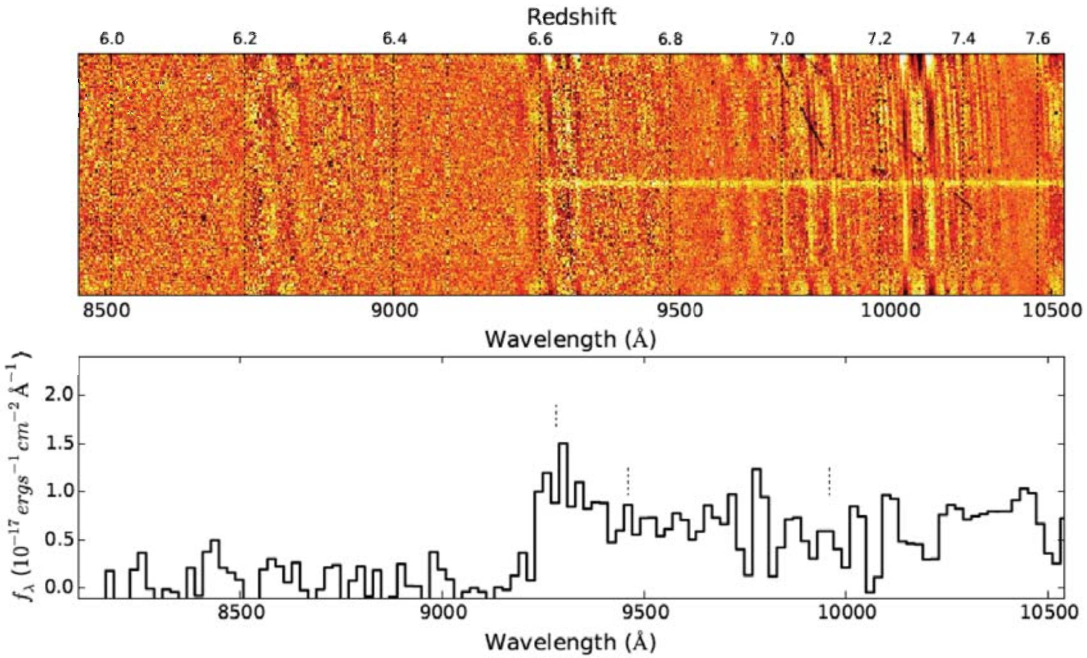

A quasar at z = 6.6 (Wang et al. 2017)

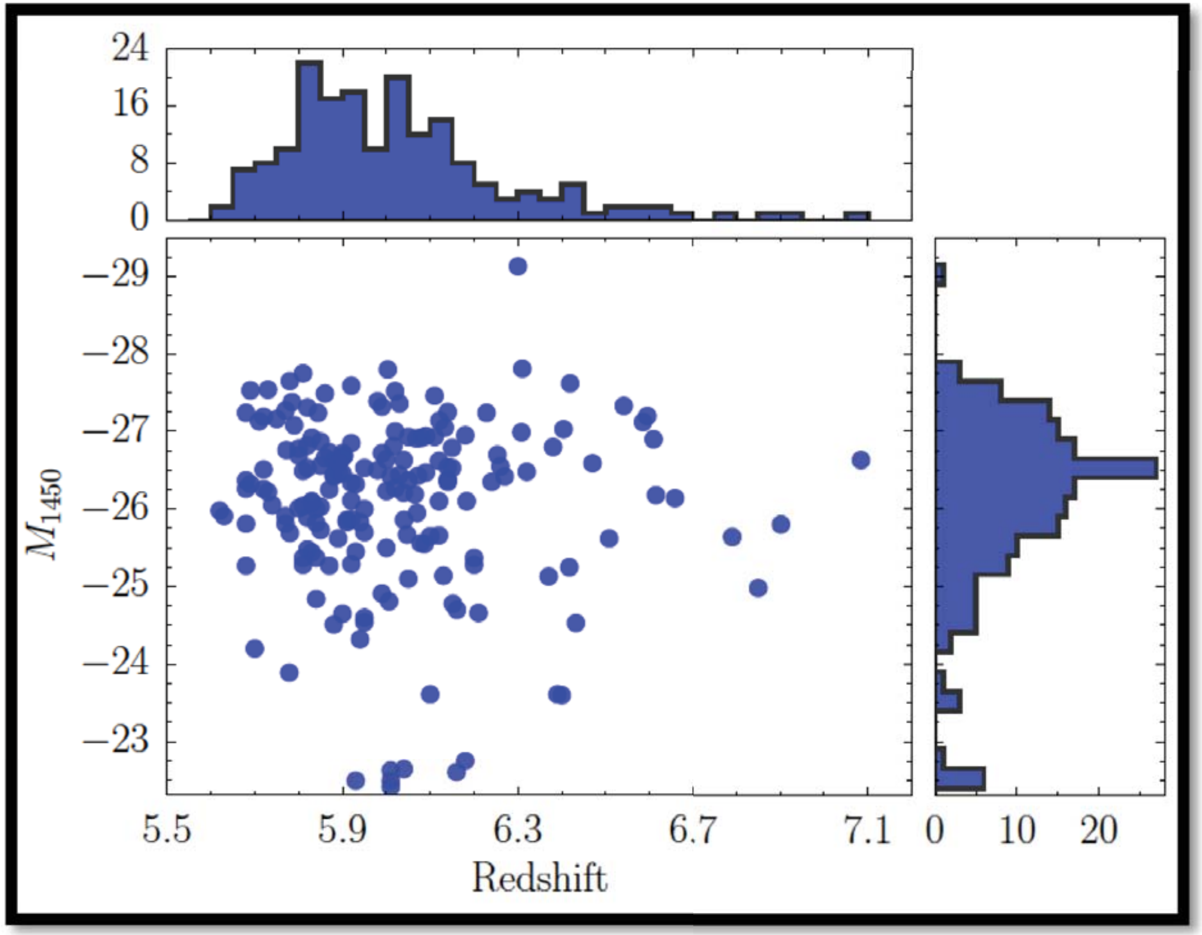

survey

>100 at
>30 at
1 at z

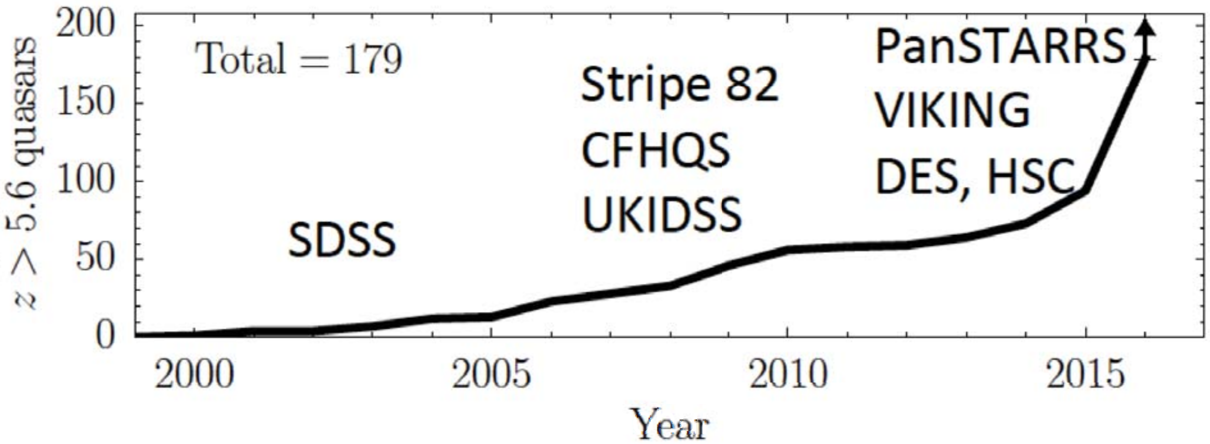

High-z quasars in the SDSS

- Quasars ($z \sim 6$) in the SDSS
  - High-z quasars in the SDSS main survey (single-epoch)
  - High-z quasars in the SDSS deep survey (Stripe 82)
  - High-z quasars in the SDSS overlap regions
- Quasars in the SDSS main survey
  - SDSS: a total of 14555 deg^2 of unique sky area (Ahn 2012)
  - 19 quasars in Fan et al. (2000−2006), including 15 with $z_{AB} < 20$ mag in ~7000 deg^2 of the main survey
- Quasars in the SDSS Stripe 82
  - Stripe 82: a total of ~300 deg^2
  - Repeatedly scanned 70–90 times
  - Two mag deeper than single-epoch data

A final SDSS sample of 52 quasars at z > 5.7

- ➢ Main survey:
  - 11,128 deg^2
  - 24 (or 29) quasars (1/460 deg^2)
  - z_{AB} ~20 mag
- ➢ Overlap regions:
  - 4022 deg^2
  - 10 (or 17) quasars
  - 20< z_{AB} <20.5 mag
- ➢ Stripe 82:
  - 275 deg^2
  - 13 quasars (1/21 deg^2)
  - z_{AB} ~22 mag

(Jiang et al. 2016)

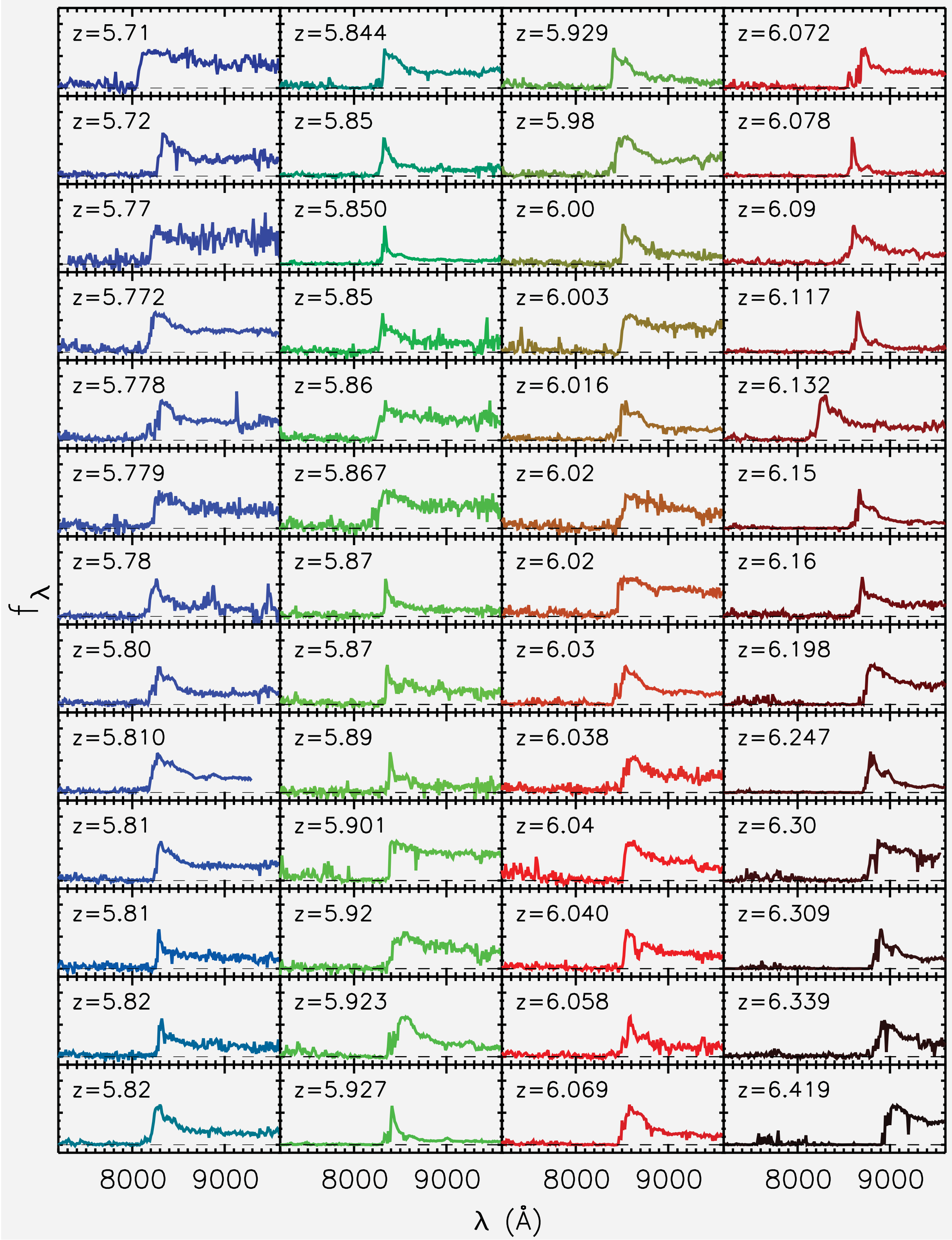

Quasar luminosity function (QLF) at z ~ 6

- Binned QLF

The available volume for a quasar with absolute magnitude M_{1450} and redshift z in a magnitude bin ΔM and a redshift bin Δz is

$$V_a = \int_{\Delta M} \int_{\Delta z} p(M_{1450}, z) \frac{dV}{dz} dz\, dM, \qquad (1)$$

where $p(M_{1450}, z)$ is the selection function used to correct for the sample incompletenesses described above. The spatial density and its statistical uncertainty are written as

$$\rho = \frac{N}{V_a}, \quad \sigma(\rho) = \frac{N^{1/2}}{V_a}, \qquad (2)$$

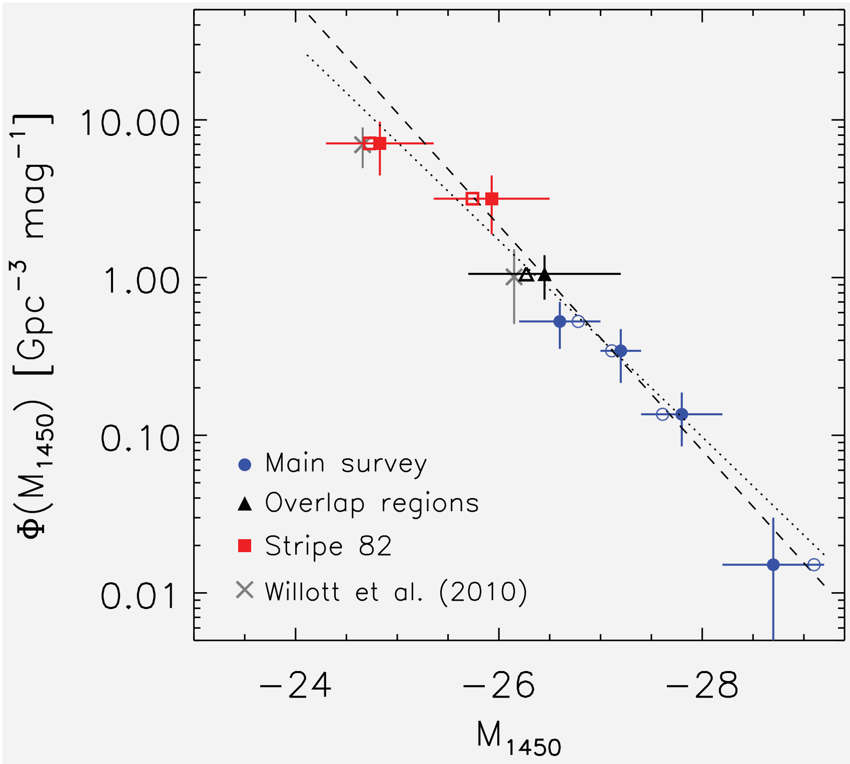

- Bright end:

$\Phi(L_{1450}) \propto L_{1450}^{\beta}$, or,

$$\Phi(M_{1450}) = \Phi^{*} 10^{-0.4(\beta+1)(M_{1450}+26)}, \qquad (3)$$

steep slope: β = −2.8

➢ Density evolution of luminous quasars at high redshift

- Double power law QLF

$$\Phi(M,z) = \frac{\Phi^*(z)}{10^{0.4(\alpha+1)(M-M^*(z))} + 10^{0.4(\beta+1)(M-M^*(z))}}, \quad (5)$$

$$\Phi^*(z) = \Phi^*(z=6)\,10^{k(z-6)}. \quad (6)$$

- Bright end:

$$\rho(<M,z) = \int_{-\infty}^{M} \Phi(M',z)\,dM'$$

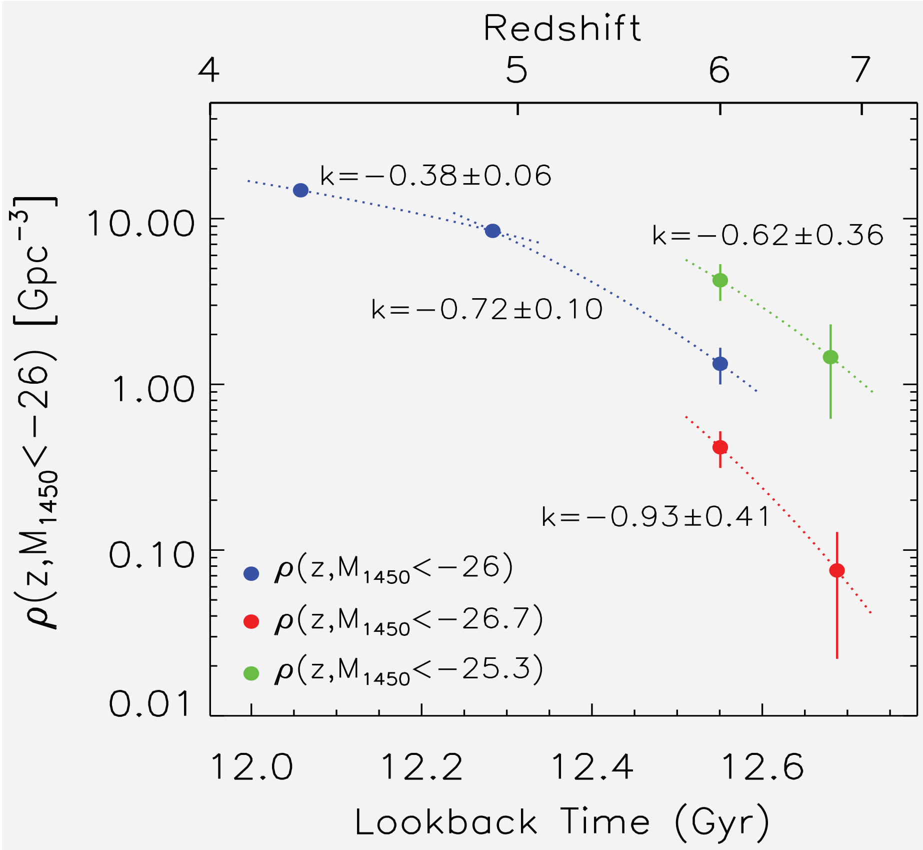

➢ Strong density evolution:

- k= −0.38 for z = 4.2 – 4.9
- k= −0.72 for z = 4.9 – 6.0
- k= −0.80 for z = 6.0 – 6.8

- Double power-law QLF

  $\phi(M_{1450}) = \phi^* / (10^{0.4(\alpha+1)(M_{1450}-M_{1450}^*)} + 10^{0.4(\beta+1)(M_{1450}-M_{1450}^*)})$

- Two faintest points from Willott 2010 and Kashikawa 2015
- Results: $\alpha=-1.9$, $M_{1450}^*=-25.2$, $\beta=-2.8$ (fixed), $k=-0.7$(fixed)

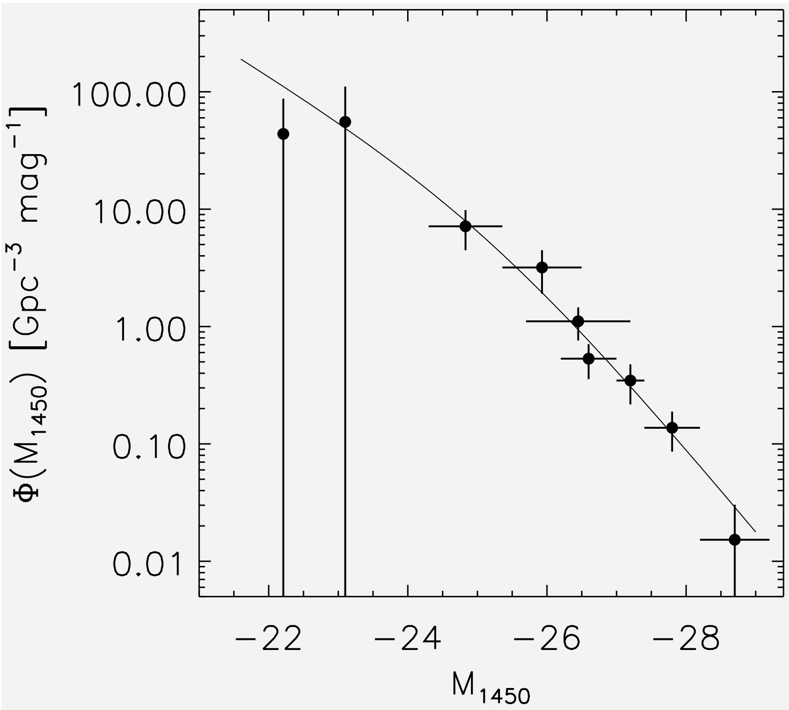

QLF at z ~ 6

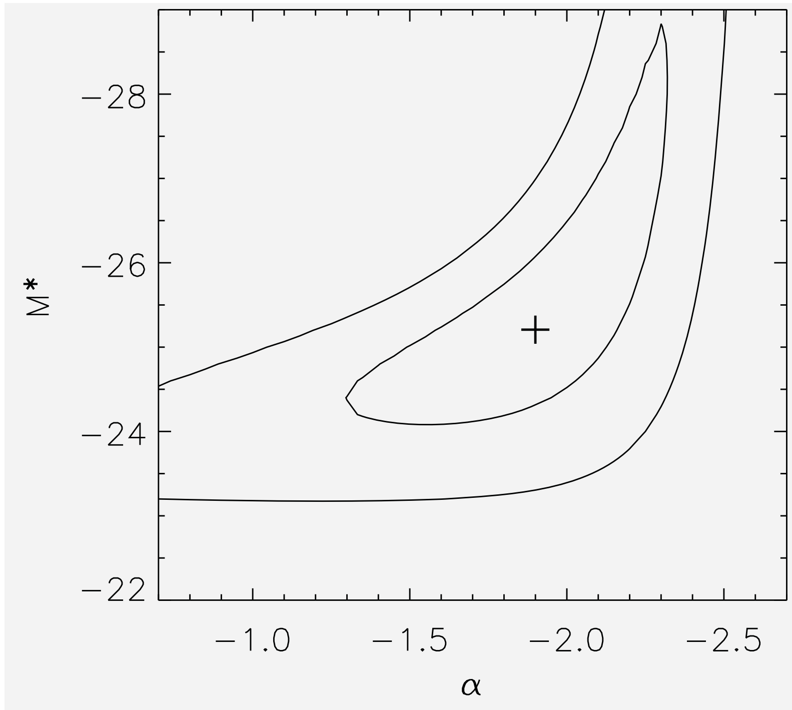

α - M_{1450}^* correlation

Quasar contribution to the UV background

- Required number of photons calculated from Madau 1999

The total photon emissivity per unit comoving volume required to ionize the universe is estimated to be

$$\dot{\mathcal{N}}_{ion}(z) = 10^{51.2}\,\mathrm{Mpc}^{-3}\,\mathrm{s}^{-1}\left(\frac{C}{30}\right) \times \left(\frac{1+z}{6}\right)^3 \left(\frac{\Omega_b h^2}{0.02}\right)^2 \quad (10)$$

(Madau et al. 1999), where baryon density $\Omega_b h^2 = 0.02$ (Spergel et al. 2007) and C is the clumping factor of the IGM. We examine the effects of three values 1, 10, and 30 for C.

- Luminosity range M_{1450}= [−30, −18]
- IGM clumping factor *C* = 1.5, 3, 5

➢ Results:

- The quasar contribution strongly depends on M*, α, and *C*
- For *C*=3, quasars/AGN cannot provide enough photons to ionize the z~6 IGM (at 90% confidence); quasars can, only if α is very steep, and/or M* is very low, and/or the IGM is homogeneous

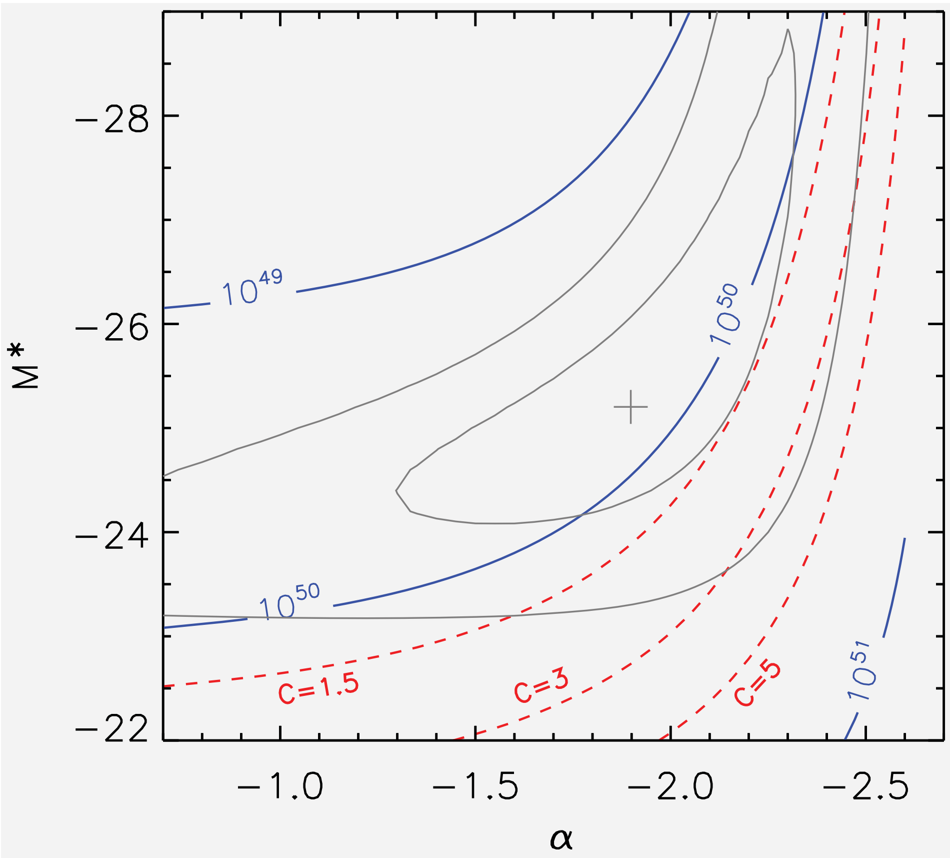

- A few more words on ionizing sources for reionization
  - One of the key science goals here
  - Key parameters: LyC escape fraction and IGM clumpiness
  - From low-z galaxies
  - From high-z galaxies
  - From deep X-ray observations
  - From faint quasars

❖ Quasar properties

- Quasars: strong radiation from X-ray to radio
- At z > 6, UV redshifted to near-IR …

AGN unification model

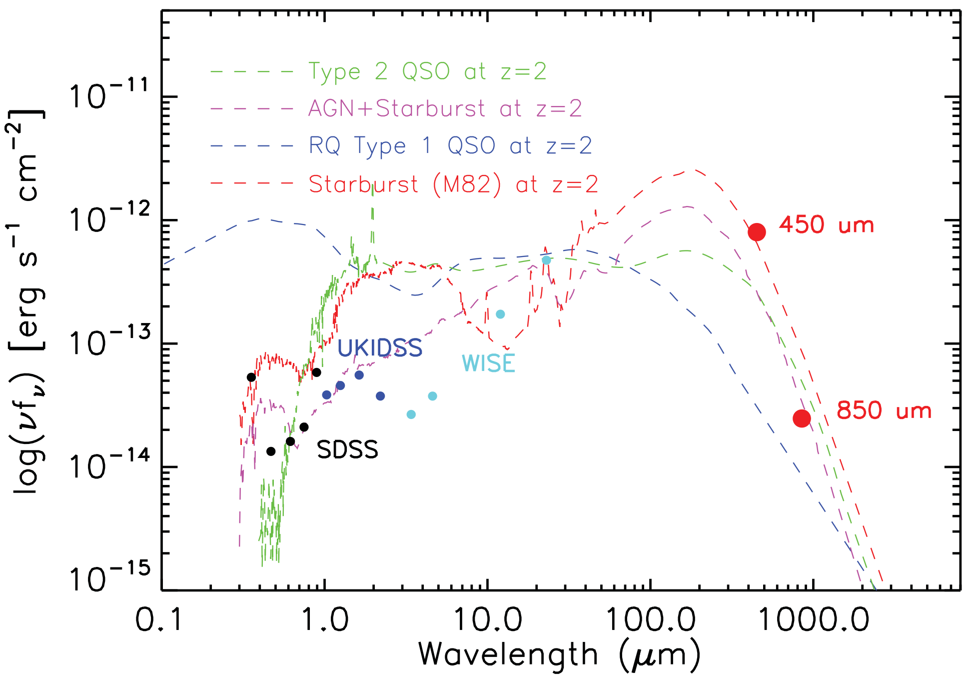

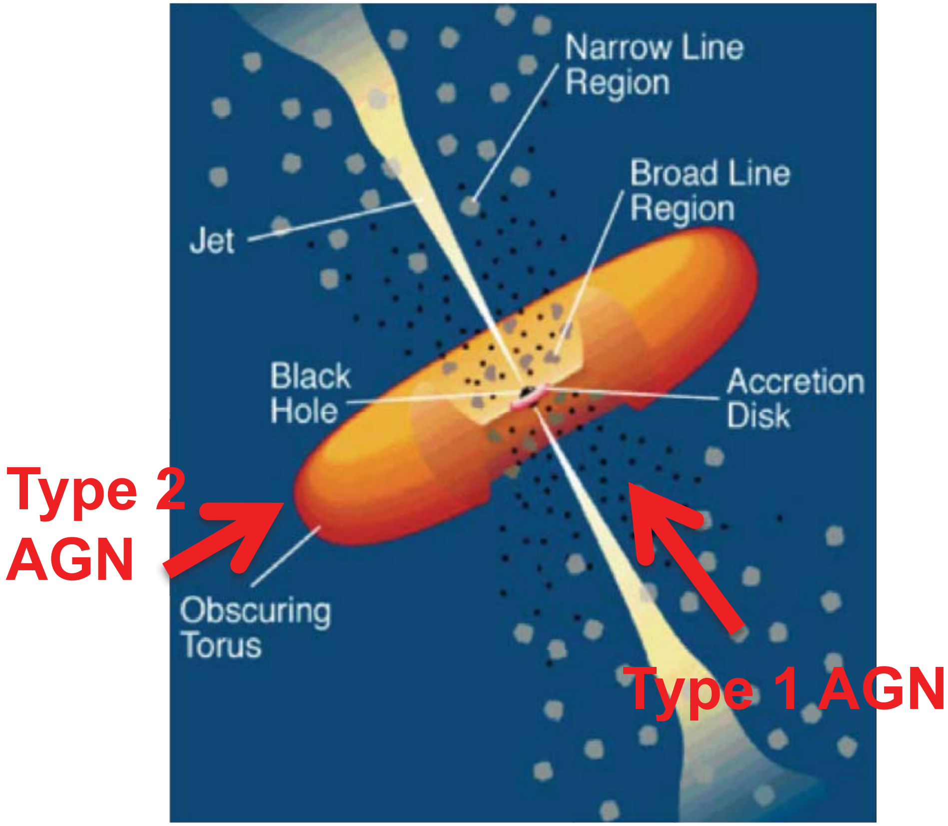

(Urry & Padovani, 1995)

- Metallicity in broad-line regions (BLRs)

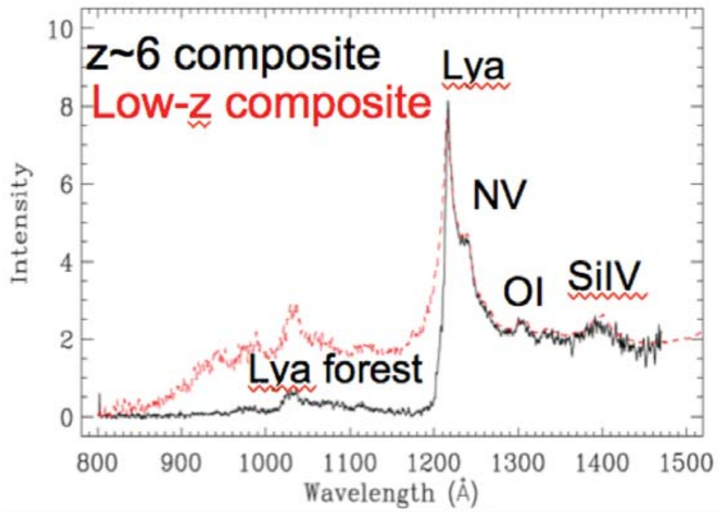

Low-z composite vs. z~6 composite

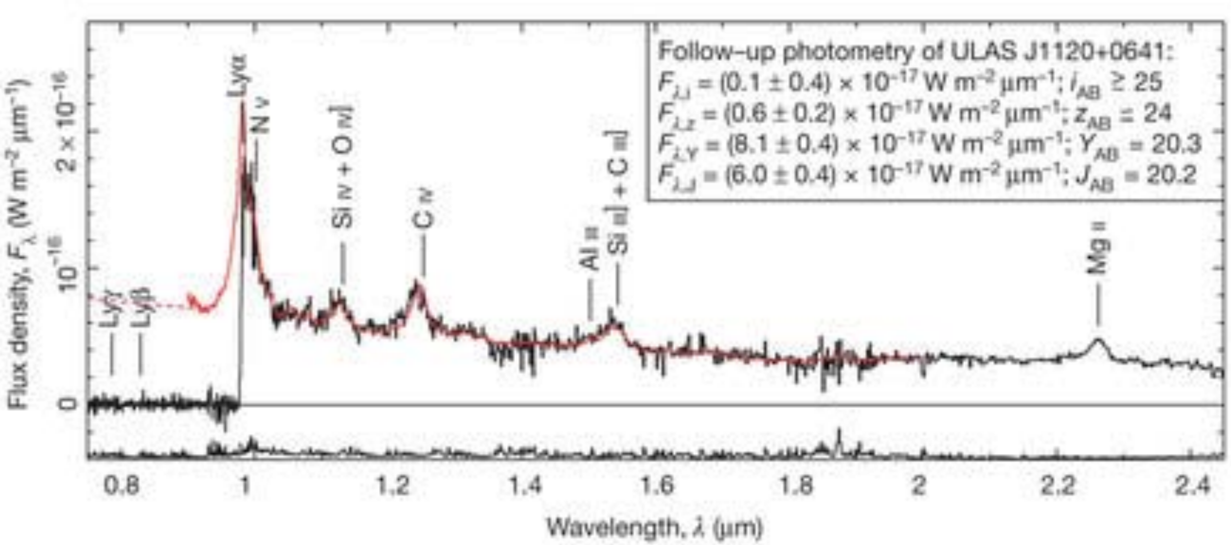

(z=7.085; Mortlock 2011)

- Photoionization models: line ratios → gas metallicity

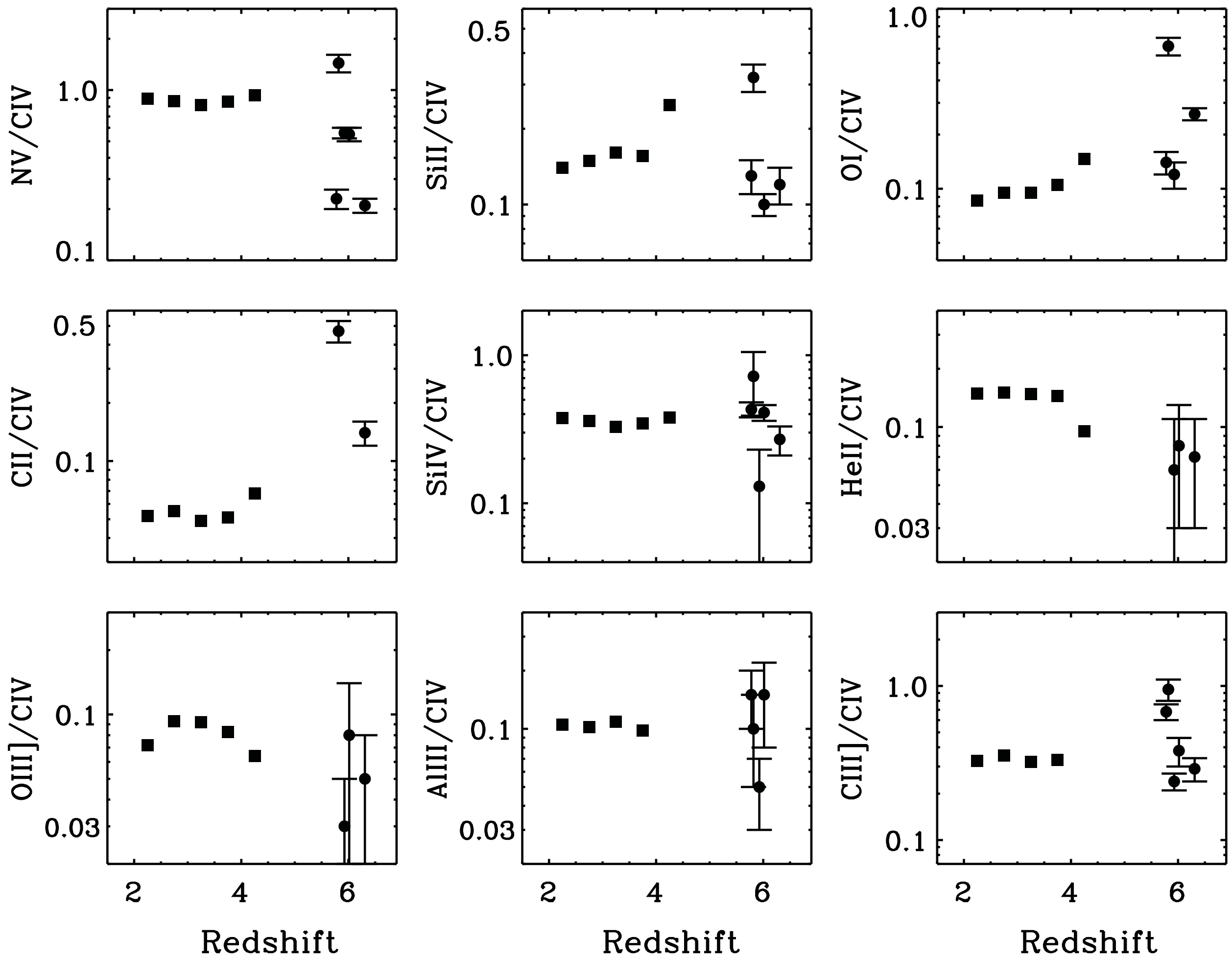

(Jiang et al. 2007)

Metallicity in BLRs

- Supersolar with $Z/Z_\odot \sim 4$
- No redshift evolution up to z ~ 6
- Vigorous star formation and element enrichment occurred in the first Gyr
- Far-IR observations: star formation rates about 1000 $M_\odot$/yr
- No redshift evolution on FeII/MgII, why interesting?

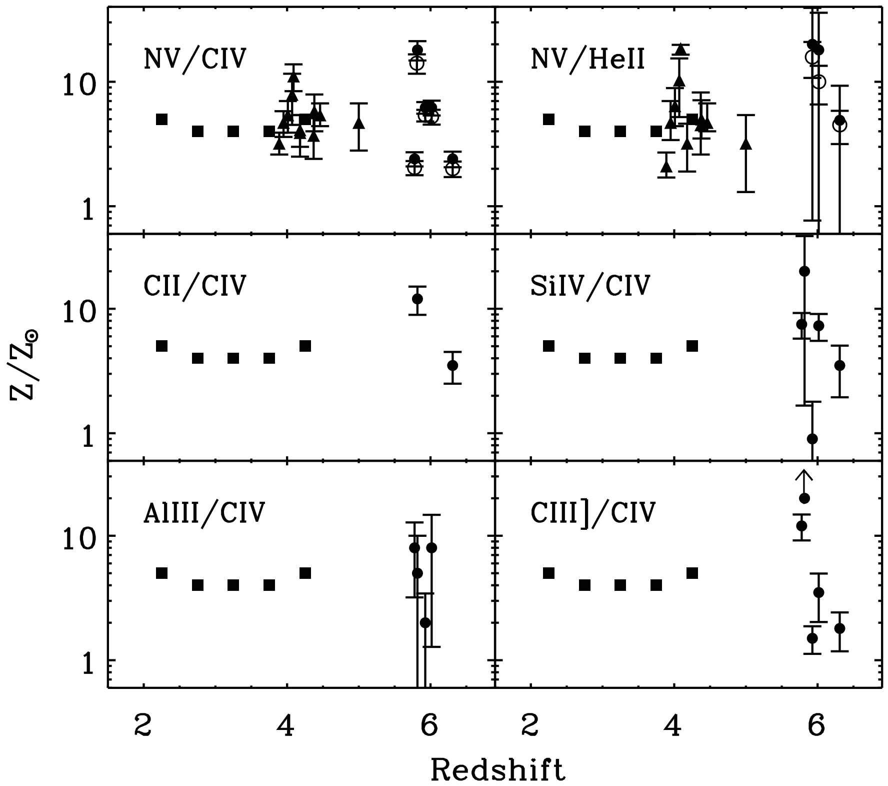

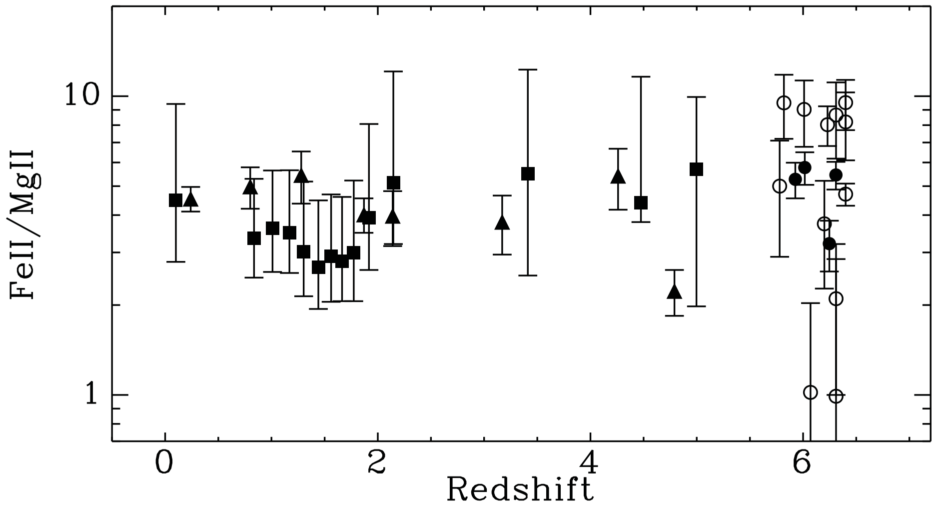

(Jiang et al. 2007)

❖ X-ray properties

- No evolution up to z ~ 6

$$\alpha_{ox} = \frac{\log\left(f_{2\,\mathrm{keV}}/f_{2500\,\text{Å}}\right)}{\log\left(\nu_{2\,\mathrm{keV}}/\nu_{2500\,\text{Å}}\right)}$$

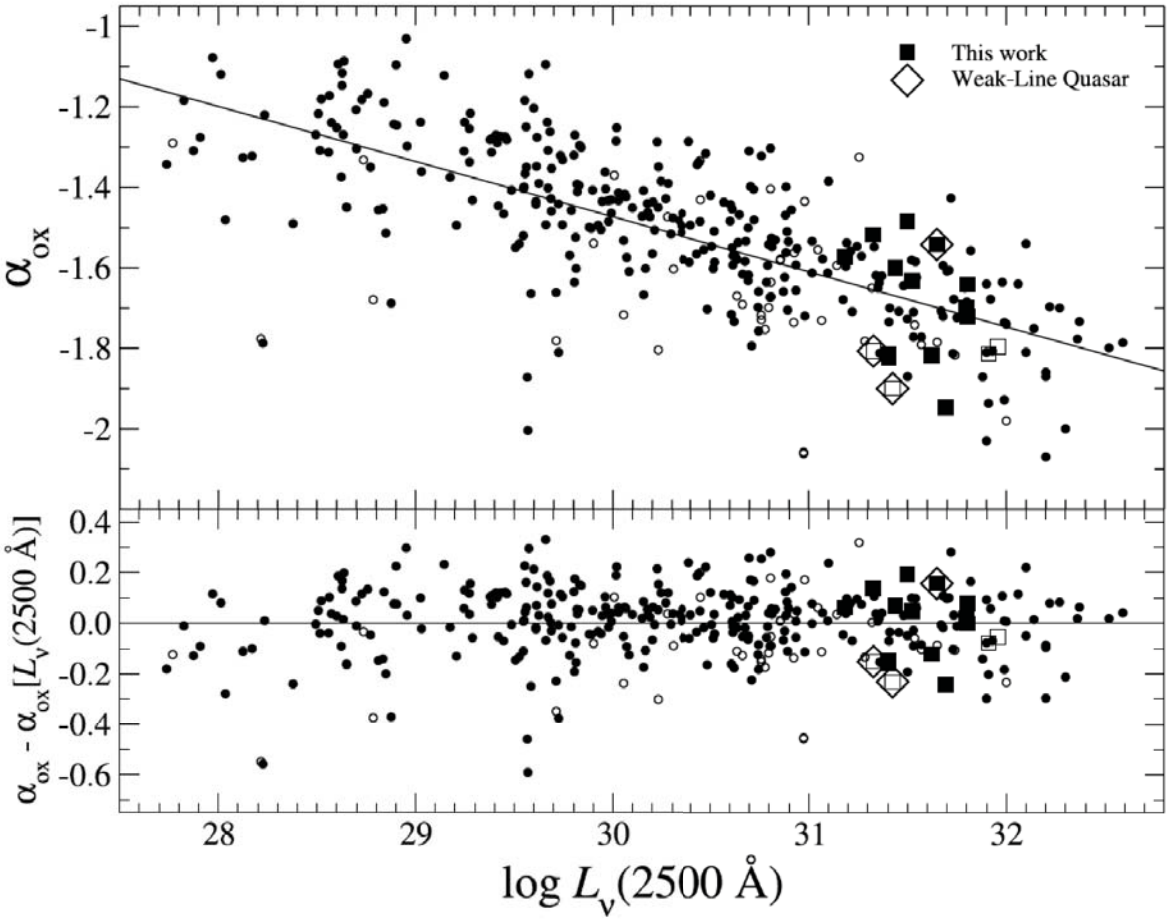

(Shemmer et al. 2006)

Quasars are boring

Quasar host galaxies at z ~ 6

- No host galaxies at z ~ 6 have been identified in the rest-frame UV
- Need future JWST …

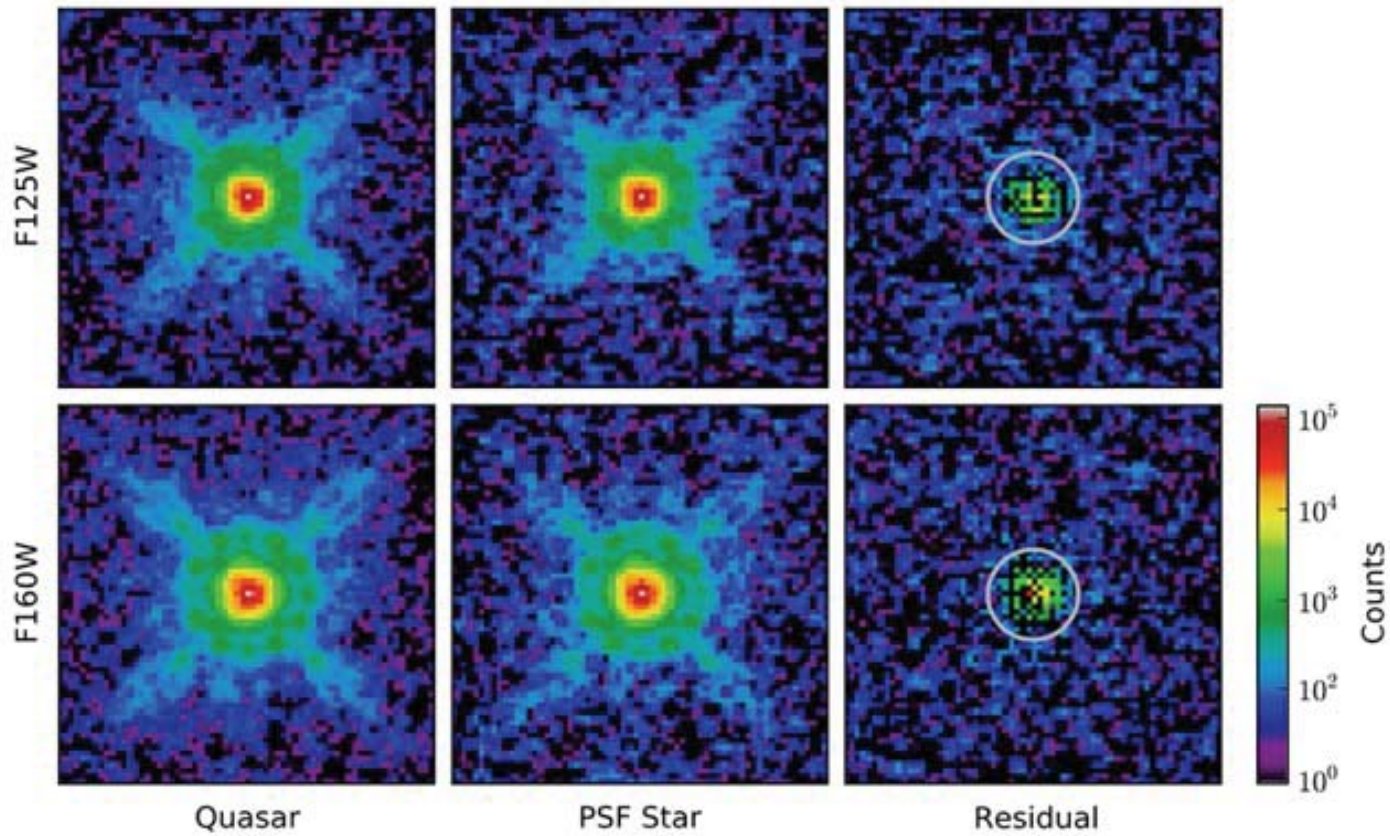

(Mechtley et al. 2012)

JWST observations of J1148 at z = 6.42

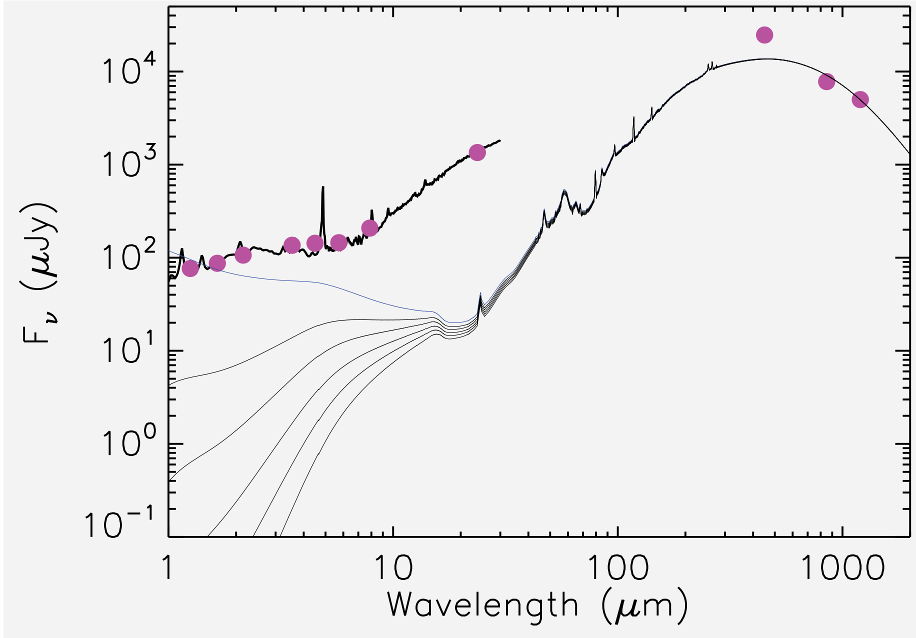

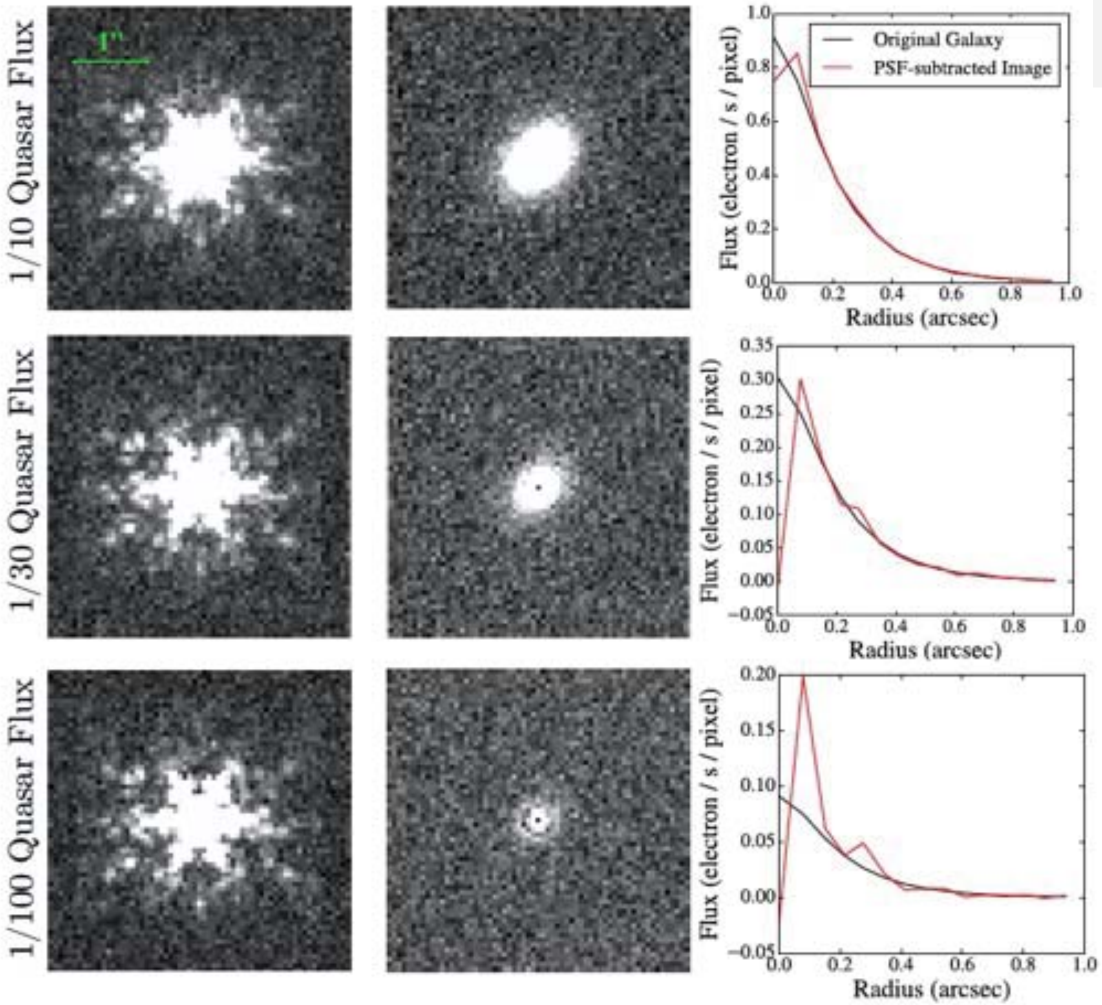

Figure 4: NIRCam simulation of 4000 sec exposure with the F360M filter using an M5 PSF star: (*left*) quasar + host; (*middle*) after PSF subtraction; (*right*) radial profile. The host galaxy has an exponential profile with $r_e = 0.3''$. Top panels: the host flux is a factor of 10 lower than that of the quasar at this wavelength. Middle panel: 1/30 flux level. Bottom panels: 1/100 flux level.

❖ SMBHs

BH mass estimate

- Low-z: reverberation mapping, etc.
- High-z: mass scaling relation

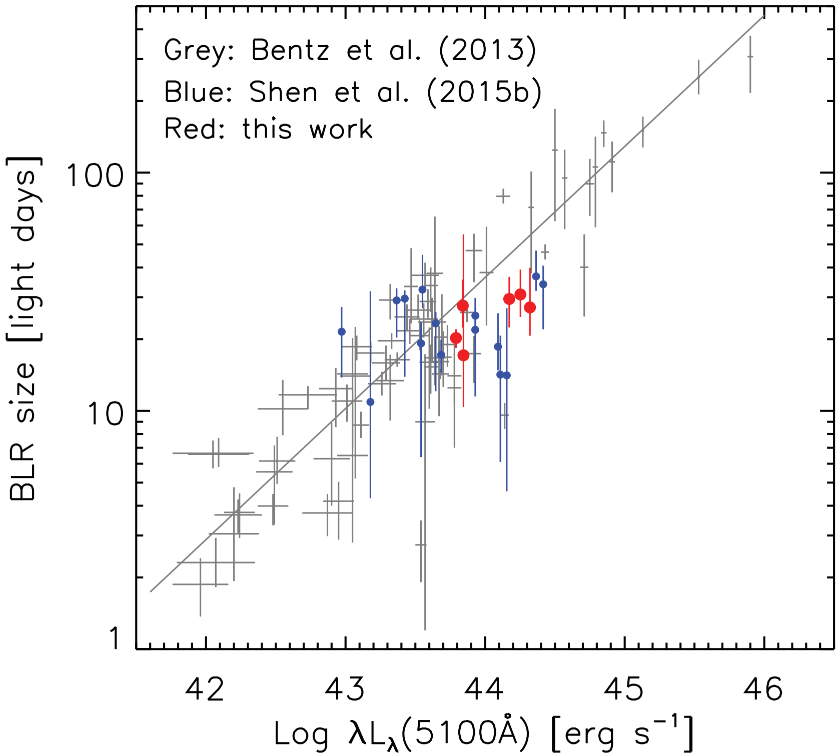

(Jiang et al. et al. 2016b)

$$M_{\mathrm{BH}} = \frac{fR\Delta V^2}{G}$$

$$\mathrm{M_{BH}(C\,IV)} = 4.57 \left(\frac{\mathrm{FWHM(C\,IV)}}{\mathrm{km\ s^{-1}}}\right)^2 \left(\frac{\lambda L_\lambda(1350\text{Å})}{10^{44}\ \mathrm{ergs\ s^{-1}}}\right)^{0.53} \mathrm{M_\odot}$$

$$\mathrm{M_{BH}(Mg\,II)} = 3.2 \left(\frac{\mathrm{FWHM(Mg\,II)}}{\mathrm{km\ s^{-1}}}\right)^2 \left(\frac{\lambda L_\lambda(3000\text{Å})}{10^{44}\ \mathrm{ergs\ s^{-1}}}\right)^{0.62} \mathrm{M_\odot}$$

(e.g. Vestergaard 2006; McLure 2004; Shen et al. 2012)

BH masses of z ~ 6 quasars

- BH masses: close to or higher than $10^9\ M_\odot$ in luminous quasars (z_{AB}<20 mag)
- Eddington ratios: close to 1

(Jiang et al. 2007)

Table 5. Central BH Masses ($10^9\ M_\odot$)

Quasar (SDSS)	L_{Bol}[a]	L_{Bol}/L_{Edd}[b]	M_{BH}(C IV)	M_{BH}(Mg II)	M'_{BH}(Mg II)[c]
J0836+0054	47.72	0.44	9.3±1.6	...	...
J1030+0524	47.37	0.50	3.6±0.9	1.0±0.2	2.1±0.4
J1044−0125	47.63	0.31	10.5±1.6	...	...
	47.40	0.61	3.2±0.6	1.1±0.1	2.2±0.3
	47.20	0.94	1.3±0.3	0.6±0.1	0.9±0.2
	47.33	1.11	...	1.5±0.3	...

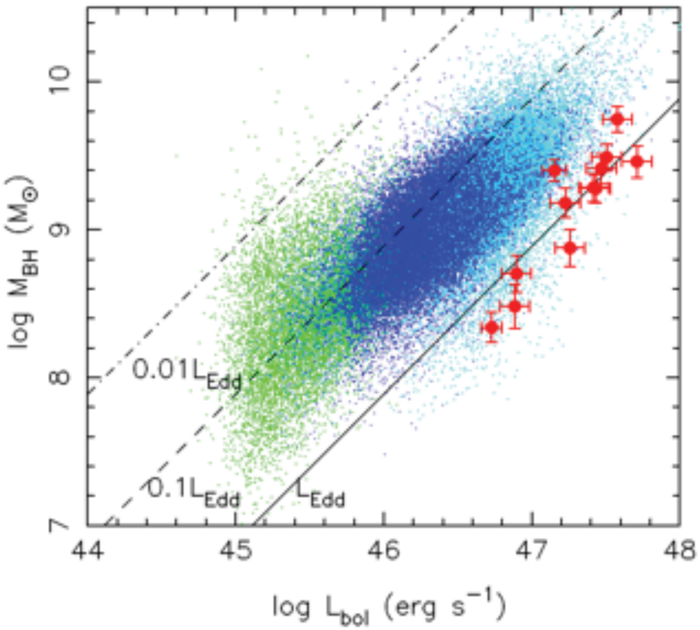

(A 12 billion solar-mass BH; Wu et al. 2015)

- Was there enough time to make such massive BHs at z~6, or, can we find lots of luminous quasars at z > 7?

It is remarkable that billion-solar-mass BHs can form less than one Gyr after the Big Bang. With the reasonable assumption that BH accretion is at the Eddington rate, the BH mass at time t is $M_t = M_0 e^{t/\epsilon\tau}$, where ϵ is the radiative efficiency, $\tau = 4.5 \times 10^8$ years, and M_0 is the initial BH mass or the seed BH mass. Seed BHs can be produced from the collapse of Population III stars or gas clouds, and their masses are roughly 10^2–10^4 $M_\odot$ (e.g. Madau & Rees 2001; Volonteri & Rees 2006; Lodato & Natarajan 2007). Consider the case in which a massive BH at $z = 6$ formed from a seed BH with $M_0 = 10^3$ $M_\odot$ at $z = 20$. The e-folding time $\epsilon\tau$ for the BH growth is roughly 4.5×10^7 years if $\epsilon \sim 0.1$. The BH grows from $z = 20$ to 6 by 15 e-foldings, or a factor of 3.3×10^6, which results in a massive BH with $M_t = 3.3 \times 10^9$ $M_\odot$ at $z = 6$, comparable to the observed BH masses in our sample. If a quasar is shining at half of the Eddington limit, its BH grows from $z = 20$ to 6 by only 7.5 e-foldings, or a factor of ~ 2000, making it very difficult to form billion-solar-mass BHs in this scenario. In addition, if Eddington-limited accretion is via standard thin disks, BHs are likely to be spun up and the radiative efficiency and Eddington timescale will increase (Volonteri & Rees 2006; Rees & Volonteri 2006). In this case it would take much longer to form massive BHs. So super-Eddington accretion or lower radiative efficiency is probably required to form BHs with $M_t = 10^9$–10^{10} $M_\odot$ by $z = 6$.

(Jiang et al. 2007)

Consider two quasars:

- ULAS J1120: 2 x10^9 $M_\odot$ at z = 7.08
- SDSS J0100: 1.2 x10^{10} $M_\odot$ at z = 6.30

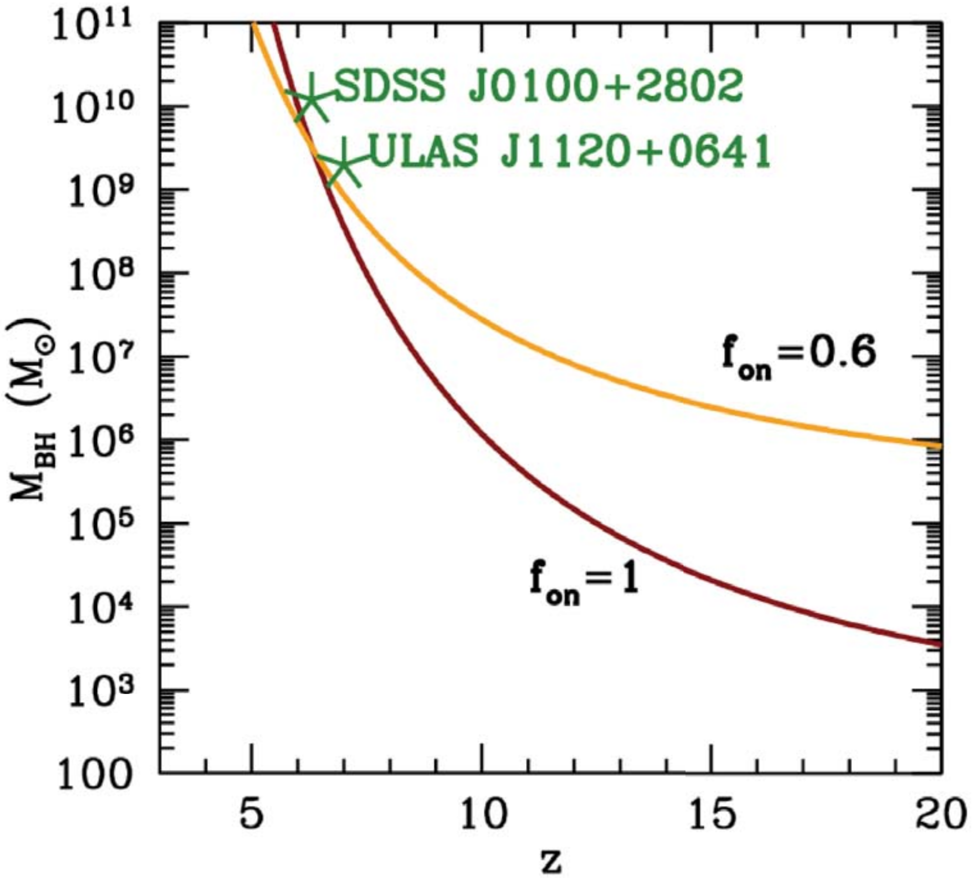

- Need to grow at the Eddington limit for the whole time (M_0 ~ 3000 $M_\odot$) or 60% of the time (M_0 ~ 10^5 $M_\odot$)

(By M. Volonteri)

SMBH seeds

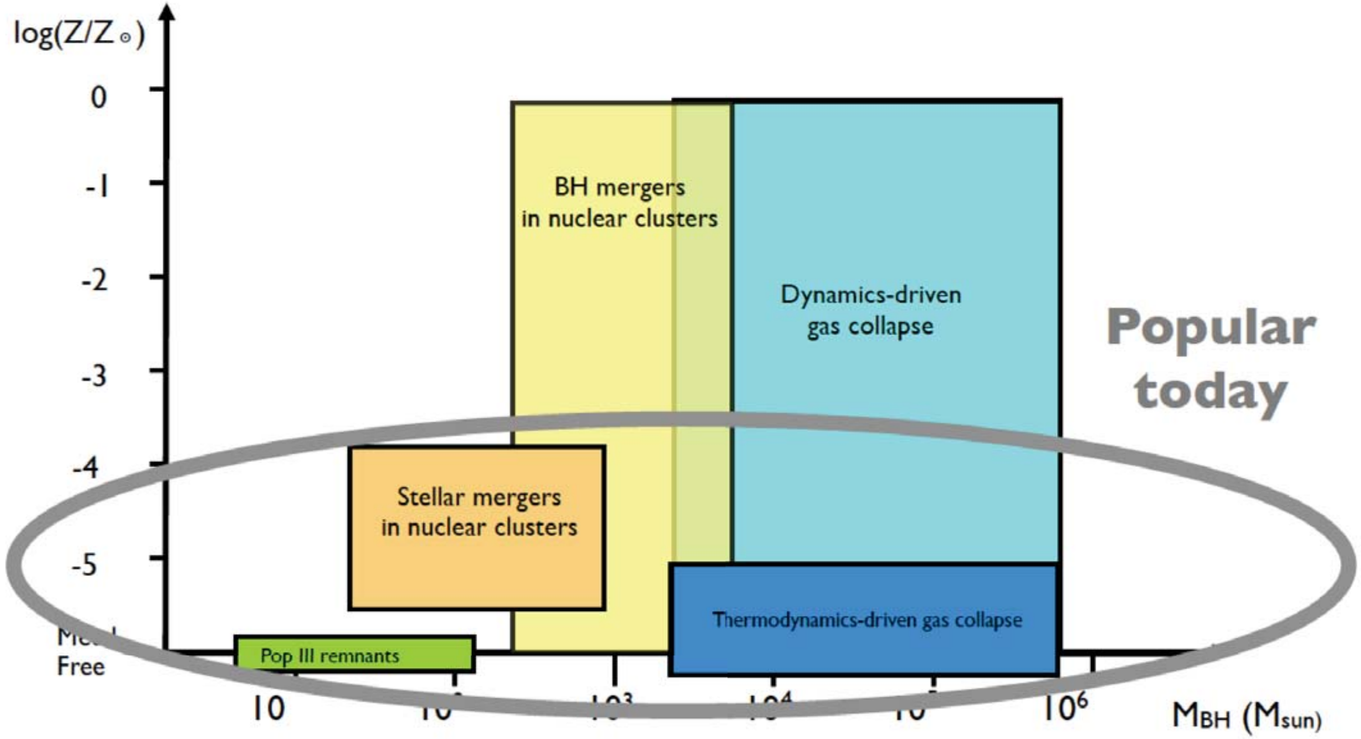

(By M. Volonteri)

Models:

- Stellar mass seeds: 1−100 $M_\odot$
- Seeds from star clusters: $10^3 - 10^4 M_\odot$
- Seeds from direct collapse of primordial gas: $10^4 - 10^6 M_\odot$
- Super-Eddington accretion (≠ Super-Eddington luminosity)

(Refs: Haiman 2000; Heger 2003; Begelman 2006; Latif 2013, 2016; Volonteri 2005)

Direct collapse model

- Currently preferred model by numerical simulations
- Direct collapse of primordial clouds → ≥ $10^5 M_\odot$ BHs
- Isothermal collapse with T ~ 8000 K
- Large inflow rate ~ 1 $M_\odot$/yr found in simulations (>0.1 $M_\odot$/yr required)
- Requires strong Lyman-Werner radiation to quench H_2 formation (like PopIII stars)

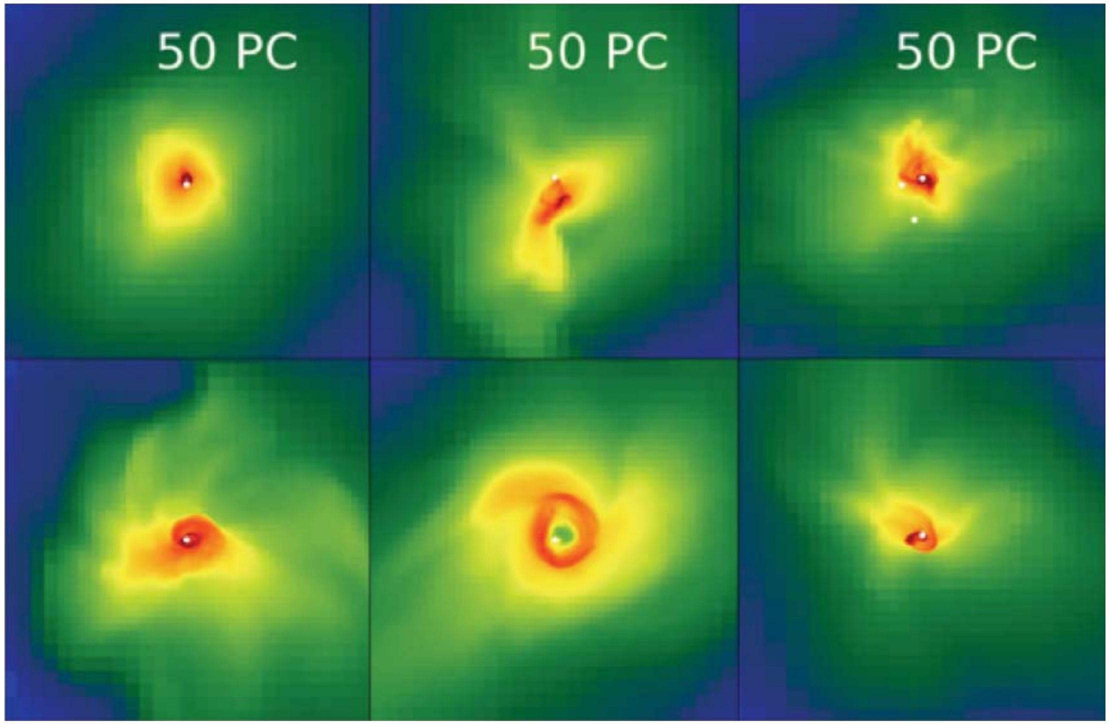

(Latif et al. 2013, 2016)

BH-Host co-evolution

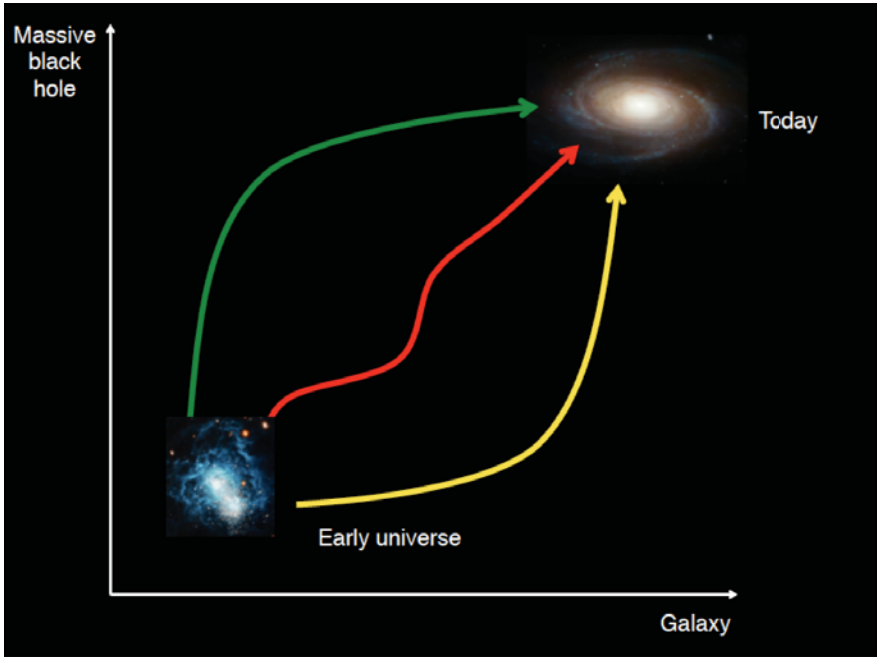

(By M. Volonteri)

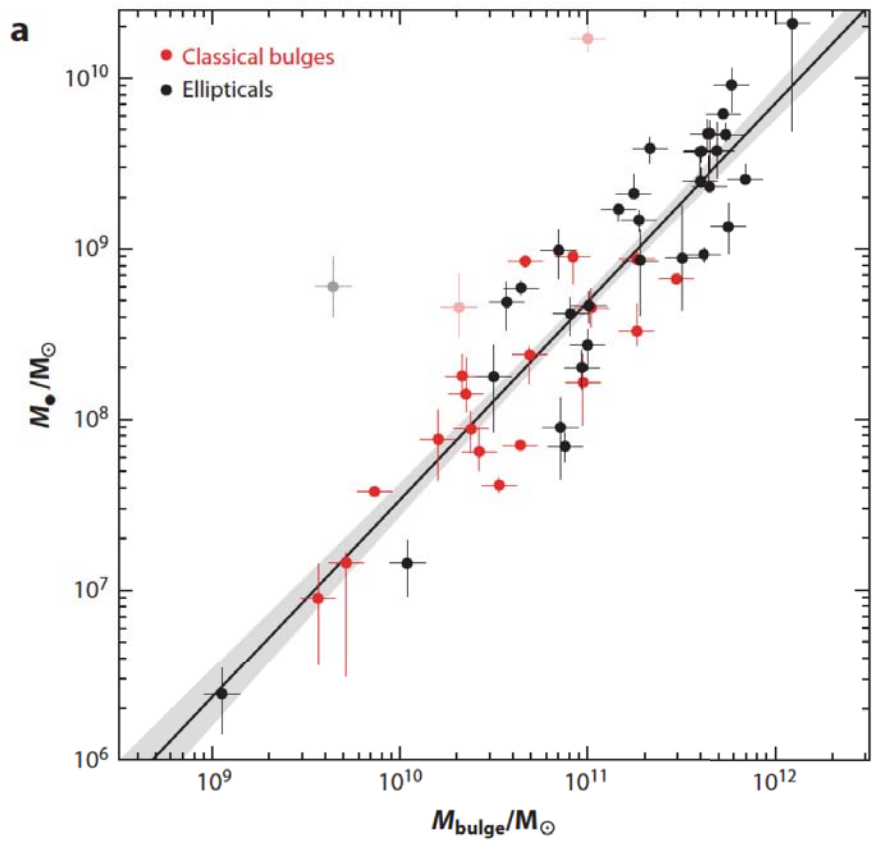

(Kormendy & Ho 2013)

黑洞和星系关系

$z \simeq 2-7$

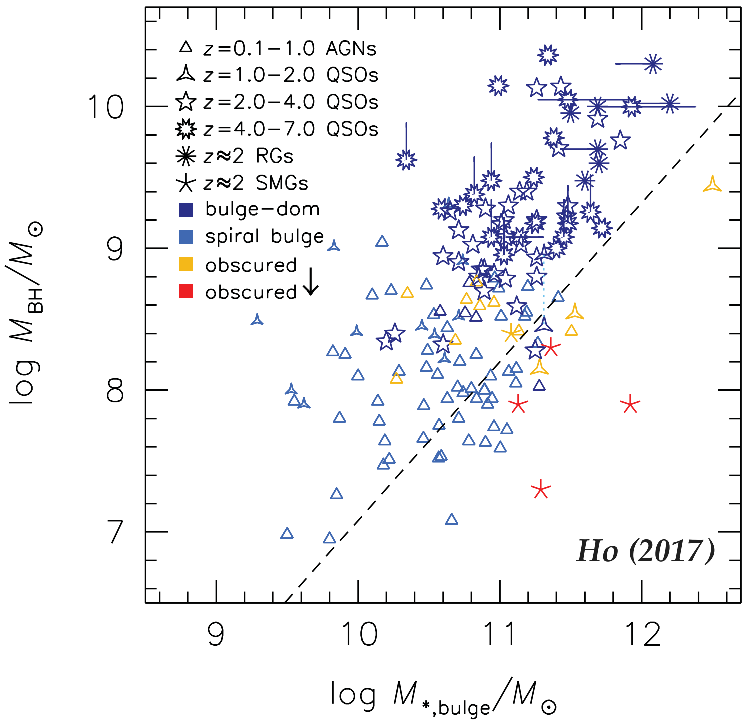

$z \simeq 0$

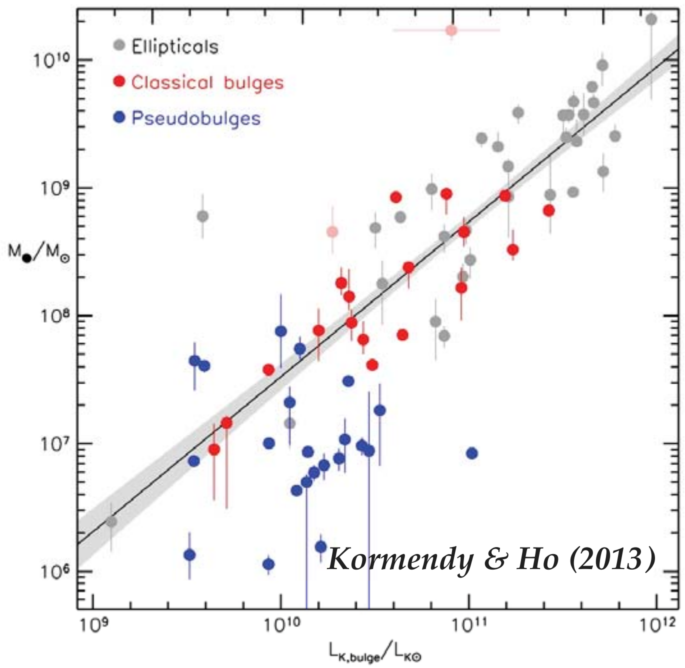

- 何时建立?
- 如何演化?
- 怎么形成?

❑ 亮点工作：ALMA揭示早期超大质量黑洞的增长

- 利用ALMA对高红移(z>6)类星体进行高精度高分辨率的[CII]观测
- 结合模型发现黑洞质量相对动力学质量比近场宇宙中的值高四倍
- 表明宇宙早期该类星体中黑洞增长先于其寄主星系的增长
- 被美国天文学会推荐为亮点文章 (AAS NOVA): http://aasnova.org/2017/09/06/alma-finds-hints-of-early-black-hole-growth/

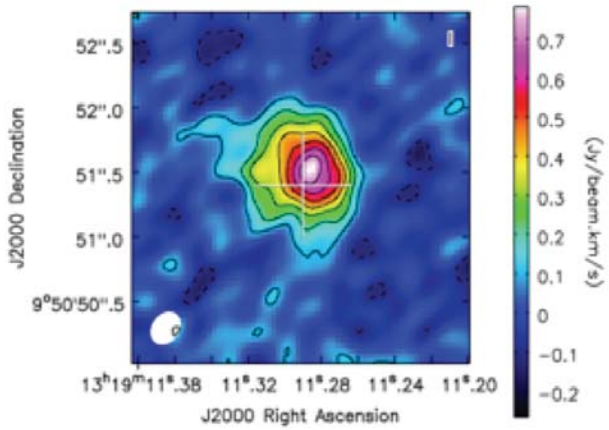

[C II] 强度图

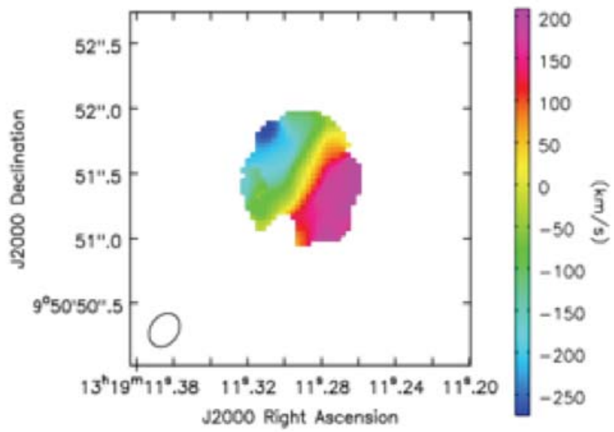

速度场

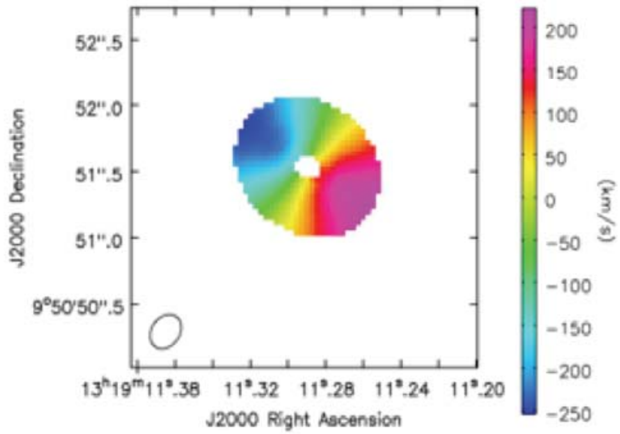

Tilted ring 模型

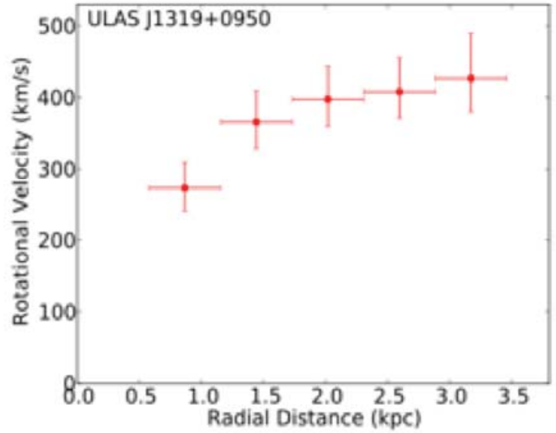

旋转曲线

(Shao, Wang, et al. 2017, ApJ, 845, 138)

❖ Probing reionization with high-z quasars

State of the IGM at z ≥ 6:

Fraction of neutral H as a function of redshift

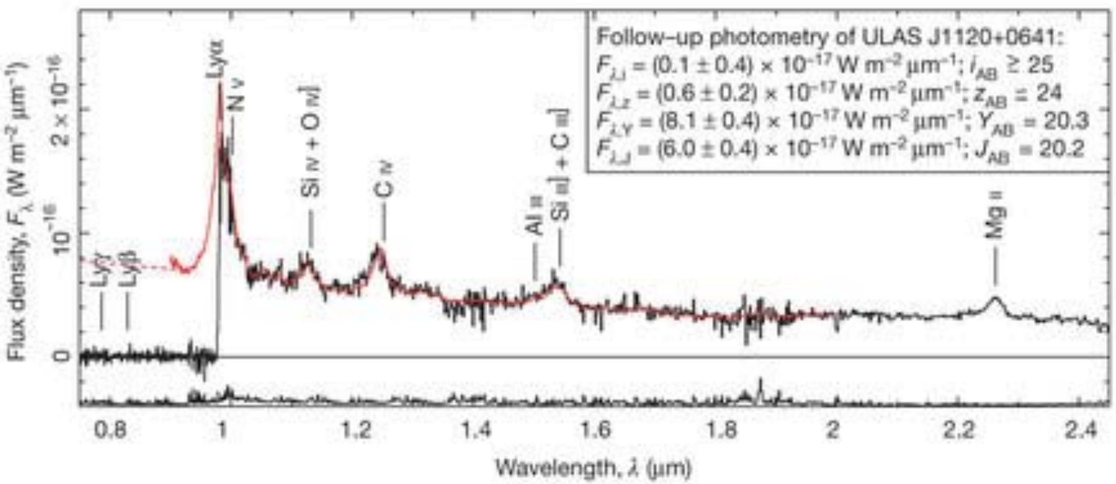

Lyα

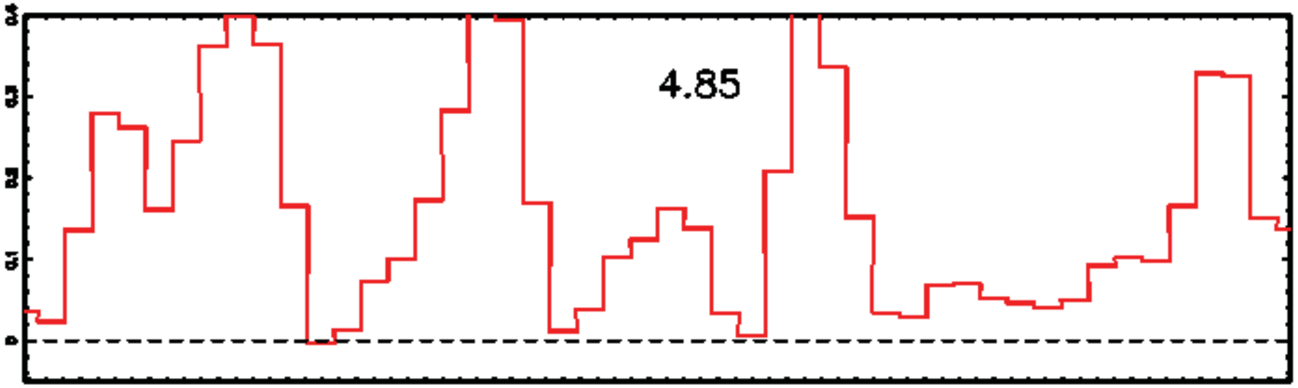

➢ State of the IGM at z~6

- Gunn-Peterson trough: Lyα forest absorption

3.1. Gunn-Peterson Effect: Basics

The Gunn-Peterson (1965) optical depth to Lyα photons is

$$\tau_{\mathrm{GP}} = \frac{\pi e^2}{m_e c} f_\alpha \lambda_\alpha H^{-1}(z) n_{\mathrm{HI}}, \quad (1)$$

where f_α is the oscillator strength of the Lyα transition, $\lambda_\alpha = 1216$ Å, $H(z)$ is the *Hubble* constant at redshift z, and n_{HI} is the density of neutral hydrogen in the IGM. At high redshifts,

$$\tau_{\mathrm{GP}}(z) = 4.9 \times 10^5 \left(\frac{\Omega_m h^2}{0.13}\right)^{-1/2} \left(\frac{\Omega_b h^2}{0.02}\right) \left(\frac{1+z}{7}\right)^{3/2} \left(\frac{n_{\mathrm{HI}}}{n_{\mathrm{H}}}\right) \quad (2)$$

(Fan et al. 2006)

First detection of complete G-P troughs

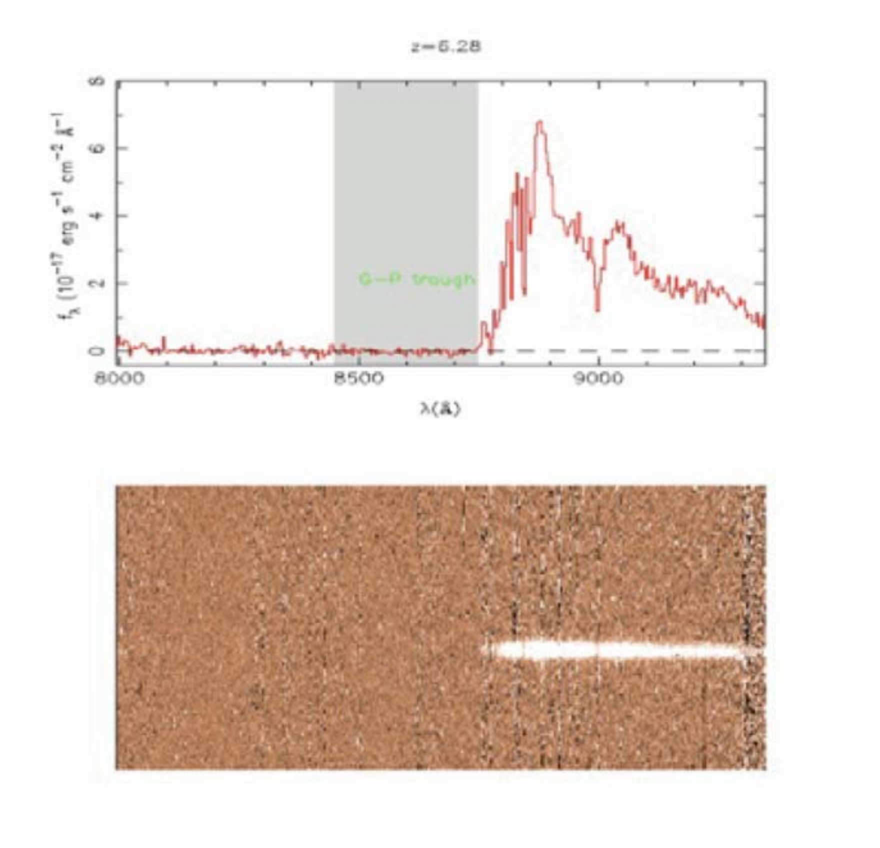

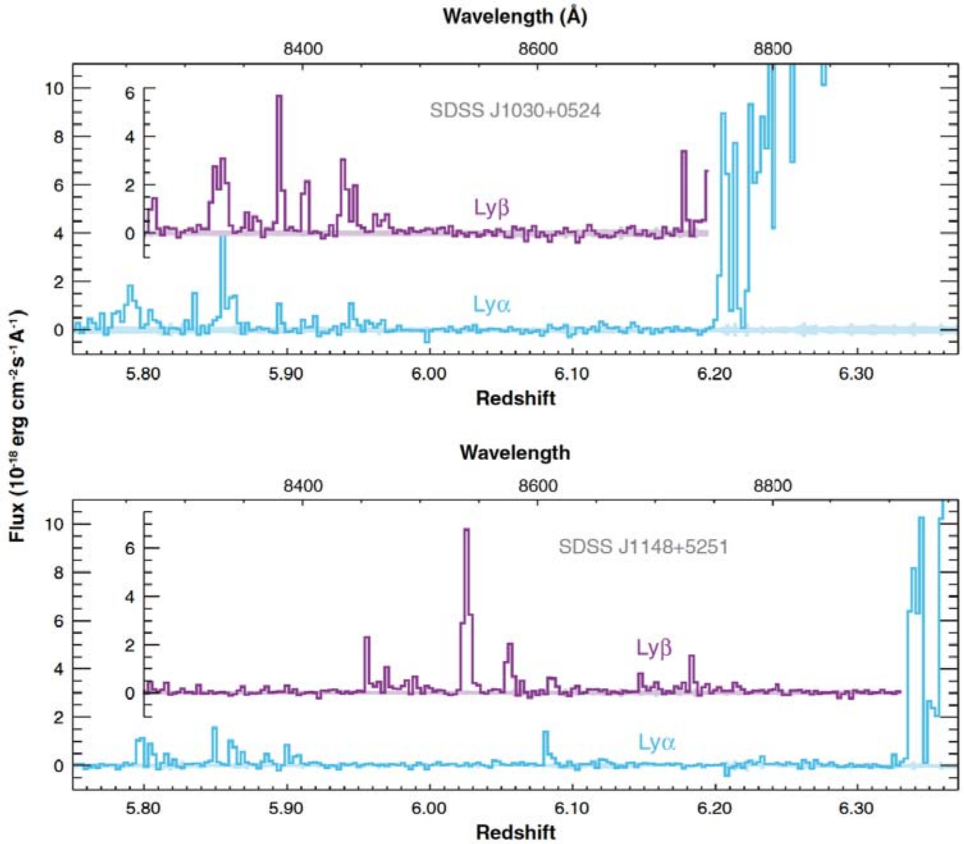

(Fan et al. 2006)

G-P optical depth: $\tau_{GP} = -\ln(f_{obs}/f_{con})$

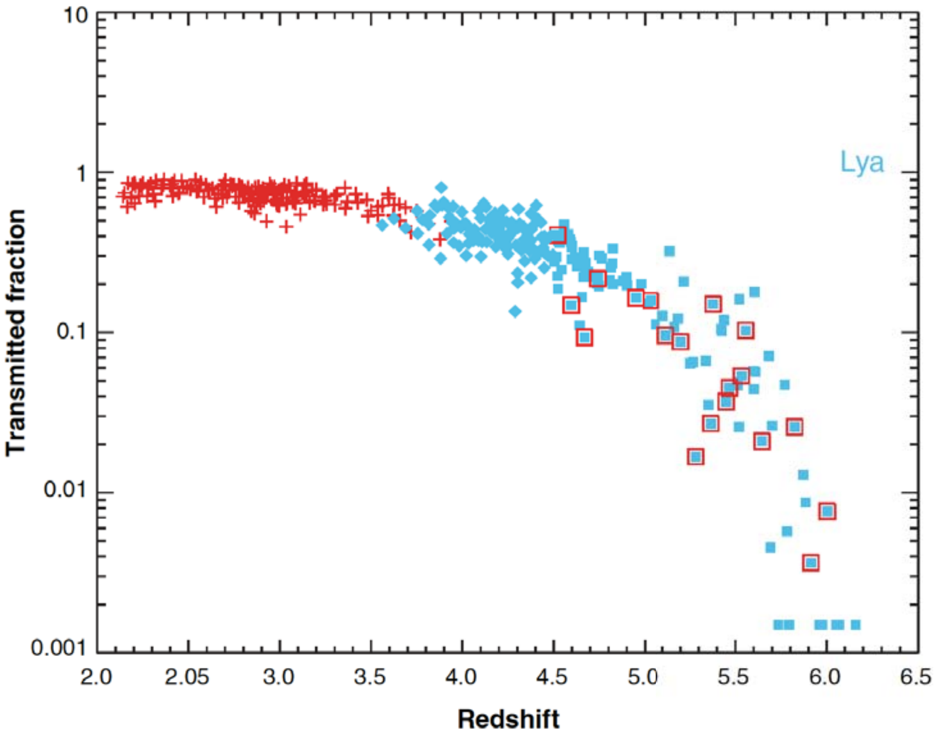

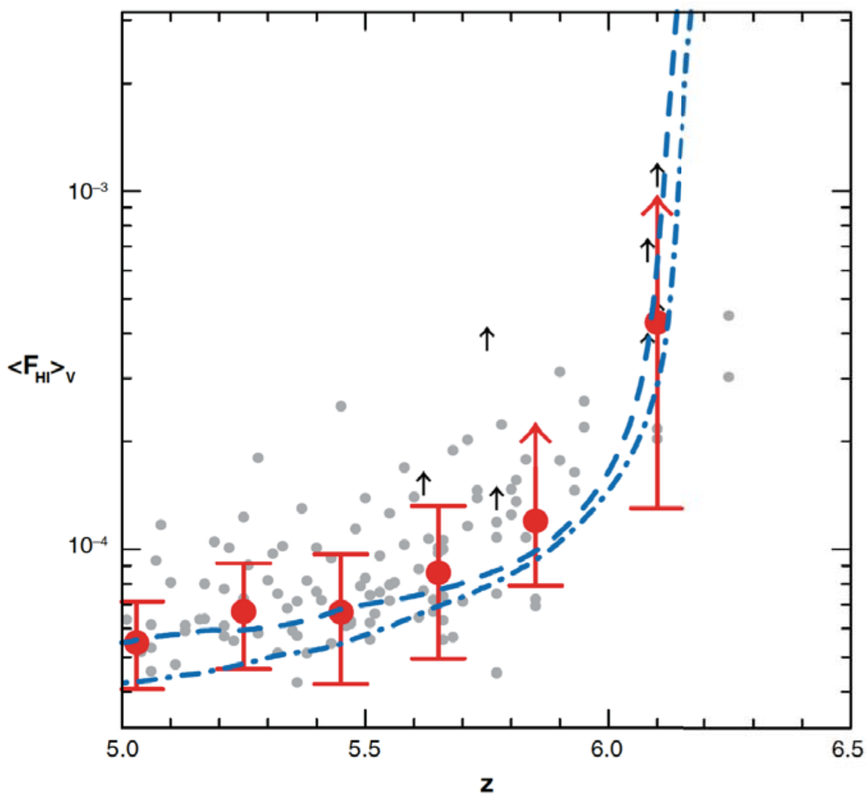

(Fan et al. 2006)

Reionization is not isotropic

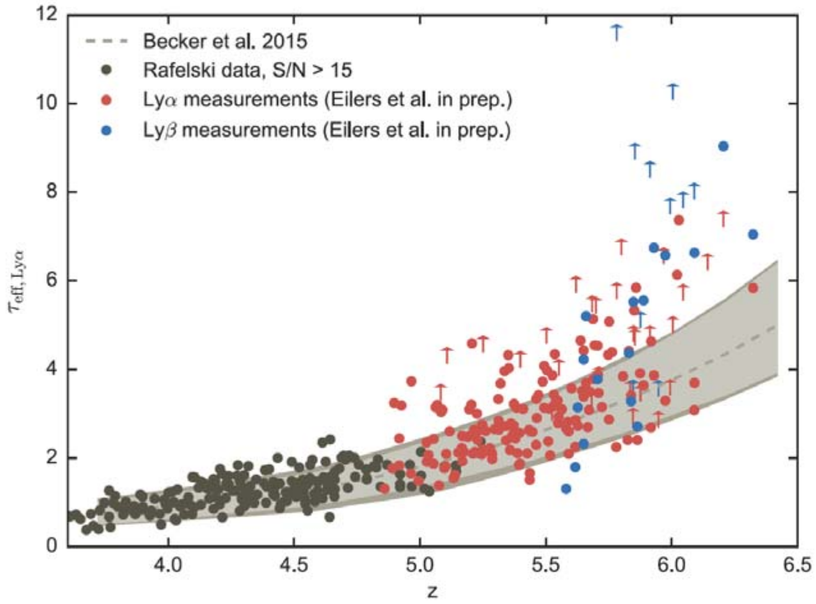

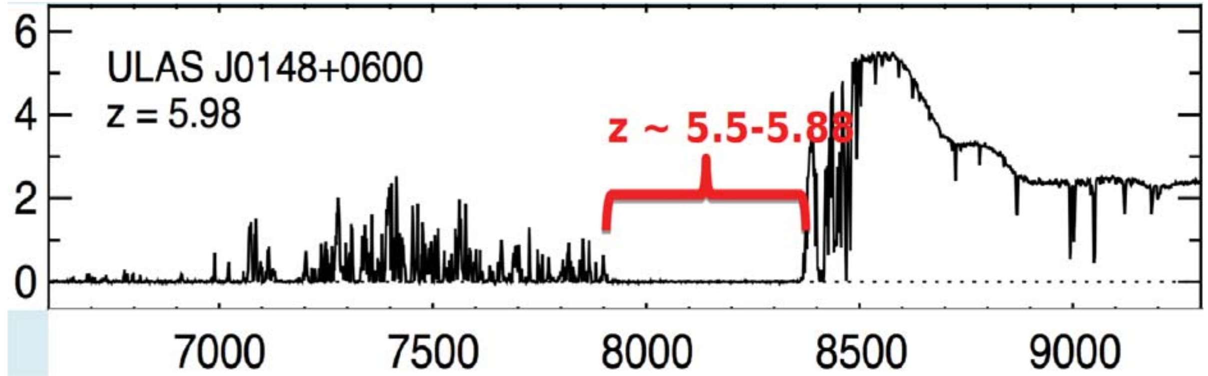

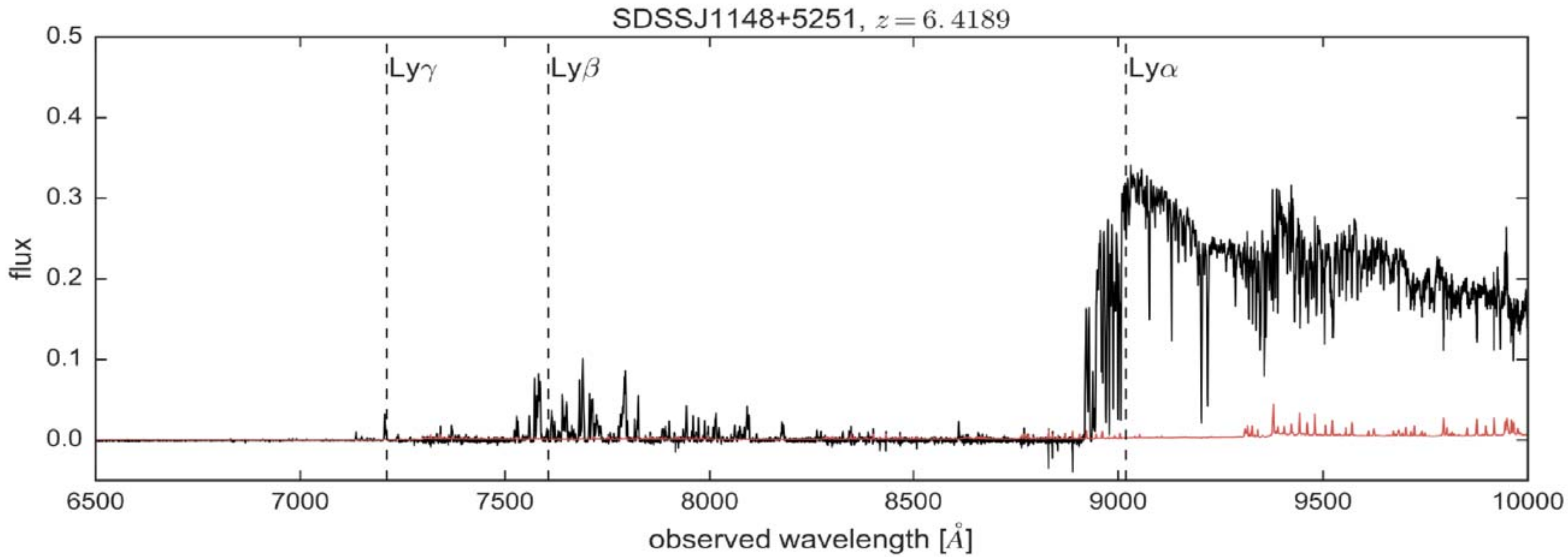

(refs: Becker et al. 2015; Davies's presentation 2016)

➢ Distributions of dark gaps

- Distributions of dark gaps, defined as regions in the spectra where all pixels have an observed optical depth larger than 2.5 for Lyα transition

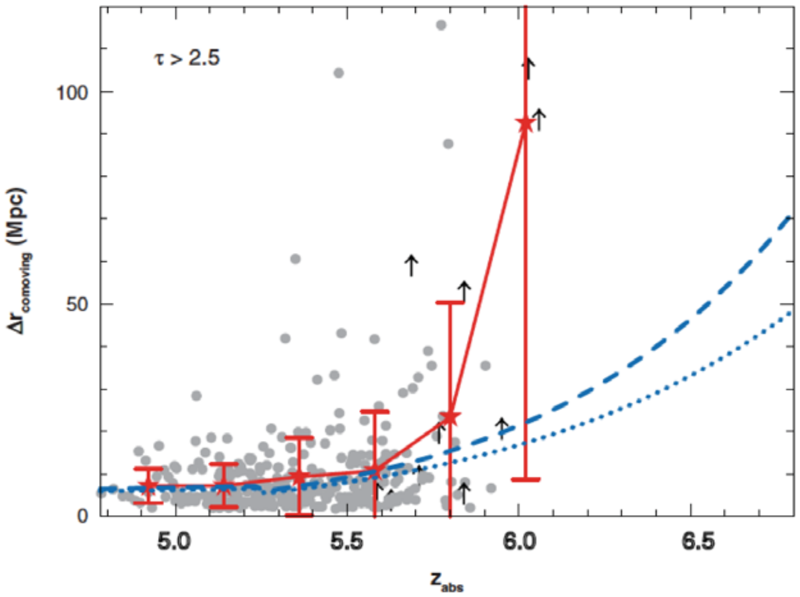

(Fan et al. 2006)

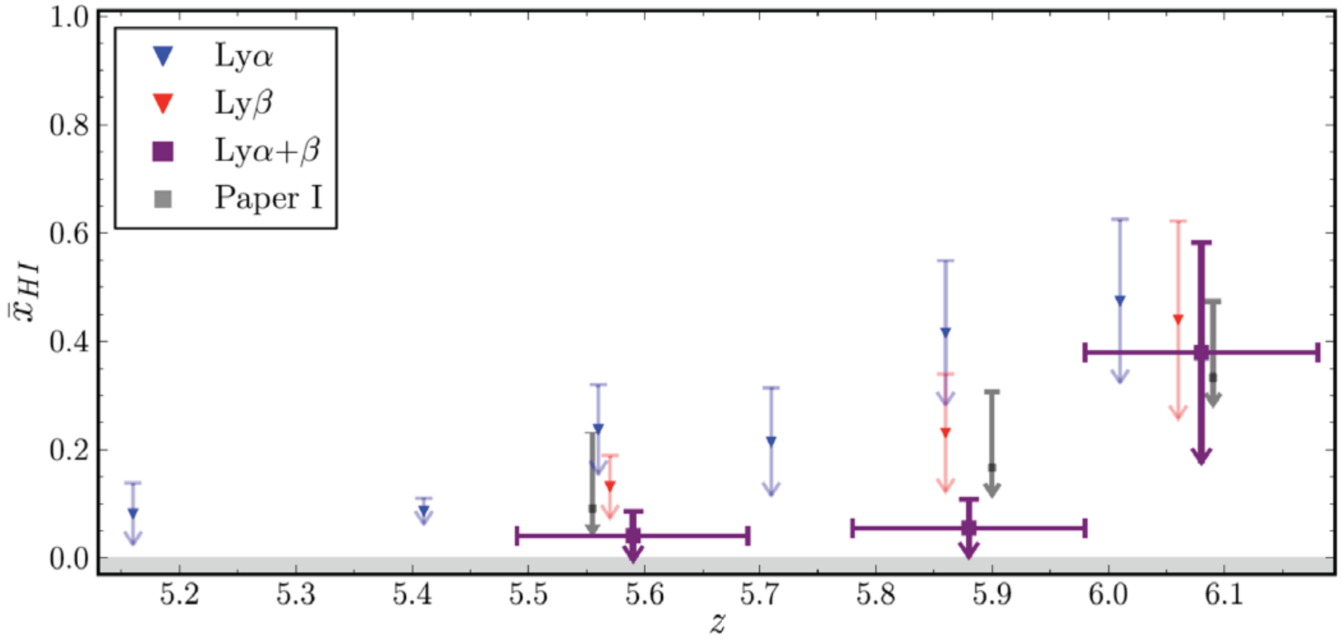

(McGreer et al. 2015)

❖ Near-zone effect, or proximity effect

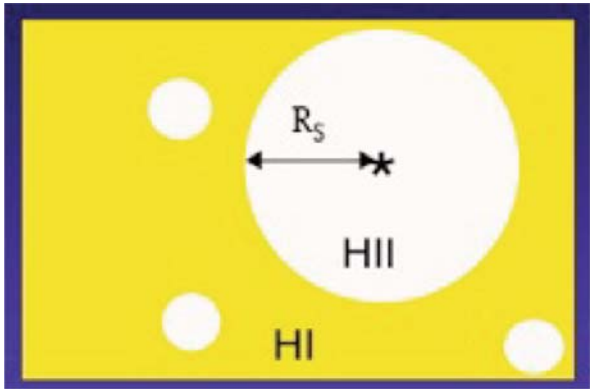

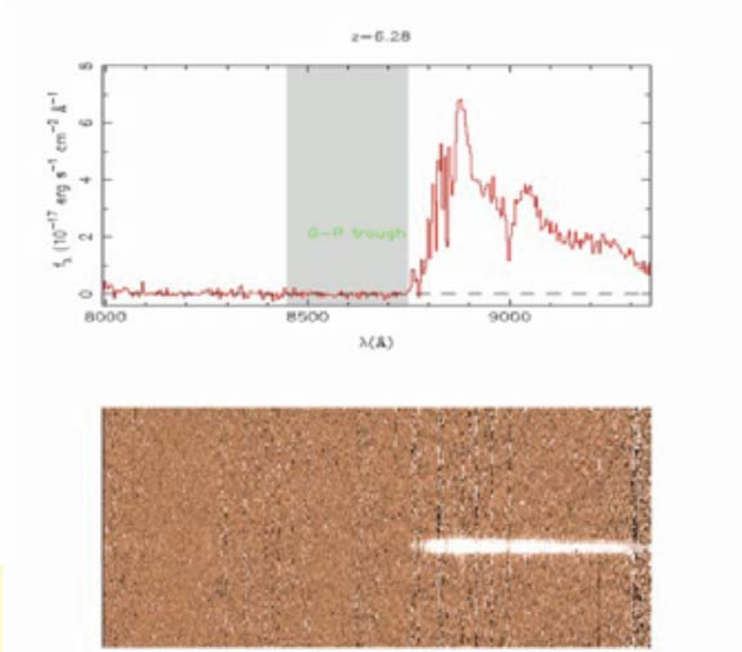

- Size of HII region

$$R_s \sim (L_Q\, t_Q \,/\, f_{HI})^{1/3}$$

- **near-zone size evolution consistent with rapid increase of neutral fraction at z>6**
- **Can be applied to higher z and f_{HI} with lower S/N data**

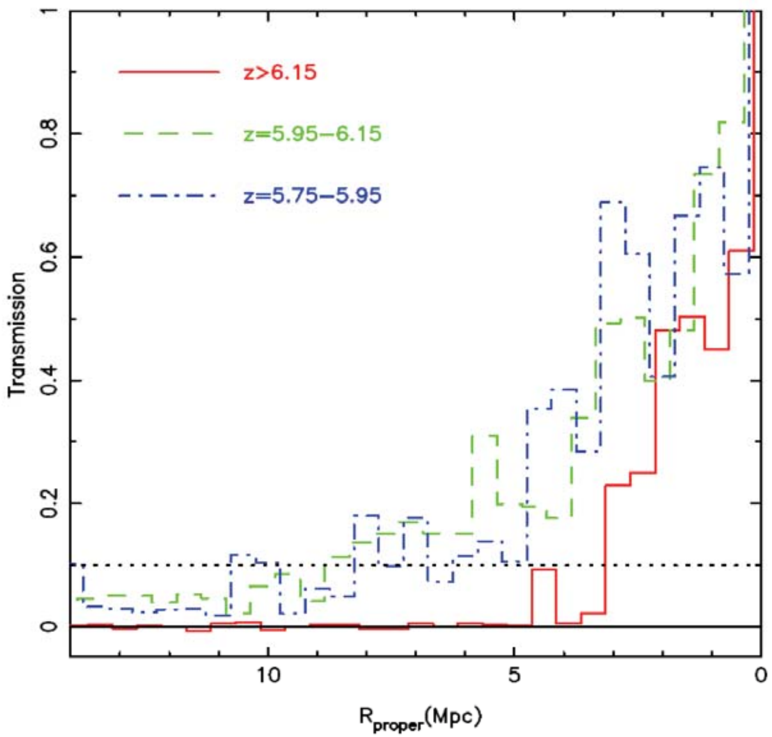

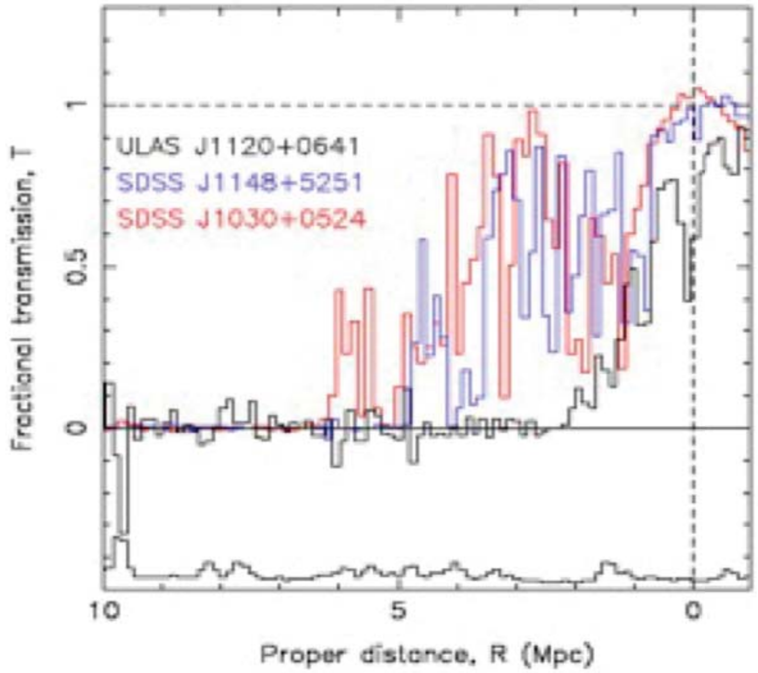

(Mortlock et al. 2011)

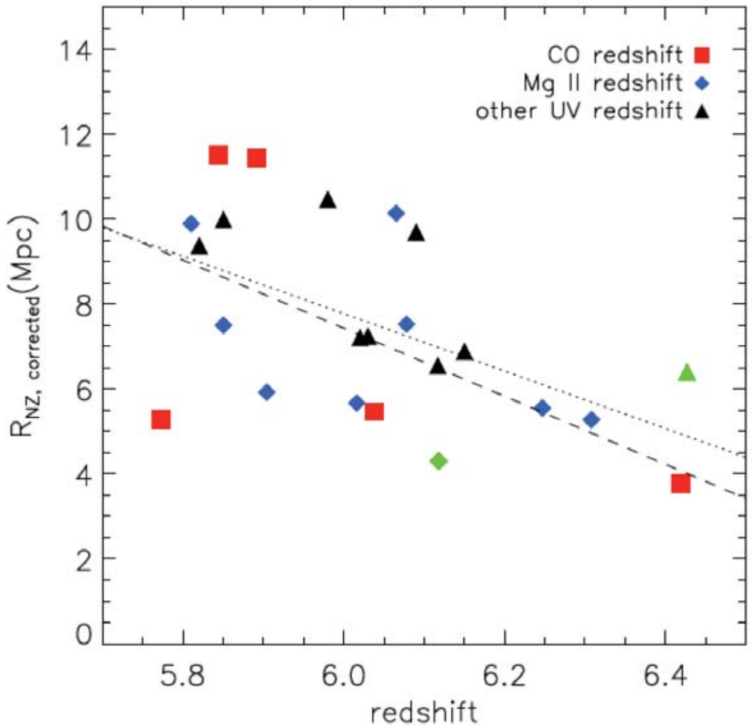

Alternatively, due to the rapid increase in the background photo-ionization rate?

(Carilli et al. 2010)

Lyα absorption damping wings

- IGM is very neutral: high column densities lead to significant absorption in the ‘wings’

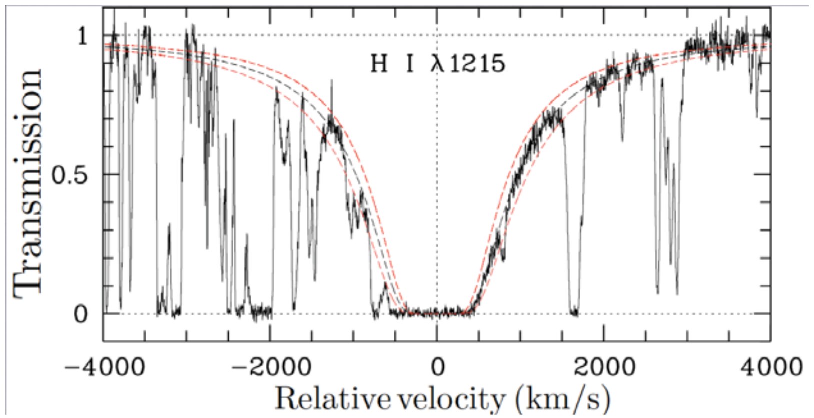

(Noterdaeme et al. 2007)

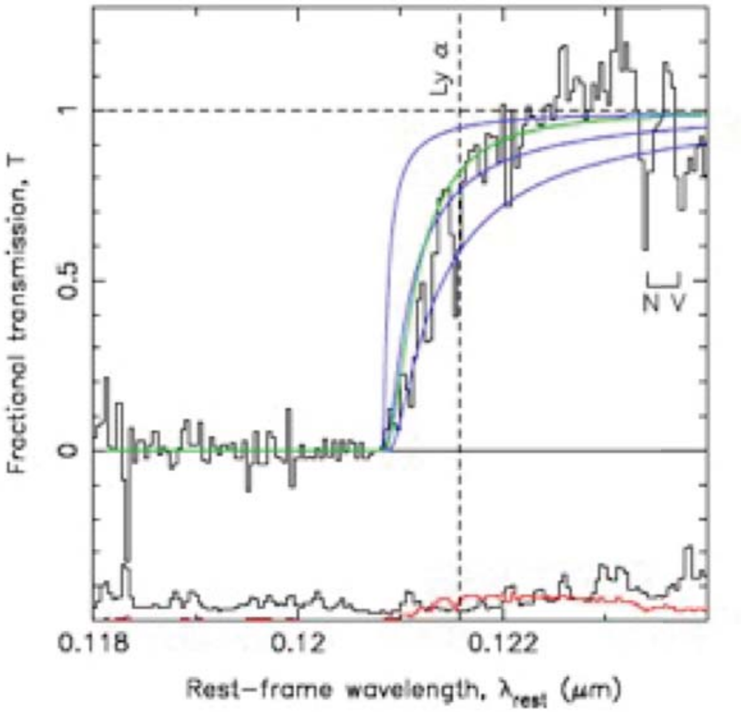

(Mortlock et al. 2011)

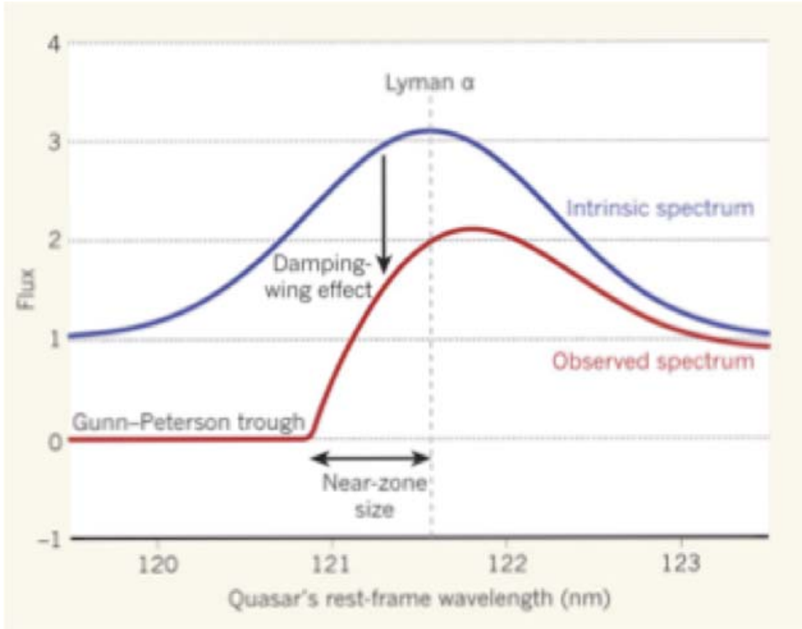

(Willott et al. 2011)

<x(HI)>~0.48+/0.27

at z=7.09

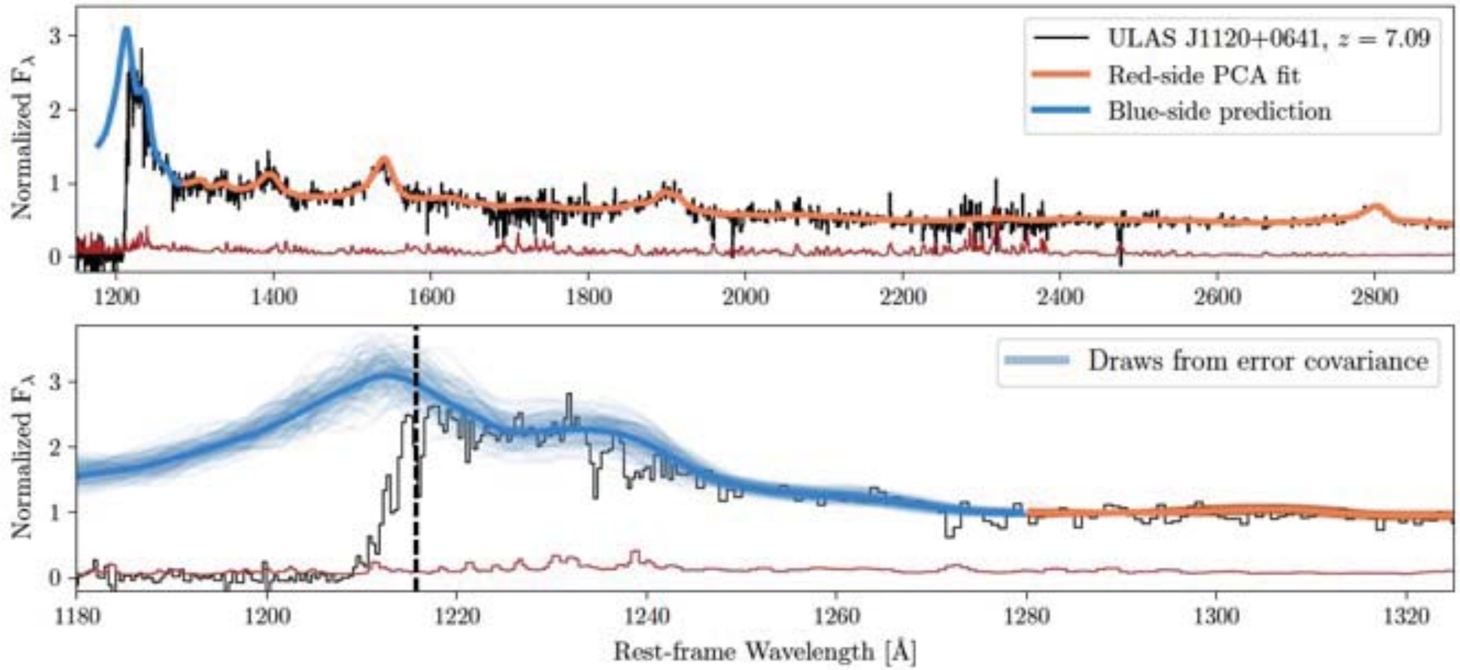

<x(HI)>~0.60+/0.22

at z=7.54

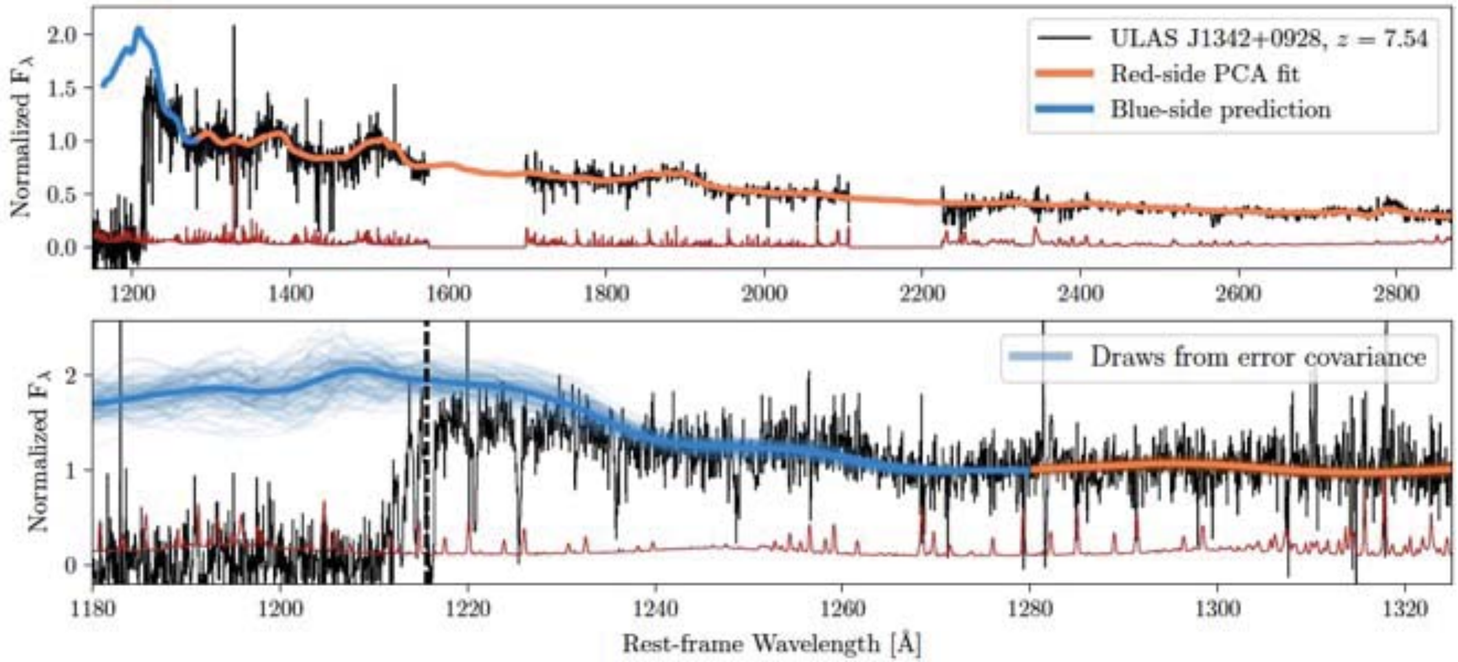

(Davies et al. 2018)

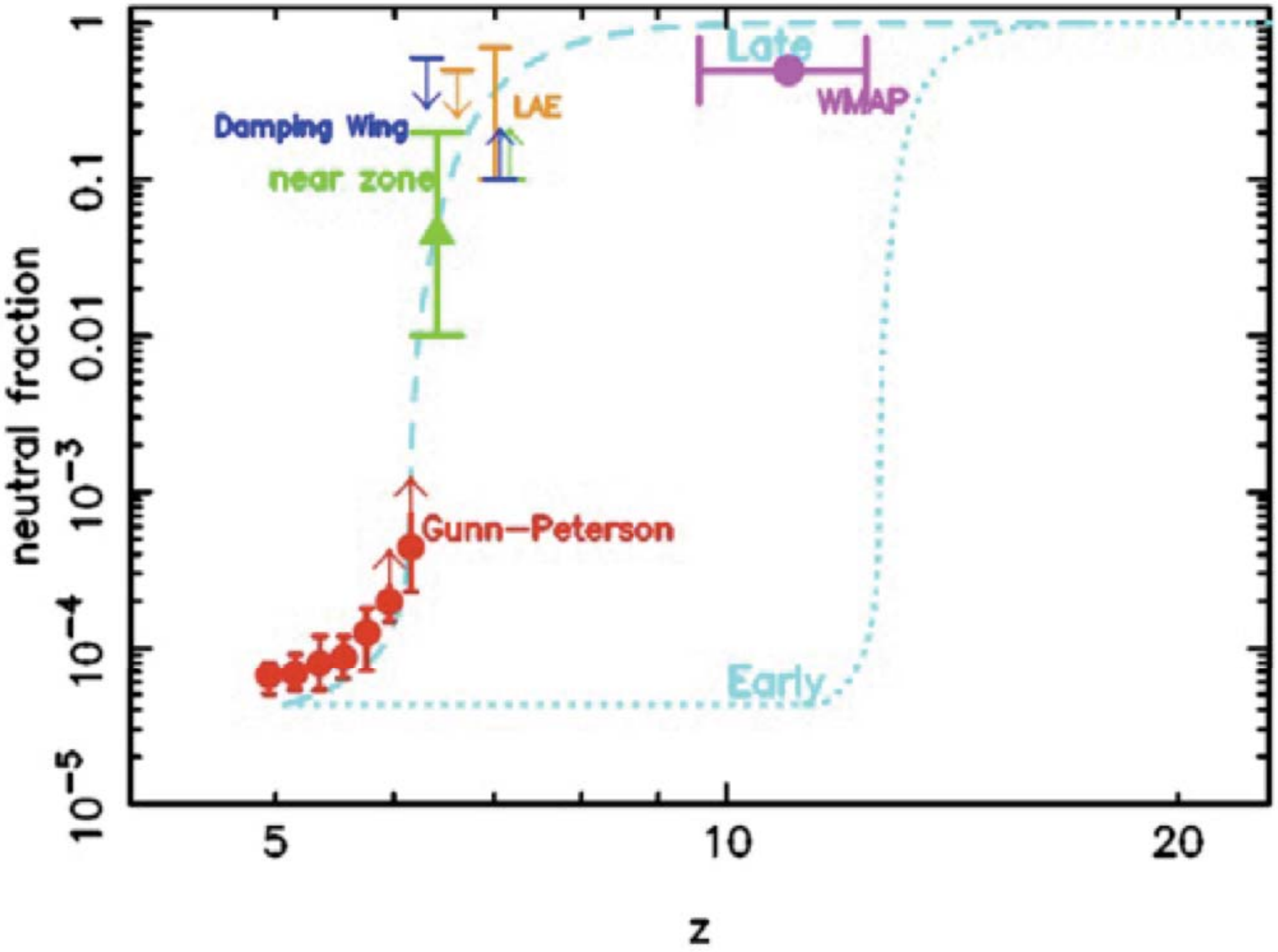

(By Xiaohui Fan)

High-redshift Galaxies at $z \geq 6$

➢ Galaxies at z ≥ 6 are faint and small

z ~ 0 galaxy, 1 min int. with SDSS

4'

SPITZER
SPACE TELESCOPE

SUBARU
National Astronomical Observatory of Japan
8.2m

29 hr int. with Subaru (z band)

4 hr int. with Keck/DEIMOS

10''

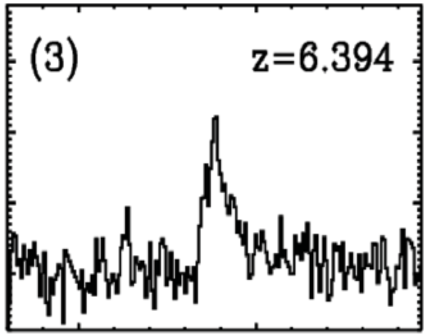

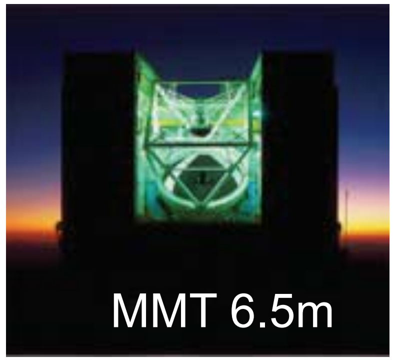

(Jiang et al. 2011)

➢ How to find these galaxies

- Drop-out technique
  → Lyman break galaxies (LBGs)
- Narrow-band technique
  → Lyman-α emitters (LAEs)

z = 3

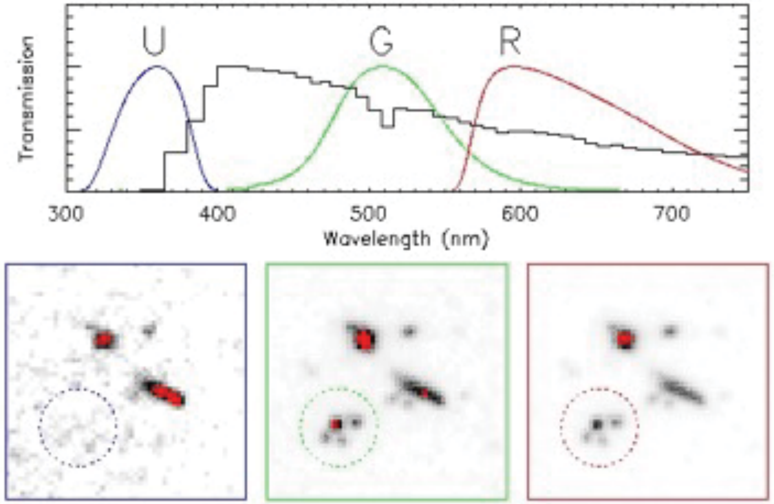

(Steidel 1993)

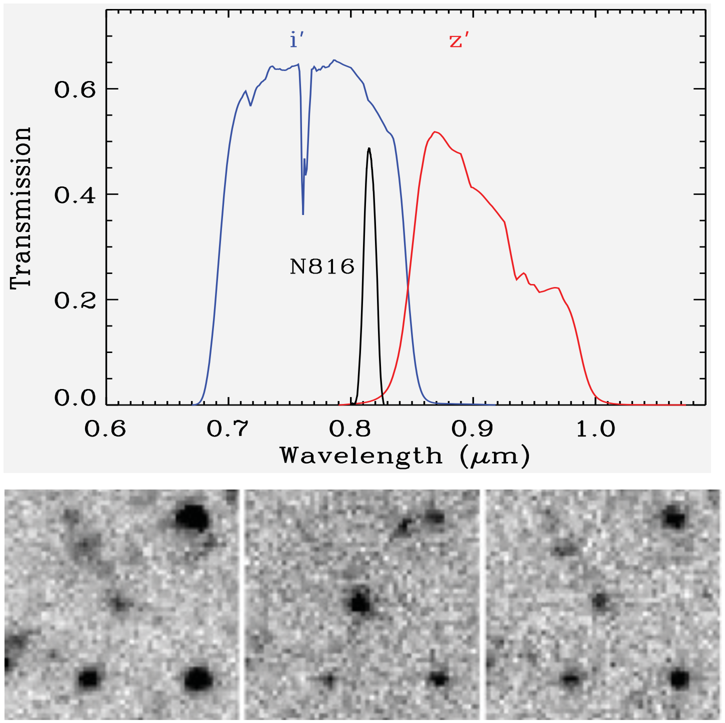

i N816 z

z = 6

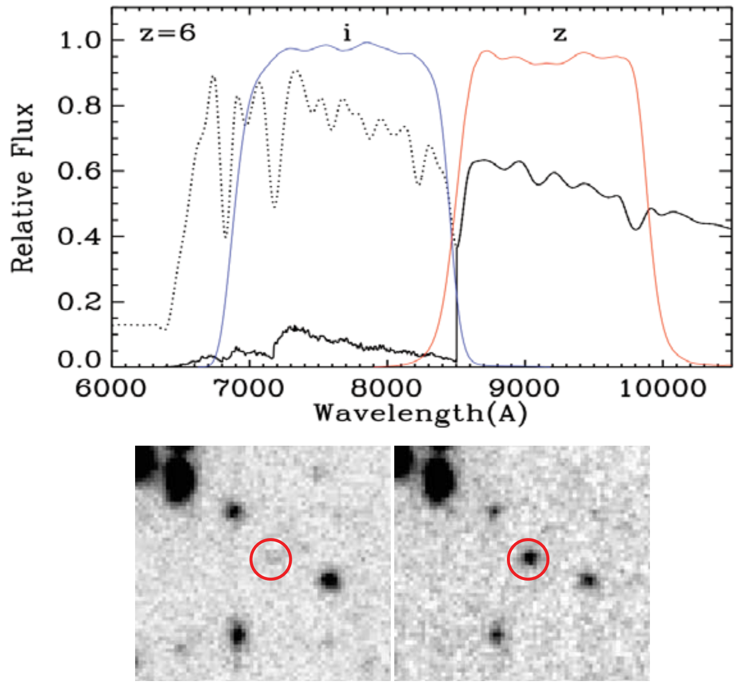

- A few examples of LAEs at z~5.7

(Jiang et al. 2018)

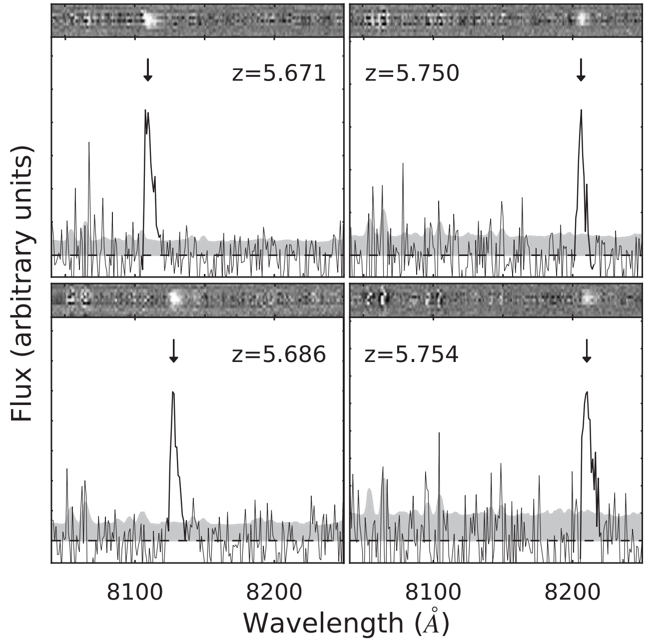

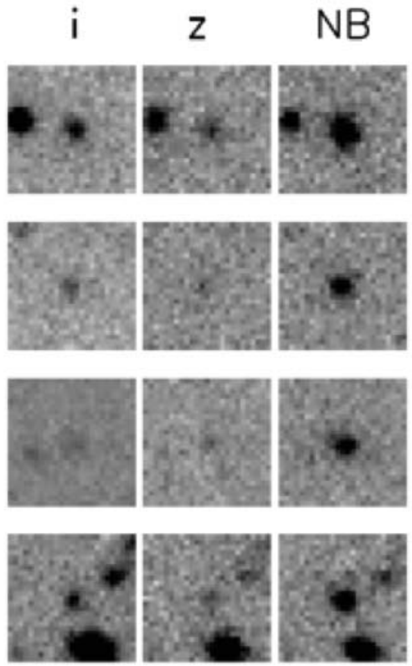

- Most galaxies do not have Lyα emission
  - Intrinsically no Lyα emission
  - Absorbed by neutral hydrogen

Lyα photons:
Resonant Scattering

UV/optical photons:
Absorption/Escape

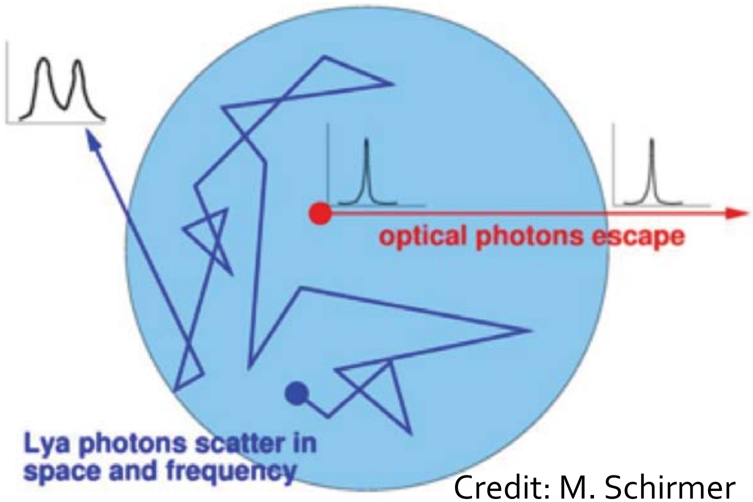

Credit: M. Schirmer

❑ Night sky emission lines and high-redshift LAE searches

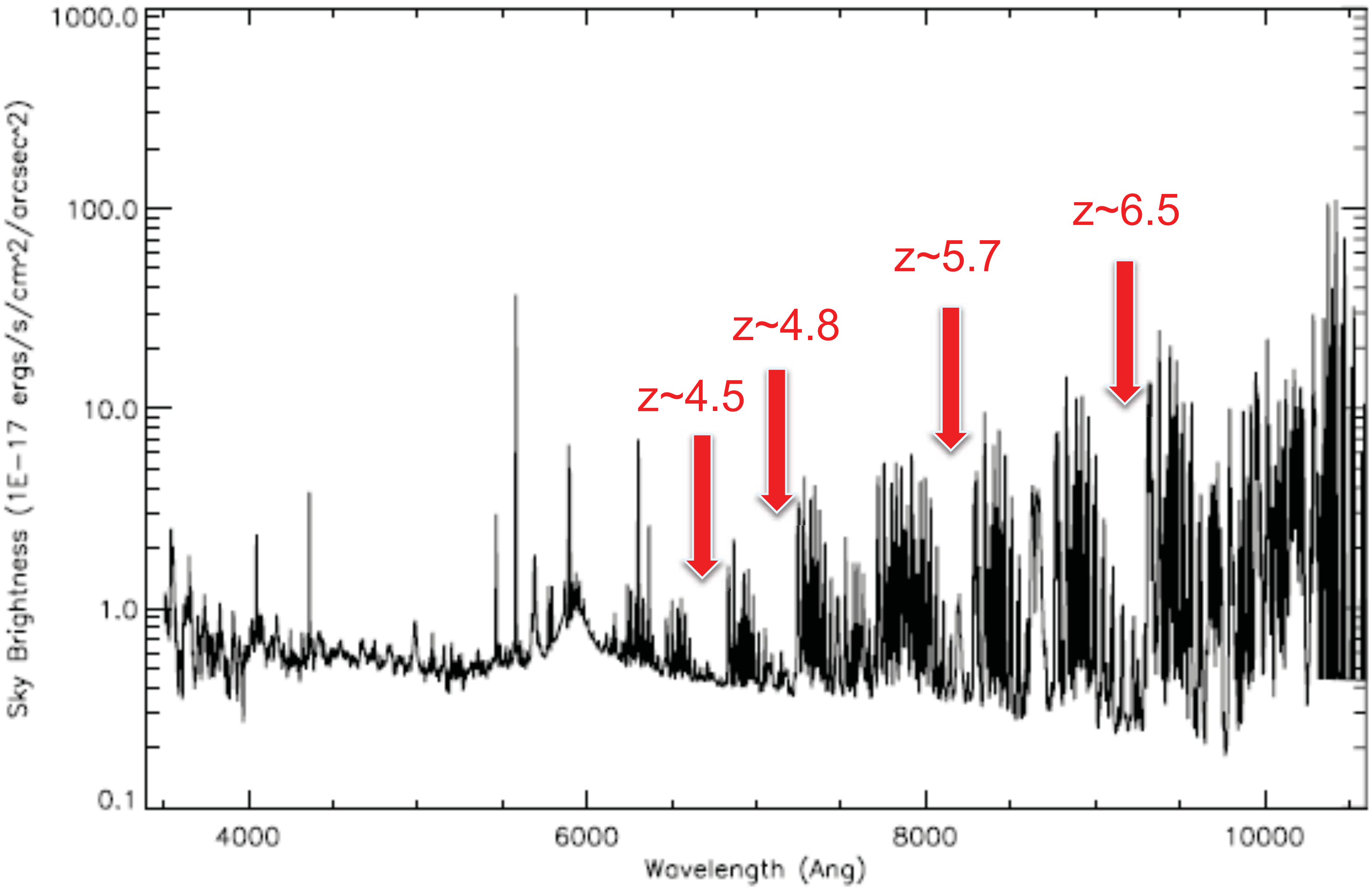

❑ Surveys of LAEs from z～1 to 7

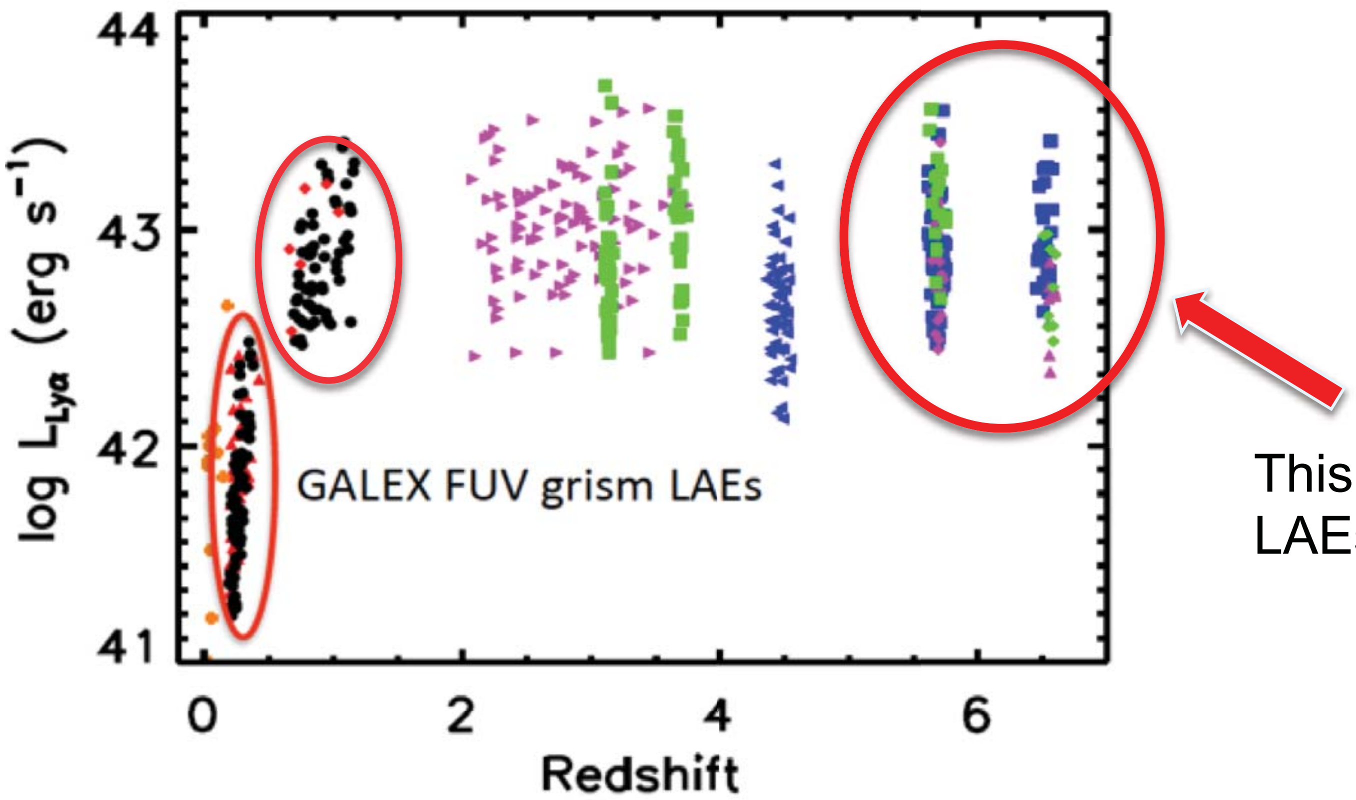

This study:
LAEs at z ~ 5.7, 6.5

- LAEs at 1<z<2 are mainly selected from GALEX grism observations
- LAEs at z>2 are mainly selected from ground-based narrow-band observations
- Most LAEs currently known at z>2 are photometrically selected candidates; spectroscopically confirmed samples are very limited

❖ Magellan M2FS survey of galaxies at 5.5 < z < 6.7

- Goal: build a large and homogeneous sample of bright LAEs (and LBGs) at 5.5 < z < 6.7
- Team (led by Jiang): PKU + Arizona + Carnegie + SHAO + ANU
- Fields: well-studied fields
  - Including COSMOS, SXDS, GOODS, SSA22, etc.
  - A total of ~ 3.5 deg^2
- Imaging data and targets
  - Subaru Suprime-Cam images in a series of broad and narrow bands
  - LAEs at z = 5.7 and 6.5; LBGs at 5.6 < z < 6.8; and many others
- Spectroscopy
  - Magellan M2FS
  - Roughly five hours per pointing

SUBARU National Astronomical Observatory of Japan

8.2m

Survey fields: well-studied fields

- Including COSMOS, SXDS, ECDFS, SSA22, A370, etc.
- Observing depth: ~ 5 hours per pointing

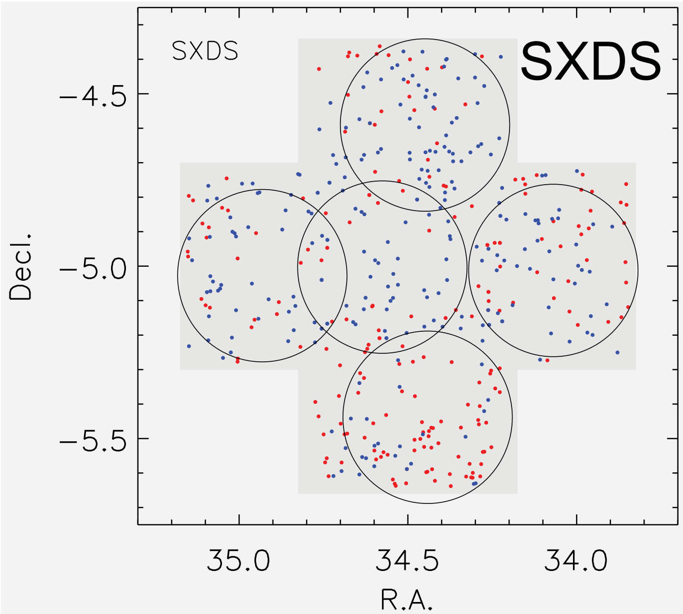

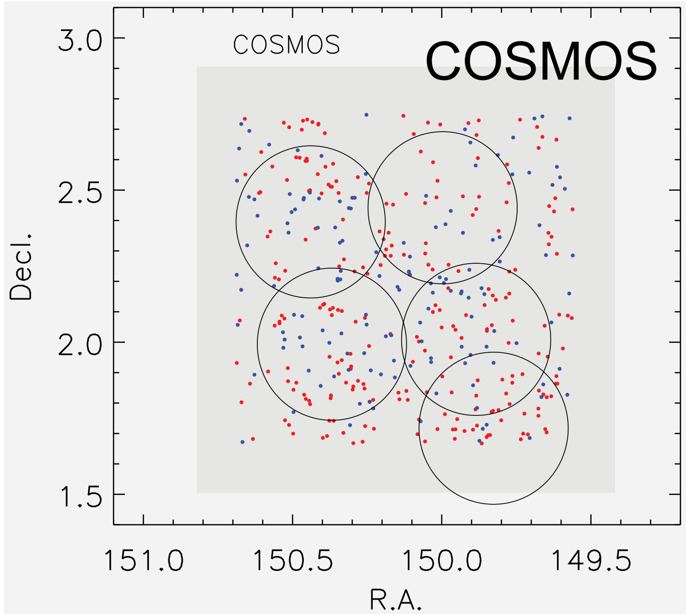

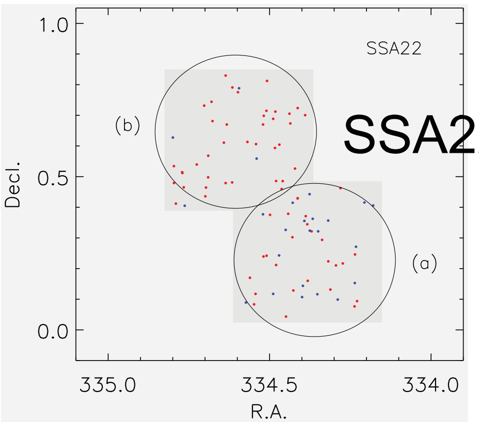

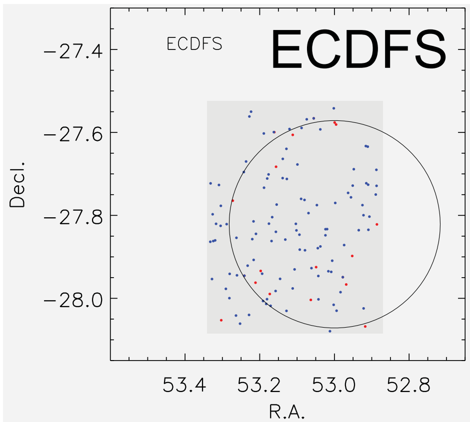

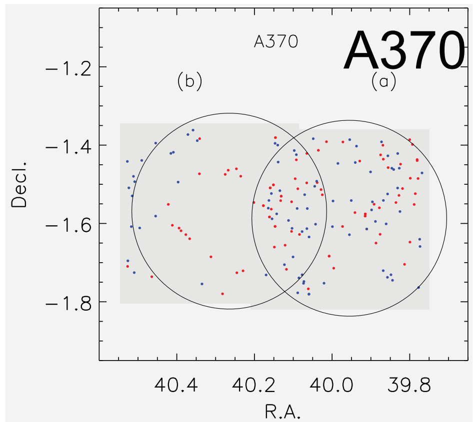

Imaging data for target selection

- Deep Subaru Suprime-Cam images in a series of broad and narrow bands
- Typical depths: BVRi~27.5 mag (all AB); z~26.5 mag; NB~25.5–26 mag

Targets

- LAEs at z ~ 5.7 and 6.5; LBGs at 5.5 < z < 6.7
- Many other targets in the same fields (we have 250 fibers)
- Narrow-band and dropout techniques

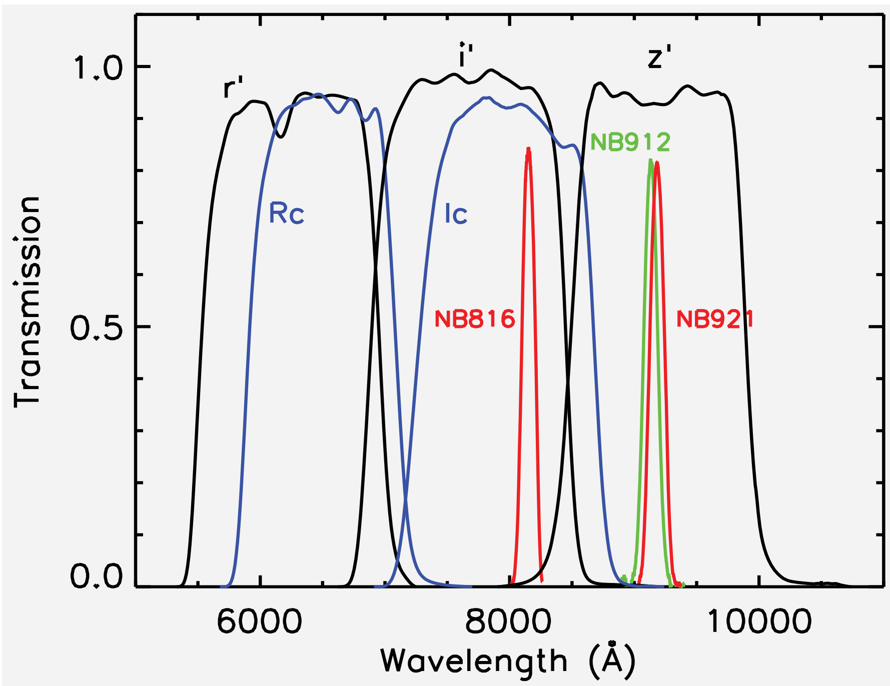

(Jiang et al. 2017)

❑ Spectroscopic observations

➢ Instrument: Magellan M2FS

- Fiber-fed, multi-object spectrograph on the Magellan Clay telescope
- 256 optical fibers
- A circular FoV of 30 arcminutes in diameter
- Low-R mode with red-sensitive gratings
- High throughput

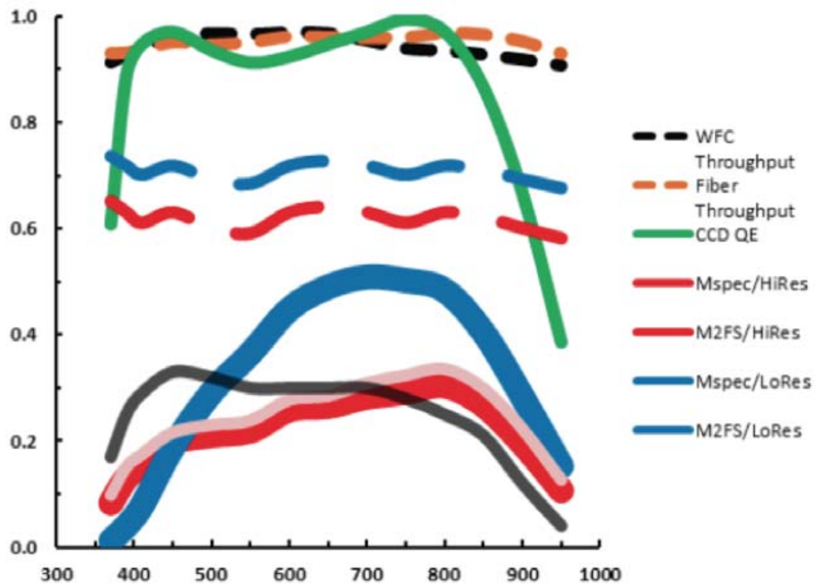

(Mateo et al. 2012)

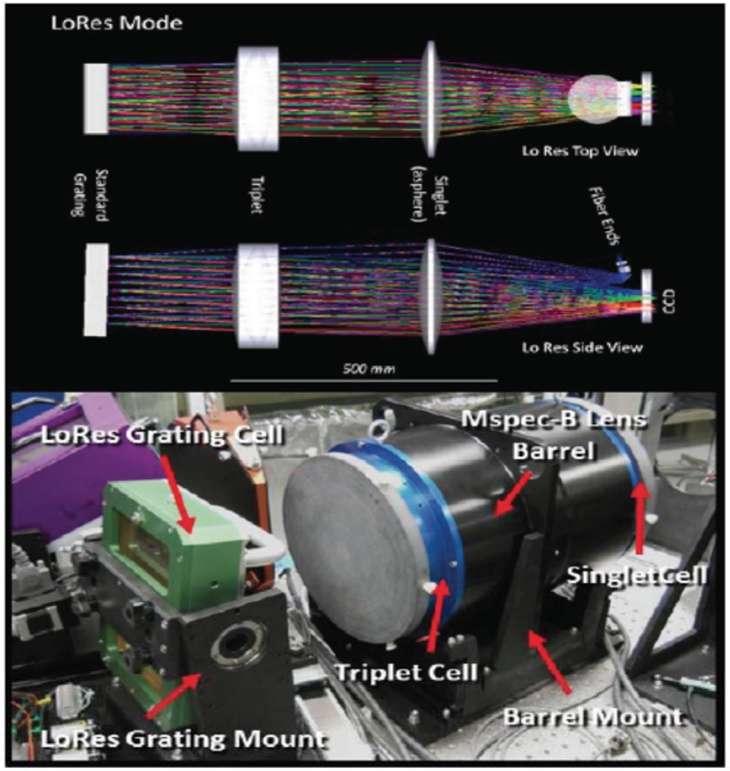

❑ Scientific goals

- A unique spectroscopically confirmed sample
  - Large area coverage (largest of its kind so far)
  - Same imaging data for target selection
  - Same target selection carried out by the same team
  - Same instrument for spectroscopic observations
  - Large number of fibers → highly complete

- Science goals (I): properties of high-z galaxies
  - Lyα LFs from a large spectroscopically confirmed sample
  - Physical properties and stellar populations (note the existence of numerous ancillary data in these deep fields)
  - Stacking images: Lyα emission halos, cool dust emission, etc.

- Science goals (II): understanding reionization
  - Evolution of Lyα LFs
  - Fraction of LBGs with strong Lyα emission
  - Patchy reionization: enhanced galaxy clustering
  - …

- Lyα LF at z=5.7
  - Lyα LF at z=5.7 is the benchmark of Lyα LF test in the epoch of reionization: little effect from IGM (ionized)

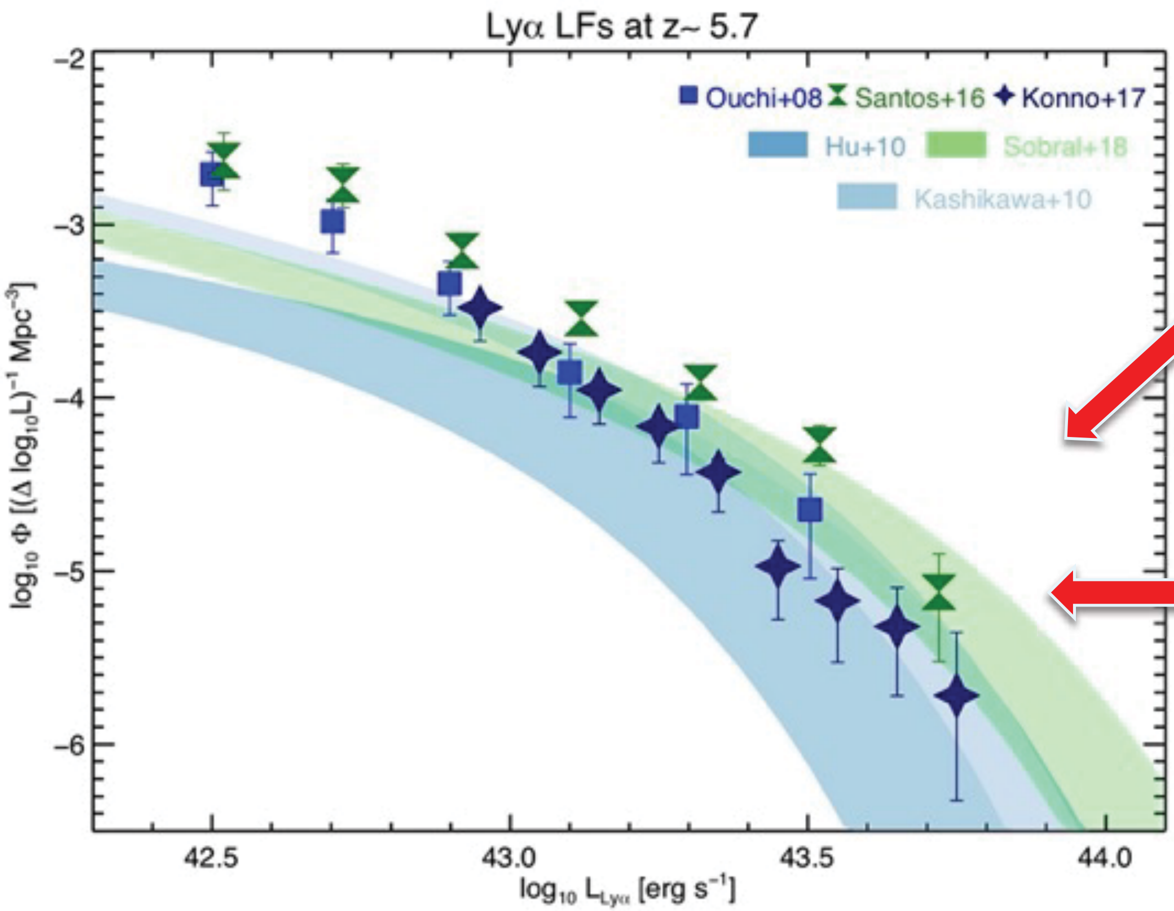

Previous studies were mostly based on photometrically selected LAEs

Large discrepancy of the z=5.7 Lyα LFs from previous studies

- Our current sample of LAEs
  - Largest spectroscopic sample: ~180 LAEs at z=5.7
  - Largest area coverage: ~2.5 deg^2

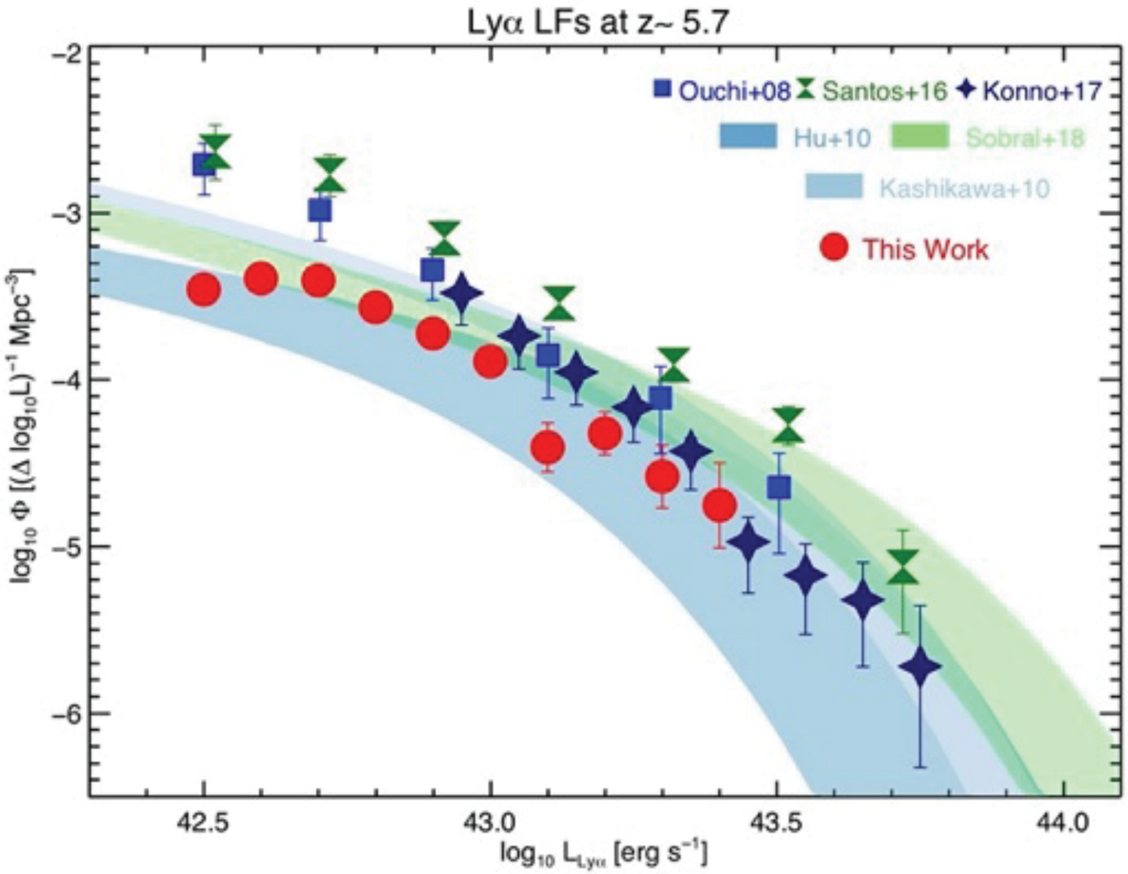

(Zheng, Jiang, et al. in prep.)

- To be completed
  - Lyα LF at z=5.7: ~2.5 deg^2 → ~3.5 deg^2
  - Lyα LF at z=6.5

❖ Preliminary results: Diffuse Lyα halos

- Lyα halos: caused by the resonant scattering of Lyα photons
- How to detect halos: stacking ground-based NB (Lyα) images
- At low redshift: mostly based on photometrically selected sample; controversial
- At high redshift: predicted by simulations

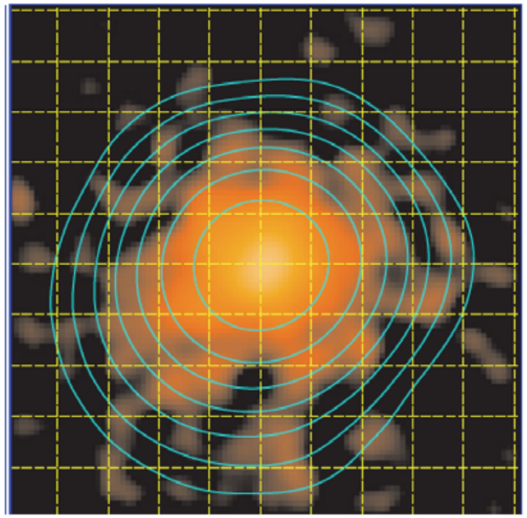

2 < z < 3 (Steidel 2011)

Lyα photons:
Resonant Scattering

UV/optical photons:
Absorption/Escape

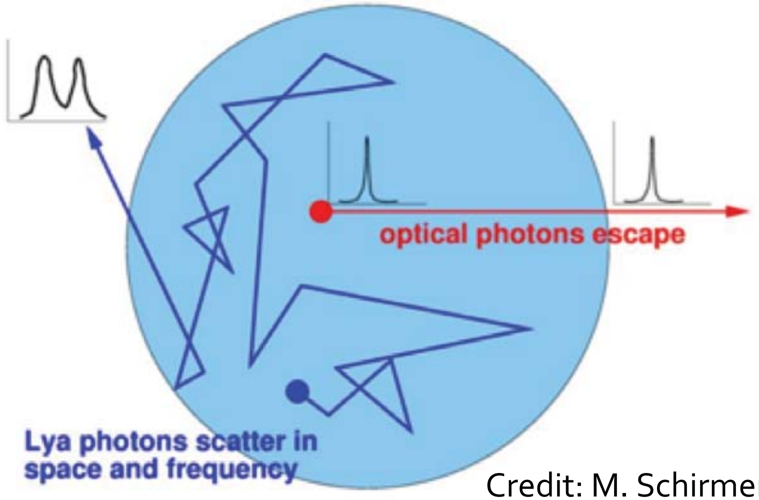

Credit: M. Schirmer

❖ Diffuse Lyα halos at z ~ 5.7

- Now we are stacking >300 spectroscopically confirmed LAEs at z ~ 5.7; Each LAE has 5~10 hr integration with Subaru Suprime-Cam

>300 LAEs

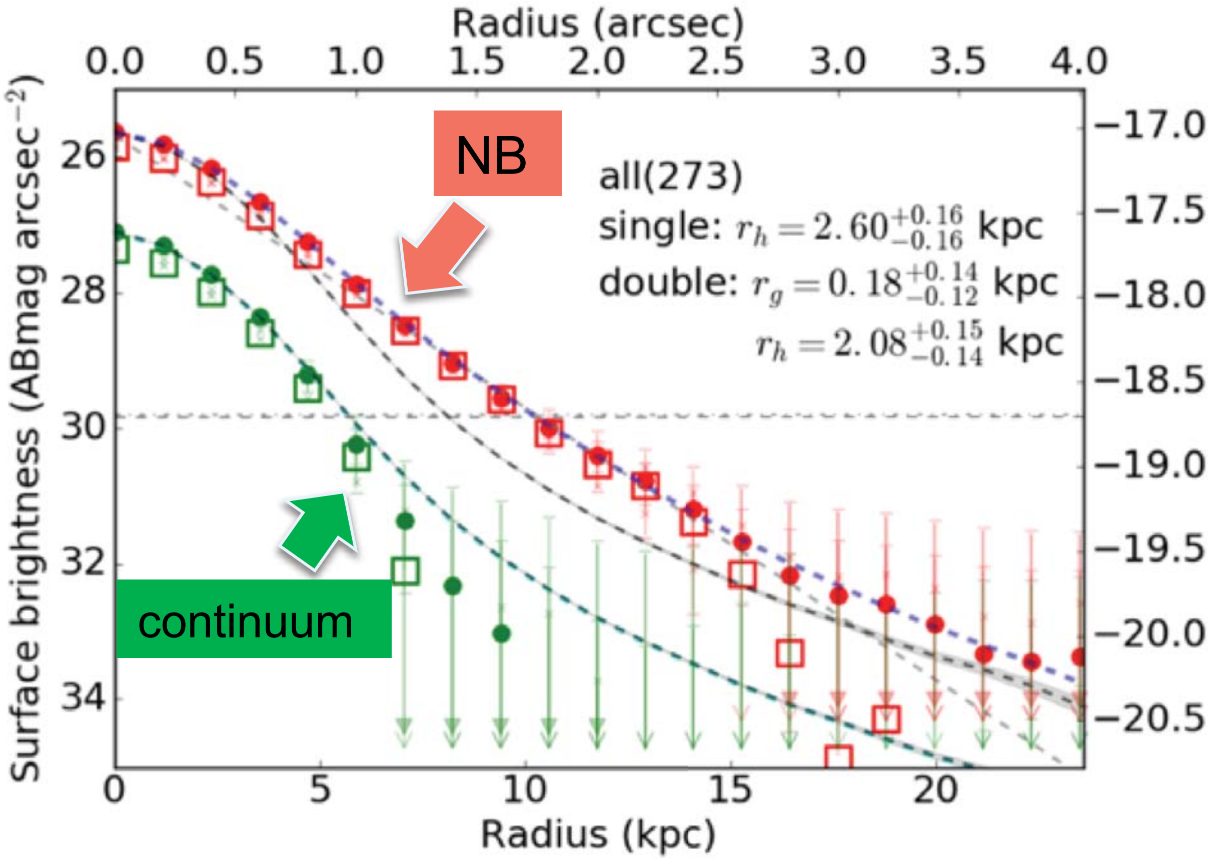

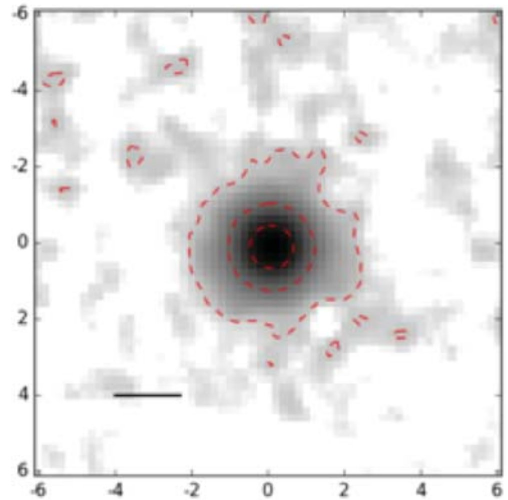

(Wu, Jiang, et al. in prep.)

Summary of halo sizes

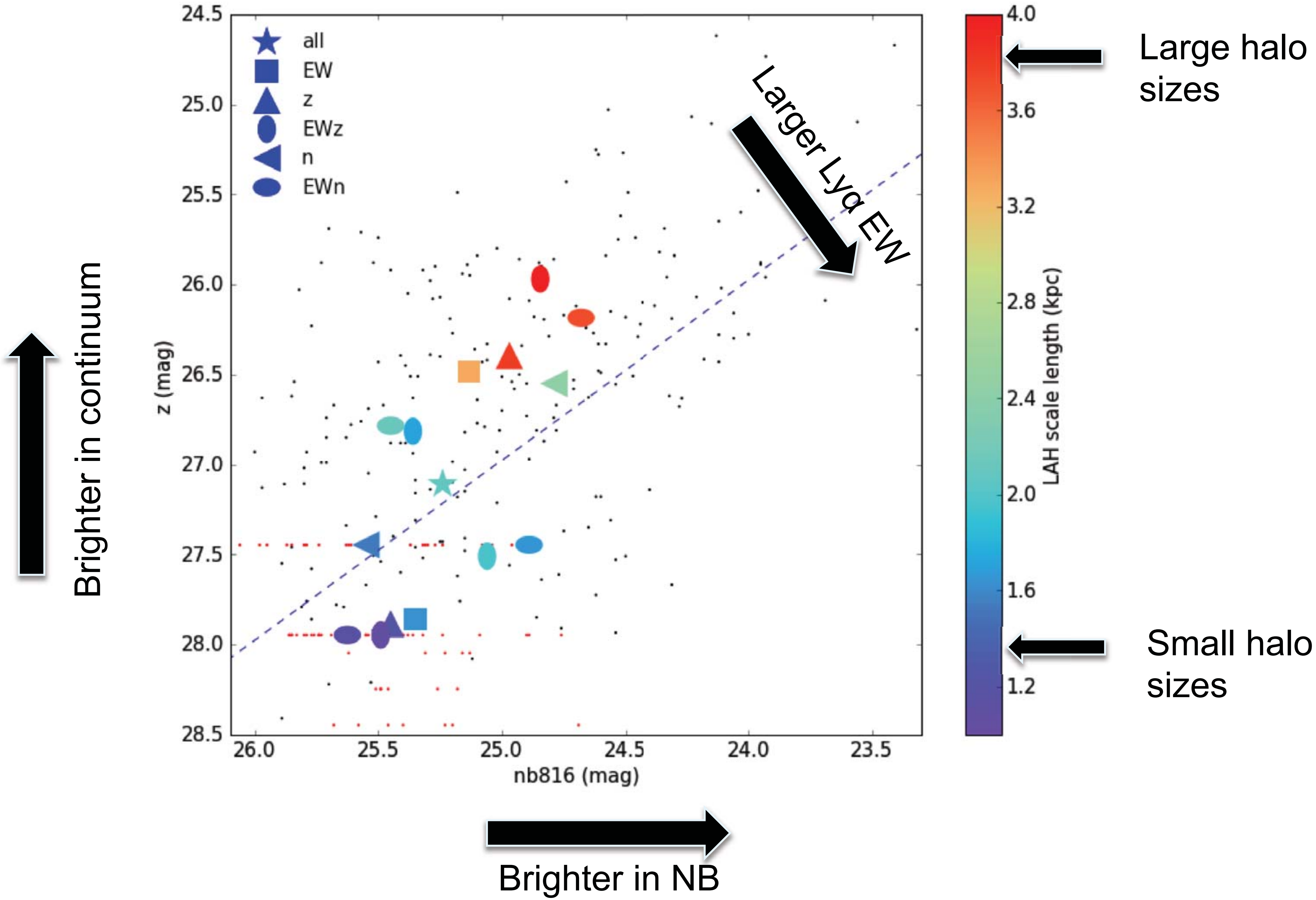

❑ Why are these halos interesting

- Closely related to an important question: how Lyα photons escape from galaxies
- What powers these halos: open question

Cold streams | Scattered light in CGM | Satellite star formation

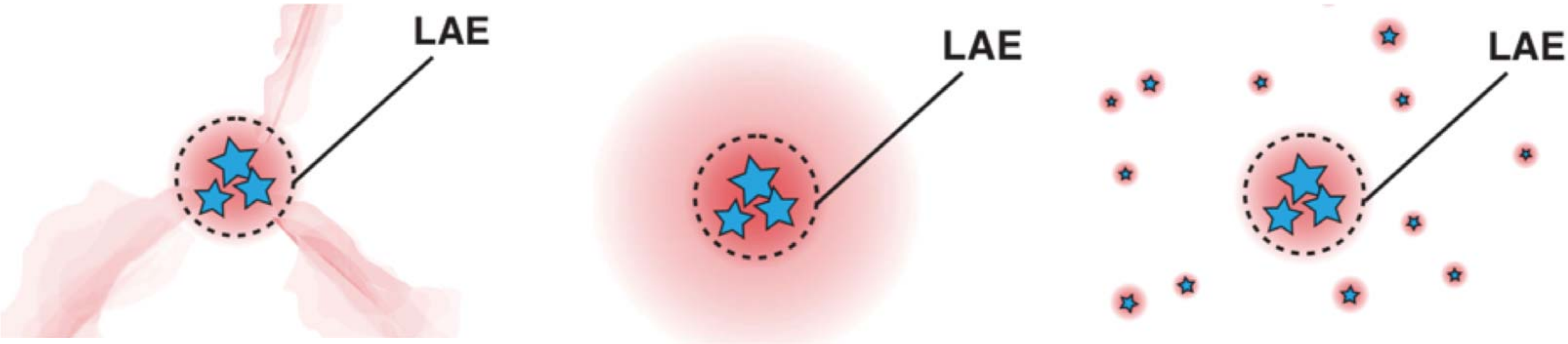

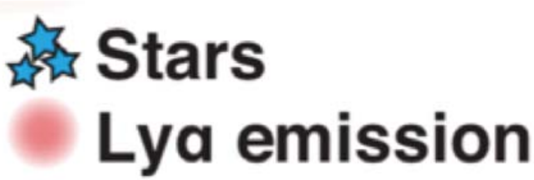

(Momose et al. 2016)

❖ Preliminary results: Large protoclusters at z> 5.5

- The largest protoclusters of galaxies extend over tens of co-moving Mpc at the epoch of their early formation
  → large-area surveys are needed to find them

- Secure redshifts are critical

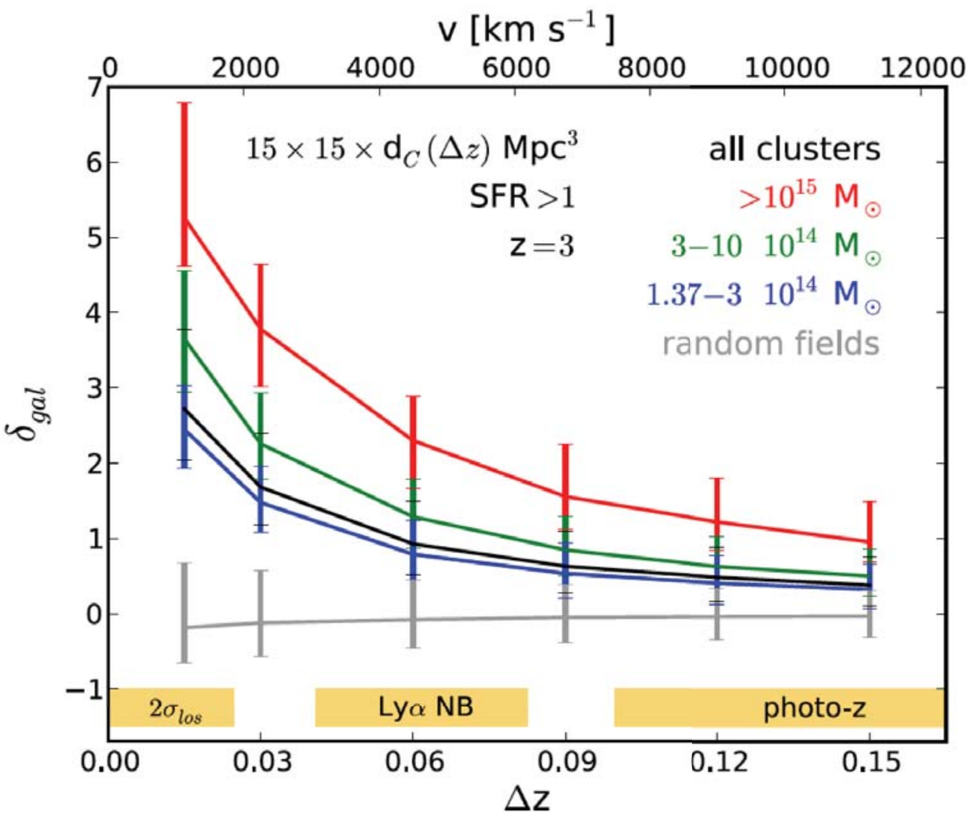

(Chiang et al. 2013)

- Discovery of a giant protocluster (SXDS_gPC) at z ~ 5.7
  - Identification of a large overdense region
  - Spectroscopic confirmation of 46 luminous LAEs (6 hour int.)

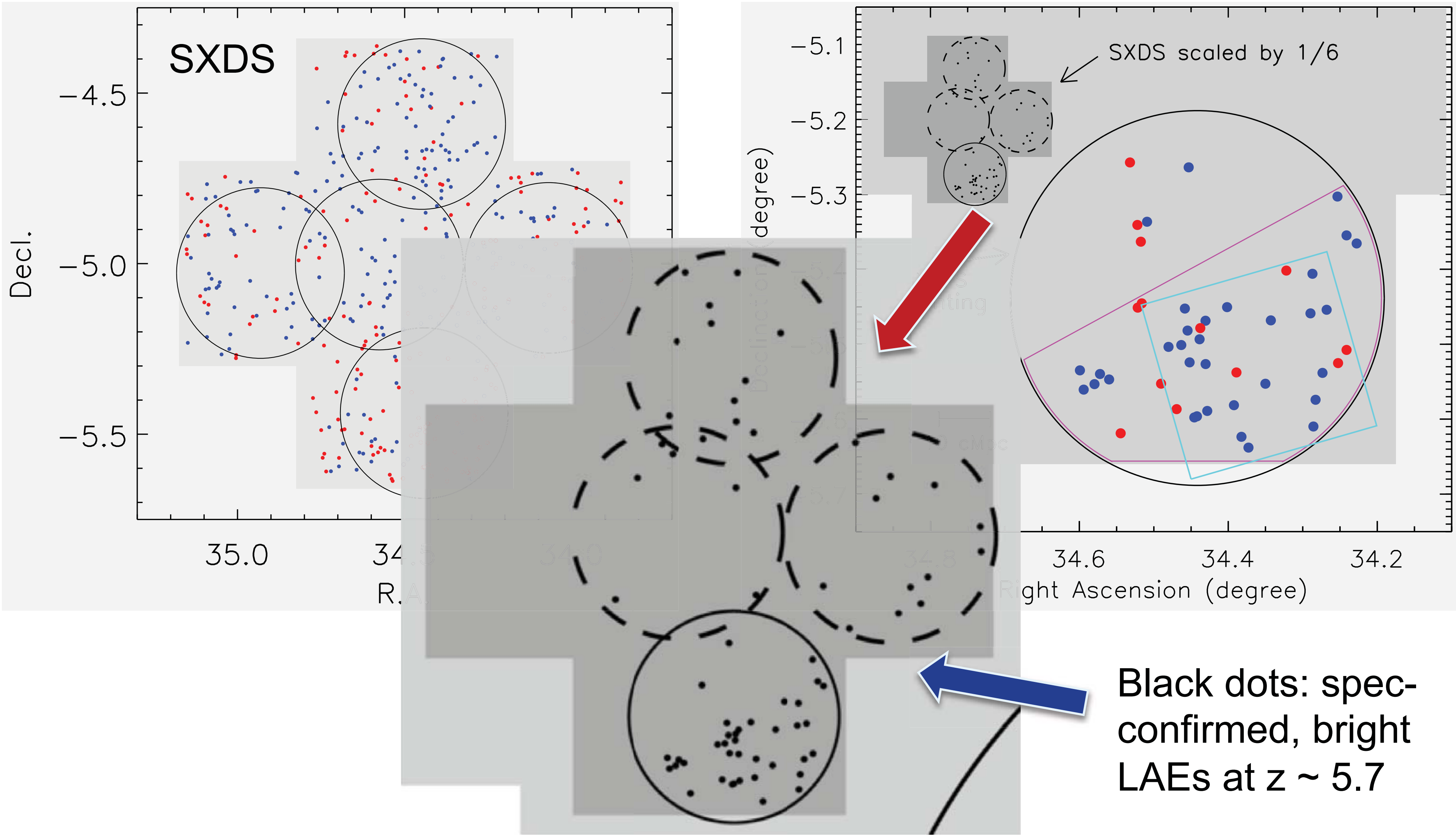

Black dots: spec-confirmed, bright LAEs at z ~ 5.7

- SXDS_gPC Galaxy overdensity $\delta_g \equiv n/\bar{n} - 1$
  - δ_g ~ 5.6 in SXDS_gPC (6.6 times the average density at z ~ 5.7); δ_g ~ 3.8 in the larger overdense region
  - The high δ_g exceeds the collapse threshold considerably in the classical theory of spherical collapse
  - Cosmological simulations also suggest that SXDS_gPC will fall into a giant galaxy cluster (see following slides)

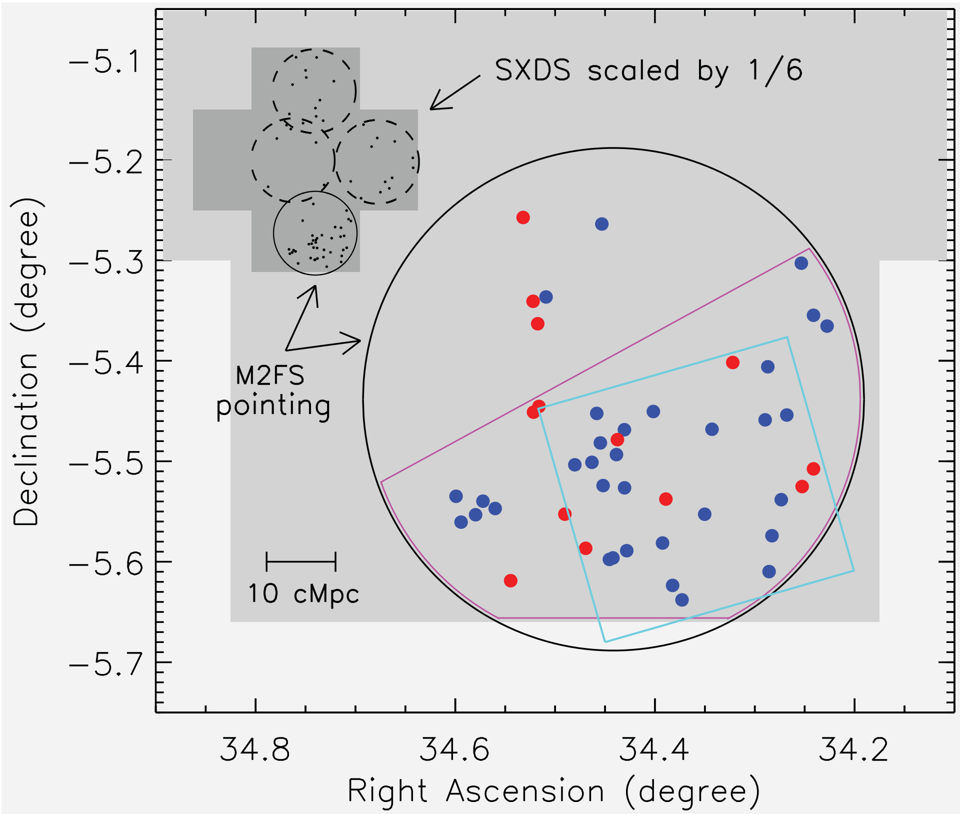

(Jiaing et al. 2018)

- Physical properties of spectroscopically confirmed galaxies at $z \geq 6$
  - These fields are (partly) covered by deep near-IR (e.g., UDS, ultraVISTA, HST CANDELS) and mid-IR imaging data (IRAC 1,2)
  - Various properties of high-redshift galaxies, such as size, morphology, UV slope, star-formation rate, age, dust, stellar mass, etc. (Note that spec redshifts remove one critical free parameter)

(Yuanhang Ning's Ph.D. thesis project)

❖ Future prospects: understanding reionization

- Increasing fraction of neutral IGM from z=5.7 towards higher redshift
- Patchy reionization

  - Lyα luminosity function
  - Enhanced galaxy clustering
  - Lyα visibility test
  - ......

➢ Enhanced clustering of LAEs

- Have we found it?
- How do we find it?
- Are z~6.5 LAEs our best chance?

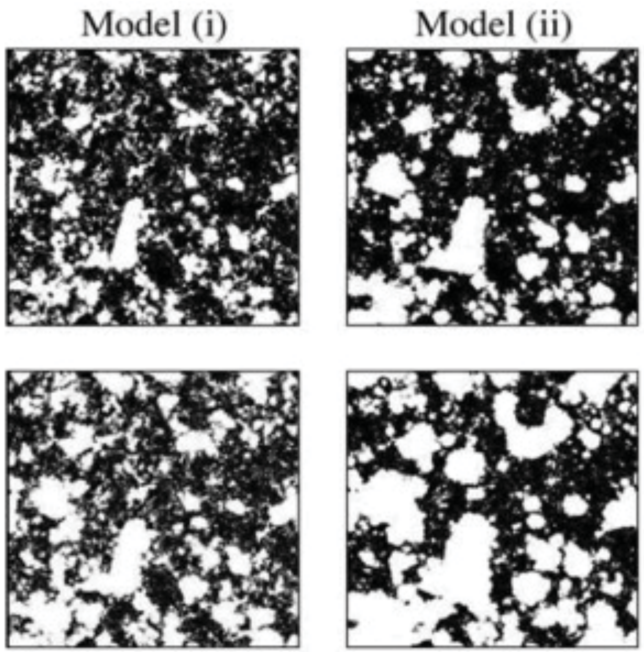

(McQuinn et al. 2007)

(Refs: McQuinn+2007; Ouchi+2010; Kashikawa+2011; Silva+2013; Treu+2013; Cai+2014; Dijkstra+2014; Jensen+2014; Kakiichi+2015)

➢ Lyα visibility test: Fraction of LBGs with strong Lyα emission

- Increases from low redshift to z~6
- Decreases towards higher redshift
- Broadly consistent with LF evolution
- But errors are very large

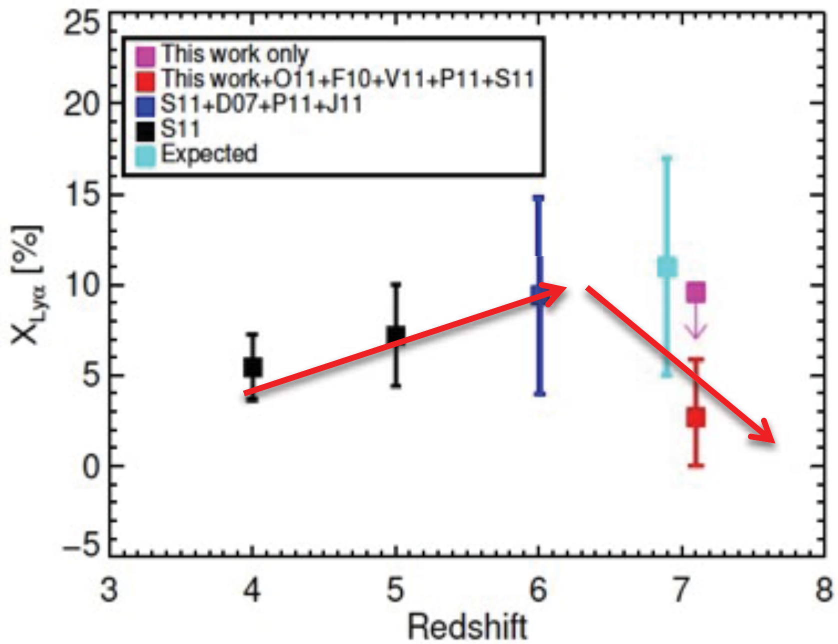

(Bian et al. 2014)

❖ Future prospects: LAEs from z ~ 2 to 7

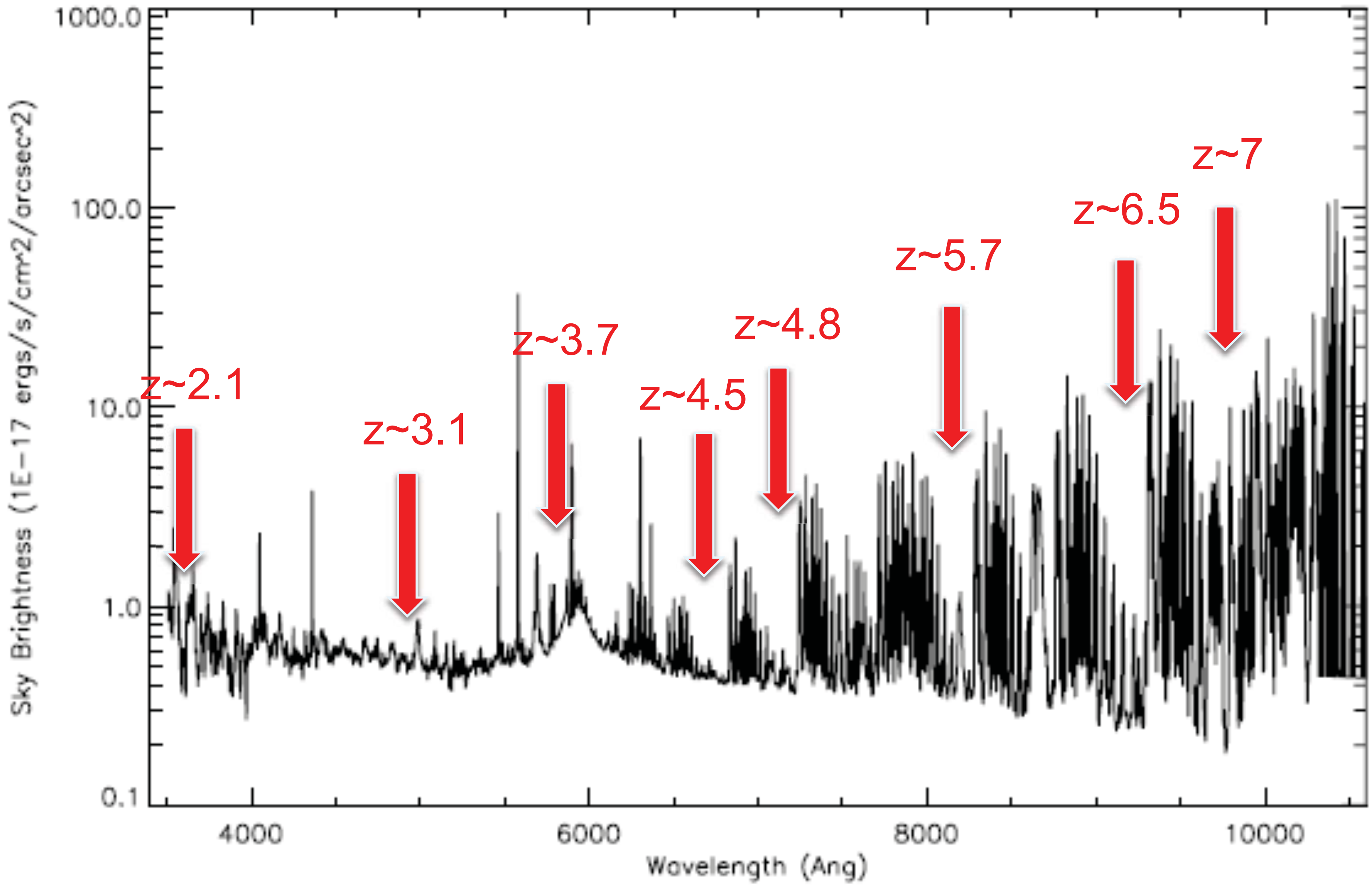

- A bigger picture:

  A systematic study of LAEs from z ~ 2 to z ~ 7

LAEs at

z = 2.1 ➡ 3.1 ➡ 3.7 ➡ 4.5 ➡ 4.8 ➡ 5.7 ➡ 6.5 ➡ 7

MMT/Hectospec
2012 − 2013

MMT/Hectospec
2016 − 2017
(Guo, Jiang, 2019)

MMT/Hectospec
Magellan/M2FS
2017 − 2019

Magellan/M2FS
2015 − 2018

DECam, Magellan/IMACS,
Gemini; 2016 − 2019; e.g.
Zheng, et al. 2017